May 2016

The Effective Use of Coal Combustion Products (CCPs) in Ashphalt Pavements

Clayton J. Cloutier
University of Wisconsin-Milwaukee

THE EFFECTIVE USE OF COAL COMBUSTION PRODUCTS (CCPs)

IN ASPHALT PAVEMENTS

by

Clayton Cloutier

A Thesis Submitted in

Partial Fulfillment of the

Requirements for the Degree of

Master of Science

in Engineering

at

The University of Wisconsin-Milwaukee

May 2016

ABSTRACT

THE EFFECTIVE USE OF COAL COMBUSTION PRODUCTS (CCPs) IN ASPHALT PAVEMENTS

by

Clayton Cloutier

The University of Wisconsin-Milwaukee, 2016

Under the Supervision of Professor Konstantin Sobolev

Hot-Mix Asphalt (HMA) is one of the most widely used construction materials. The National Asphalt Paving Association (NAPA) estimated that there are over 2.6 million miles of roadway surfaces paved in the United States and 94% of these roads are paved with asphalt. NAPA also estimates that approximately 550 million tons of asphalt worth over $30 billion a year is produced in the United States. At such a huge production rate, innovative solutions need to be developed so that asphalt pavements last longer and can also reduce the production and maintenance costs. Producing sustainable asphalt materials can provide for improved infrastructure which is required for the operational needs of society.

Coal Combustion Products (CCPs), such as fly ash materials, are by-products of the coal combustion process. Fly ash is one of the most commonly used by-product pozzolan. These materials are unique in that they have a spherical shape and the small spherical particles can improve the workability and reduce the porosity when mixed with other binding materials. In 2006, the American Coal Ash Association (ACAA) reported that there has been 72.4 million tons of coal ash produced in which only about 52,608 tons of fly ash was used as mineral fillers in asphalt applications. Since 2006, there has been no data on the use of fly ash in asphalt applications. Researchers have found beneficial

uses of fly ash in asphalt mastics and asphalt pavements. However, this research has been limited to older testing procedures and only few researchers have reported on the effects of CCPs in asphalt using Superpave® protocol. By further systematic investigation of the effect of CCPs in asphalt, better conclusions can be made regarding the potential favorable effects of CCPs in asphalt.

This research investigated the effects of CCPs in asphalt mixtures in terms of asphalt film thickness, workability, aging resistance, moisture damage resistance, intermediate-temperature fatigue cracking resistance, and low-temperature thermal cracking resistance. Control mixtures (5.5% binder content) were compared to ASHphalt mixtures with a 10% (by mass) binder replacement with CCP. The CCPs used were a WE05 (Class C), TA11 (Class F), LG14 (Class F), and SF15 (SDA – Spray Dryer Absorber material). For the Control and ASHphalt mixtures, it was verified that no major differences were observed or recorded for aggregate coating quality or mixing performance. Compaction efforts were reduced for ASHphalt mixtures (compacted at 145^{o}C) as compared to the Control mixtures (compacted at 140^{o}C). The minor increase in compaction temperature was negligible but was necessary to reduce the material viscosity so that compaction efforts were more comparable to the Control mixtures. The addition of CCPs resulted in an enhanced aging resistance for mixtures with LG14 (F) and SF15 (SDA). Indirect Tensile Testing (IDT) proved that the ASHphalt mixtures developed higher strengths than the Control mixtures, especially for WE05 (C) and TA11 (F) mixtures. Moisture damage resistance was evaluating using Tensile Strength Ratio (TSR) and it was discovered that all ASHphalt samples, especially LG14 (F), developed a better TSR than the Control samples. Fatigue testing was performed at intermediate temperatures (20 ± 1^{o}C) to evaluate the number of cycles each sample could withstand before a drop in E* (Complex Modulus). Every ASHphalt material performed better than the Control mixtures for fatigue testing, especially TA11 (F) mixtures as this material withstood 149,250 cycles before failure with a vertical deformation rate of 6.52E-06 mm/cycle. Thermal cracking resistance was evaluated at low temperatures (-18 ± 1^{o}C) by using the Semi-Circular Bending (SCB) test. For Fracture

Energy (G_f) all ASHphalt mixtures performed better than the Control mixture, specifically LG14 (F) as this mixture performed the best. For Fracture Toughness (K_{IC}), only LG14 (F) performed better than the Control mixture. Lastly, all mixtures demonstrated lower Stiffness (S) values, especially TA11 (F), than the Control mixture and this was desirable.

TABLE OF CONTENTS

LIST OF FIGURES

LIST OF TABLES

LIST OF EQUATIONS

LIST OF ABBREVIATIONS

AASHTO	American Society of State Highway and Transportation Officials
ASTM	American Society for Testing Materials
CCPs	Coal Combustion Products
ESALS	Equivalent Single Axle Load
E*	Complex Modulus
G_f	Fracture Energy
G_{mb}	Bulk Specific Gravity
G_{mm}	Maximum Specific Gravity
HMA	Hot Mix Asphalt
ID	Indirect Tensile Test
JMF	Job Mix Formula
K_{IC}	Fracture Toughness
PG	Performance Grade
S	Stiffness
SDA	Spray Drying Agent
SEM	Scanning Electron Microscope
SGC	Superpave® Gyratory Compactor
T_f	Film Thickness
V_a	Air Void Content
VFA	Voids Filled with Asphalt
VMA	Voids in Mineral Aggregates

ACKNOWLEDGEMENTS

I would like to express my sincere gratitude to Dr. Konstantin Sobolev, Dr. Ahmed Faheem, and Dr. Emil Bautista for their knowledge and expertise during all of the project developmental stages. Their help and recommendations have been vital to this research.

I would also like to thank EPRI (Electric Power Research Institute), We Energies, and Payne & Dolan as the primary sponsors of the research project. Their help and generosity made this research possible.

In addition, I want to thank all the other lab colleagues that helped me out during this process: Brian Mullen, Leif Jackson, Andrew Sinko, and Emily Szamocki. All of the help that they provided made the project what it is today.

CHAPTER 1.

SCOPE OF WORK

1.1 INTRODUCTION

Asphalt cement is one of the oldest materials used in the construction field. Asphalt was first used as a construction material in Sumeria (Mesopotamia), around 6,000 B.C., as a shipbuilding material. From there, asphalts were then used in places like Egypt around 2600 B.C. as a material for waterproofing, mummification, and building structures. In various parts of the world, asphalt continued to be used as mortar for buildings and paving blocks, caulking for ships, and numerous waterproofing applications. In the United States, the first known natural asphalt pavement was laid in 1876 on Pennsylvania Avenue in Washington, D.C. Before the mid-1850s asphalt came from natural pools at different locations in the world such as Trinidad Lake. With the discovery and refining of petroleum in Pennsylvania, asphalt became very well-known. By 1907, most of the asphalt came directly from the distillation process from petroleum refineries than from the natural deposits. Today, almost all asphalt materials come from refined petroleum (Roberts et al. 1996).

Asphalt concrete is composed of two different ingredients: asphalt cement and aggregates. Asphalt cement consists of approximately 5% of the total mixture mass whereas the aggregates consist of the remaining 95% mass. Asphalt cement, or binder, is a mixture of petroleum hydrocarbons with different chemical structures. The primary elements present in asphalt are carbon and hydrogen. Other elements present are sulfur, nitrogen, oxygen, vanadium, and nickel. Asphalt binder is a strong and durable material that has great adhesive and waterproofing features. Asphalt binder can be very elastic and brittle at low temperatures and can be very fluid (viscous) at high temperatures. At intermediate temperatures, asphalt cement is considered a viscoelastic material since it demonstrations both elastic

and viscous properties. Due to these variations in material behavior at different temperatures, asphalt cement is considered a thermoplastic material (Roberts et al., 1996).

Asphalts used in the construction industry are typically classified as asphalt cements, emulsified asphalts, and cutback asphalts. The most common type of asphalt material is Hot Mix Asphalt (HMA). Hot Mix Asphalt is widely used as a material in the construction of flexible pavements. The asphalt cement can be heated in terms of temperature to make the material less viscous so that it can flow easier which aids in compaction. This allows the material to liquefy and then be mixed with aggregates to make asphalt concrete. Since the asphalt material is sticky, it adheres to the aggregate particles to produce HMA.

Aggregates are used in asphalt applications because they act as a stone framework which is important in terms of material strength. Aggregates in asphalt pavements range from coarse aggregates to fine aggregates. According to the American Society for Testing and Materials (ASTM) the No. 4 sieve size (4.75 mm) separates the coarse and fine aggregates (ASTM C136). Anything above the No. 10 sieve size (2.00 mm) is considered gravel, boulders, or cobbles, whereas anything below the No. 10 sieve size (2.00 mm) is considered either sand or mineral fillers. Mineral fillers are classified as the portion of the fine aggregates that pass the No. 200 sieve (0.075 mm). These mineral fillers usually take up less than 8% of Hot Mix Asphalt (HMA), by mass, but have a large effect on the HMA field performance. Properly classifying and grading aggregates is critical for asphalt mixtures.

In recent years, researchers in the materials construction field have explored the use of by-products, such as fly ash, and how these materials can improve other material properties. Fly ash has been used in Portland cement concrete, however it has not been widely investigated in asphalt pavements. It has been reported that the introduction of fly ash into asphalt mixtures (ASHphalt) improves the performance of HMA in terms of mixing, compacting, aging, moisture damage

resistance, rutting resistance, fatigue resistance, and low-temperature thermal cracking (Carpenter, 1952; Bautista et al., 2015; Bianchetto, Martinez, Miro, & Perez, 2005; Faheem & Bahia, 2009; Goetz, Tons, & Rozi, 1983; Henning, 1974; Howell, Hudson, & Warden, 1952; Sobolev et al., 2013; Suheibani, 1986; Zimmer, 1970). Fly ash improves these characteristics because it has a distinct spherical shape with beneficial chemical properties. Using fly ash in asphalt mixtures is important because it can reduce costs associated with asphalt production and at the same time enhance certain properties of regular asphalt mixtures.

Fly ash in asphalt related applications has not been entirely assessed. This research evaluates possible advantages of Coal Combustion Products (CCPs) when incorporated into asphalt mixtures. Utilizing waste products is critical in terms of sustainability. Reducing the amount of energy consumption in asphalt production is vital. Not only this, but reducing the efforts in pavement maintenance costs is also an important goal. Integrating CCPs into asphalt mixtures could potentially reduce energy consumption, production costs, and even maintenance costs and this is why this research is so important.

1.2 PROBLEM STATEMENT

The National Asphalt Paving Association (NAPA) estimates that there are over 2.6 million miles of paved roads in the United States and 94% of these roads are paved with asphalt. NAPA also estimated that there are around 4,000 asphalt plants in the United States. Every year, these asphalt plants produce approximately 550 million tons of asphalt worth over $30 billion a year. Evaluating different and more effective methods for asphalt production is important. As the infrastructure in the United States continues to deteriorate, while the population continues to grow, innovative solutions need to be developed to withstand the effects of these problems.

1.3 RESEARCH HYPOTHESIS

Adding Coal Combustion Products (CCPs), such as fly ash and Spray Dryer Absorber (SDA) materials, to asphalt mixtures can improve the overall performance of asphalt pavements.

1.4 RESEARCH OBJECTIVES

The overall goal of this research was to understand the potential benefits of adding different Coal Combustion Products (CCPs) to asphalt mixtures. The following objectives of this study were established:

- To evaluate aggregate coating when CCPs are introduced into the asphalt mixture.
- To investigate the constructability of ASHphalt mixtures.
- To examine the aging transitions and performance of aged asphalt mixtures with and without CCPs.
- To explore the moisture damage resistance of ASHphalt mixtures.
- To assess the strength of the ASHphalt mixtures in terms of fatigue and thermal cracking resistance.

1.5 THESIS OUTLINE

This thesis is structured into five primary sections with the following contents:

Chapter 1: Scope of Work – This chapter includes a background on HMA application, as well as an introduction to fly ash applications and potential reasons why Coal Combustion Products (CCPs) should be used in asphalt pavements. The problem statement, research hypothesis, and research objectives are also included.

Chapter 2: Literature Review – This chapter gives a detailed description of asphalt characteristics, the importance of aggregates, asphalt mixtures, and Coal Combustion Products (CCPs).

Chapter 3: Preliminary Study – This chapter explains a full preliminary study that was conducted to evaluate the feasibility of adding CCPs to asphalt mixtures.

Chapter 4: Materials and Testing Methods – This chapter explains the materials and testing methods that were used throughout this research. There is a detailed description about the CCPs that were used as well as the aggregates and asphalt binder. This chapter also explains the testing methods that were used to evaluate aggregate coating, asphalt constructability, aging comparisons, moisture damage resistance, and fatigue and thermal cracking resistance.

Chapter 5: Results and Analysis – This chapter includes a detailed analysis of all the results that were obtained throughout this research. Comparisons were made between asphalt mixtures with and without CCPs. Aggregate coating, constructability, aging comparisons, moisture damage resistance, and fatigue and thermal cracking resistance were all analyzed.

Chapter 6: Conclusions – This chapter explains the research results. The main points are presented and conclusions are made based on the results that were found throughout the research.

Chapter 7: Future Work – This chapter explains potential research options for future work.

Chapter 8: References – This chapter gives a list of all the references that were used throughout this thesis research.

CHAPTER 2.

LITERATURE REVIEW

2.1 ASPHALT BINDER

2.1.1 Chemical Composition

Asphalt is defined by the American Society for Testing Materials (ASTM) as a "dark brown to black cementitious material in which the predominating constituents are bitumens which occur in nature or are obtained in petroleum processing" (Asphalt Institute, 2003). Asphalt is made from crude petroleum which is a product that can be found naturally in the world. About 90 to 95 percent by weight of asphalt bitumen is composed of hydrogen and carbon, which is why it is referred to as a hydrocarbon. The carbon atoms can arrange in different configurations which allows the asphalt to behave in different ways. There are three distinct arrangements that carbon can configure: straight or branched chains, simple or complex saturated rings, and one or more stable six-carbon condensed unsaturated ring structures. The remaining portion of asphalt contains both heteroatoms (hydrogen, nitrogen, and sulfur) and metals. The heteroatoms and metals provide asphalt with many unique characteristics because they are reactive with other molecules. The type, rather than quantity, of each element is more critical to the overall asphalt molecular composition. Since asphalt is derived from an organic petroleum product, the molecular structure is diverse and very dependent on the crude source. Table 2.1 shows the elemental analysis of representative petroleum asphalts (Peterson, 1984).

Table 2.1 Elemental Analysis of Representative Petroleum Asphalts

Elements	B-2959 Mexican Blend	B-3036 Arkansas-Louisiana	B-3051 Boscan	B-3602 California
Carbon (%)	83.77	85.78	82.9	86.77
Hydrogen (%)	9.91	10.19	10.45	10.93
Nitrogen (%)	0.28	0.26	0.78	1.1
Sulfur (%)	5.25	3.41	5.43	0.99
Oxygen (%)	0.77	0.36	0.29	0.2
Vanadium (ppm)	180	7	1380	4
Nickel (ppm)	22	0.4	109	6

As previously mentioned, the heteroatoms attach to the carbon atoms in different configurations. Within these molecular configurations, there is an imbalance of electrochemical forces. For this reason these asphalt molecules are considered to be polar. Each polar group, therefore, has an electropositive charge and an electronegative charge. Since similar charges and opposite charges have different effects with each other, these characteristics influence asphalt properties and performance. These polar groups can also vary depending on the source of the asphalt material and this can influence the performance of the asphalt material. Non-polar groups in asphalt act as solvents for the polar groups and this also affects the physical and aging properties of the asphalt cement (Roberts et al., 1996).

There are many different molecular structures comprising asphalt cements. Researchers have focused on categorizing these structures into major fractions (Figure 2.1). Asphalt cement consists of both asphaltenes and maltenes (petrolenes). Asphaltenes are dark brown friable solids that are chemically complex and have the highest polarity when compared to the other asphalt components. The asphaltenes are responsible for the adhesive properties of asphalt which is directly related to viscosity. When the asphaltene content is less than 10%, the compaction effort is very high and it is difficult to compact the asphalt concrete to the appropriate density. Maltenes, on the other hand,

consist of both resins (highly polar hydrocarbons) and oils (aromatics and saturates). Resins are dark brown and semisolid or solid, and are temperature dependent which affects the viscosity of the overall asphalt material. When heated, these resins act as a fluid material, but at low temperatures these resins become brittle. The resins are responsible for dispersing asphaltenes in the oil, which is a clear or white liquid that, during oxidation, produces asphaltene and resin molecules. This compatible and balanced system is what makes asphalt suitable as a binder material in the construction industry (Domone & Illston, 2010; Mamlouk & Zaniewski, 2006; Roberts et al., 1996).

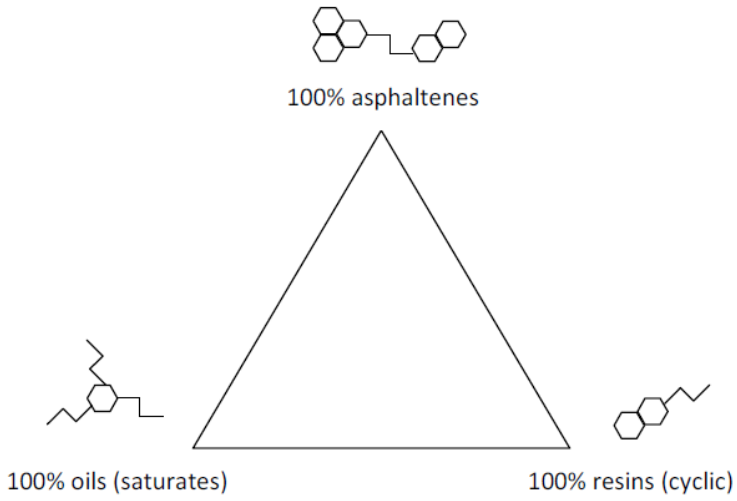

Figure 2.1 Chemical Composition of Asphalt Binder (Bentur et al., 1998)

2.1.2 Oxidation and Age Hardening

Asphalt cement is chemically organic and thus reacts with atmospheric oxygen. Bituminous materials are exposed to the environment and therefore these materials can harden and age. However, the rate of oxidation and age hardening both depend on the natural conditions, such as temperature, as well as the chemical composition of the bituminous material. The oxidation process occurs more quickly at higher temperatures. Oxidation alters the structure and composition of the asphalt molecules and changes the rheological properties of asphalt cement so that it becomes more

brittle, especially at lower temperatures. Since rheological properties are critical in asphalt development, oxidation and age hardening are important factors to consider (Asphalt Institute, 2001; Domone & Illston, 2010).

During the oxidation process, oxygen molecules from the atmosphere form asphaltenes by combining with resins and oils. The polarity and molecular weight fraction both increase while the molecular weight components decrease. Due to this result, the viscosity of the bituminous materials increases. The asphalt also becomes unstable because there are discontinuities between the saturates and the other components. This instability within the material creates a lack of cohesion and this can lead to cracking. Volatiles are also lost in the oxidation process. If the bitumen is subjected to higher temperatures, and if there is a large portion of low molecular weight components, there will be a loss of volatiles and this will lead to a more rapid age hardening process (Domone & Illston, 2010).

A large amount of oxidation and age hardening occurs during the HMA process when the asphalt is heated for mixing and compacting. At the beginning of the mixing process, the asphalt binder is placed into the mixer and mixed with heated aggregates. During this mixing process the hot asphalt cement is exposed to air temperatures from 275 to 325^{o}F (135 to 163^{o}C). The asphalt cement at this time also exists in thin films, while it coats the aggregates, and this allows oxidative hardening to occur at a faster rate. High temperatures change the rheological properties of the asphalt cement by decreasing penetration and increasing the viscosity. The reason this happens is because of oxidation and because of the loss of more volatile components (Roberts et al., 1996).

After the short-term oxidation during mixing, transportation, and placement, the asphalt then experiences a long-term form of oxidation, exposure during service life called age hardening. Once the asphalt pavement has been compacted and opened to vehicle traffic, the age hardening process continues, but at a slower rate. This process usually happens until the asphalt reaches its limiting

density (compaction to percent air voids) under the traffic loads. During the construction process volatilization occurs which associated with the process of volatile components evaporating from the asphalt pavement. Physical hardening also occurs when asphalt has been exposed to low temperatures (typically less than 0°C) for long periods of time. Also, if the HMA pavement has a higher air void content than designed, there is a larger amount of air, water, and light that can penetrate the pavement and cause the pavement to age faster. This is why asphalt compaction in the field is a critical parameter (Kandhal, Sandvig, Koehler, & Wenger, 1973).

One way to represent the aging of asphalt materials is by an aging index. The aging index is calculated as the ratio of the viscosity of the aged bitumen to that of the original bitumen. It practice, the aging index is almost always larger than 1.0. This means that as the material ages, it becomes harder, brittle, and more viscous. Figure 2.2 shows a graphical representation of the aging process throughout the asphalt pavements life-cycle (Shell Bitumen, 2003).

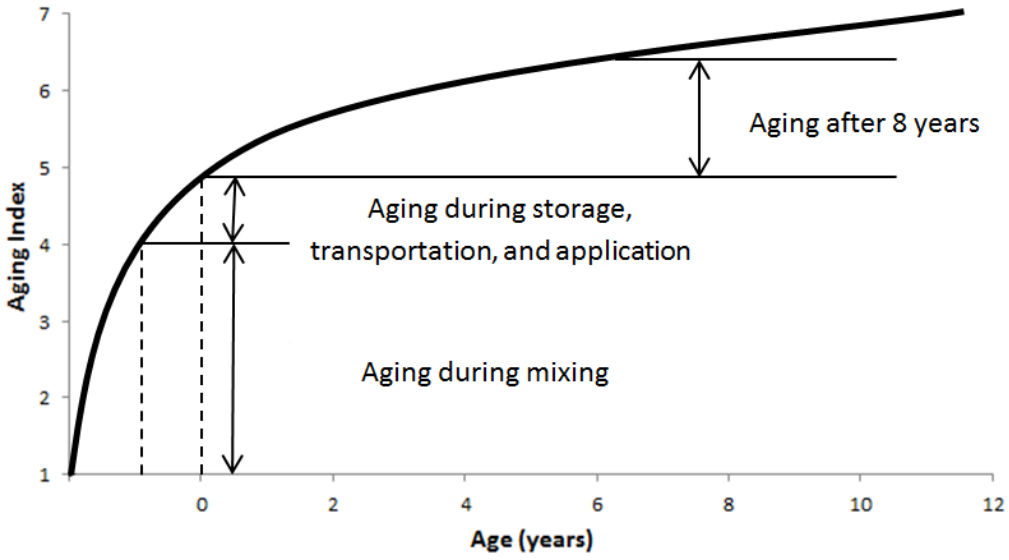

Figure 2.2 Aging Characteristics during Different Periods of the Asphalt Life-Cycle

2.1.3 Performance Grading System

In 1987, the Strategic Highway Research Program (SHRP) developed a new system for HMA characterization based on a pavement-temperature performance rather than an air-temperature performance. The final outcome from this SHRP effort resulted in what is known as Superpave® - *Su*perior *Pe*rformance Asphalt *Pave*ments. The main reasons for developing Superpave® were to extend the pavement life, reduce the life-cycle costs, to reduce the maintenance costs, and to minimize premature failure (McGennis et al., 1994). With these ideas in mind, a new system of asphalt grading was also developed, as well as a detailed specification for mineral aggregates. The new system of asphalt selection is based on a temperature design to describe the viscoelastic and failure properties of asphalt binders which can more realistically relate to asphalt concrete properties and field performance (McGennis et al. 1995).

The new Superpave® grading system introduced a Performance Grading (PG) classification. This means that the asphalt binder is selected based on its performance in relation to temperature. The asphalt binder is selected based on maximum, minimum, and intermediate pavement design temperatures. This Performance Grade philosophy ensures that the selected binder will meet the performance requirements at the selected temperatures. The PG binders are defined by a term such as PG 58-28. The first number, 58, refers to the high-temperature grade which means that the binder is capable of physically performing at 58^{o}C. This temperature is selected based on the seven-day average maximum pavement temperature. The second number, -28, refers to the low-temperature grade. This means that the binder possesses adequate physical properties in pavements down to at least -28^{o}C. The intermediate temperature is the average of the maximum and minimum pavement design temperatures plus 4^{o}C. When testing asphalt binders or mixtures, it is critical to conduct a

thorough analysis at all three temperatures (McGennis et al., 1994). Table 2.2 shows common types of asphalt binder grades identified by Superpave® performance specifications.

Table 2.2 Common Types of Performance Graded Asphalt Binders

High-Temperature Grades (°C)	Low-Temperature Grades (°C)
PG 46	-34, -40, -46
PG 52	-10, -16, -22, -28, -34, -40, -46
PG 58	-16, -22, -28, -34, -40
PG 64	-10, -16, -22, -28, -34, -40
PG 70	-10, -16, -22, -28, -34, -40
PG 76	-10, -16, -22, -28, -34
PG 82	-10, -16, -22, -28, -34

2.1.4 Temperature Susceptibility

Asphalt cement is a material that undergoes extreme changes when temperature fluctuates. At low temperatures asphalt cement can be very elastic and brittle, at high temperatures it can be very fluid and viscous, and at intermediate temperatures it can be considered a viscoelastic material since it exhibits both elastic and viscous properties. Because of the variations in behavior (temperature dependent) asphalt cement is considered a thermoplastic material. Temperature susceptibility, therefore, is the rate at which the consistency of the asphalt binder changes with respect to the change in temperature. Figure 2.3 demonstrates the linear inverse relationship that asphalt has on both viscosity and temperature; as temperature increases, viscosity decreases. Since asphalt cement exhibits these extreme variations in material properties (with temperature), Superpave® methodology was developed to control high-temperature pavement rutting, intermediate-temperature fatigue, and low-temperature thermal cracking (Asphalt Institute, 2001, 2003; Roberts et al., 1996).

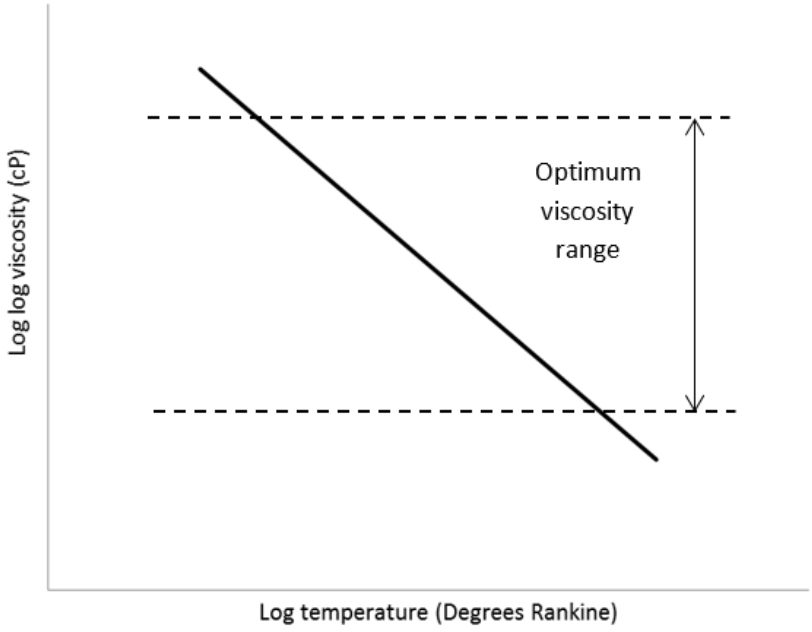

Figure 2.3 Viscosity-Temperature Relationship of Asphalt Binders

2.1.4.1 High-Temperature Behavior

At high temperatures, most asphalt cements act as a viscous, Newtonian material where the shear stress and shear strain are proportional. Viscosity is the material property that characterizes the resistance of liquids to flow. Therefore, for Newtonian fluids, the viscosity is independent of the shear rate. Also, at higher pavement temperatures, a high stiffness, which is the relationship between stress and strain as a function of time of loading and temperature, is generally a desirable property because this allows for the pavement to resist rutting (Asphalt Institute, 2003; Finn, 1967; Kandhal et al., 1988; Kandhal, Sandvig, & Wenger, 1973).

2.1.4.2 Intermediate-Temperature Behavior

At intermediate temperatures, asphalt binders are considered a viscoelastic material because these demonstrate characteristics of both a viscous liquid and an elastic solid. For this reason, the response can be represented by a spring-dashpot model (Figure 2.4). Forces that are exerted on the

asphalt material cause parallel reactions and also cause an immediate elastic response. Mostly all of this response is recoverable with time while some of the response is plastic and can't be recovered. The non-recoverable aspect can be related to repeated cyclic loading and unloading of the material and this can result in fatigue failure (Asphalt Institute, 2003).

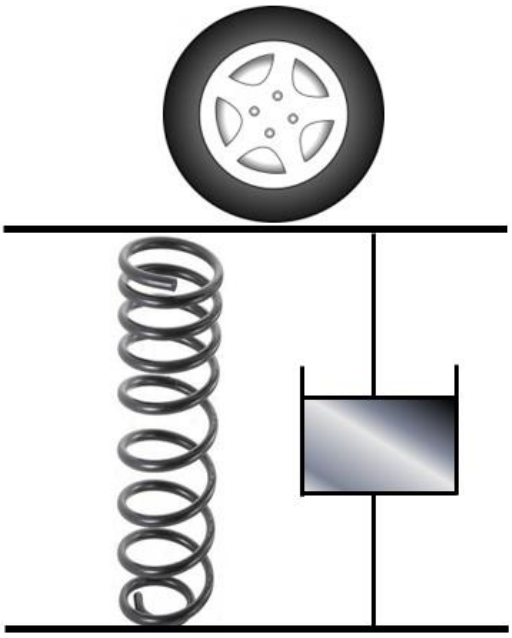

Figure 2.4 Spring-Dashpot Model of Viscoelastic Asphalt Behavior

2.1.4.3 Low-Temperature Behavior

At low temperatures, most asphalt cements act as an elastic, or non-Newtonian, material where the ratio of shear stress to shear strain is not proportional. At these lower temperatures the material behaves elastically like a rubber band in which it deforms under load but then returns to its original shape once it is unloaded. Typically at lower temperatures however, a low stiffness is generally desired because this allows the asphalt material to resist low-temperature cracking. If the material is stressed beyond the material capacity or strength, the brittle elastic solids can fracture and this

results in thermal cracking (Asphalt Institute, 2003; Finn, 1967; Kandhal et al., 1988; Kandhal, Sandvig, & Wenger, 1973).

2.2 MINERAL AGGREGATES

2.2.1 Aggregates in Engineering Applications

Aggregate selection is critical in engineering applications. Determining the appropriate chemical and physical properties of aggregates is important for every construction project because these properties dictate the quality of the material. The characteristics of aggregates vary drastically, however, because most aggregates are produced in a quarry or gravel pit where there are significant differences between the aggregate sources. This makes it obvious that during any construction project the aggregates need to be monitored and tested so that they continuously meet the requirements of the project. Specifications, especially in respect to grading requirements, need to be met to ensure the quality of the aggregates for every engineering project (Goetz & Wood, 1960; Meininger & Nichols, 1990).

During typical construction projects, such as subgrade developments or any paving applications, a large quantity of aggregates are used. Since there is a large amount of material quantity that is being consumed, there are high costs associated with these materials as well as availability concerns. Using locally available aggregates is very important especially to control the transportation or delivery costs. Reducing the amount of costs associated with transporting the aggregate from the quarry to the job site needs to be evaluated and this can be a challenge at times. Pricing and availability are both criteria that are always evaluated during any project, but the main aggregate characteristics are what dictate the application of the material. These aggregates can be used as a base material, in portland cement or asphalt paving applications, or even in concrete building construction. Typically in portland cement concrete, aggregates consist of approximately 79 to 85% by mass. In asphalt pavements,

aggregates consist of about 92 to 96% of the total mass where the remaining percent is asphalt binder. Considering these large amounts of aggregates in these applications, it makes it clear that proper aggregate determination is vital (Mamlouk & Zaniewski, 2006).

2.2.2 Physical Properties of Aggregates

Aggregates are used in asphalt applications because they act as a stone framework which is important in terms of material strength. Most aggregates that are selected for asphalt mixtures are typically from natural sources (sands, gravels, or crushed rocks). There are many different individual particle characteristics that are important when determining the type of aggregate to be used and when determining the aggregate application. The main importance of the aggregate in HMA applications is to provide both strength and stability. These properties are evaluated based on the particle shape, size texture, cleanliness, durability, toughness, and absorption (Mamlouk & Zaniewski, 2006; Roberts et al., 1996).

Aggregate shape, size, and texture are key factors that dictate the packing density of HMA mixtures. These parameters determine how the particles will pack together into a dense configuration and at the same time determine the movement of the aggregates in the mixture. In mixtures with small aggregates, the packing density is greater than those with large aggregates. Mid-size and small-size aggregates fill the void spaces between large aggregates which is why an optimal combination of aggregates is necessary for HMA mixtures. For compacted HMA mixtures, angular-shaped and rough particles experience greater internal friction and interlock which means that there is greater stability and greater strength. Asphalt cement tends to form stronger mechanical bonds with angular-shaped and rough-textured particles which aids in higher overall strengths. The downfall with these types of particles is that they need larger amounts of added asphalt binder in order to increase the workability. On the other hand, round-shaped particles can be coated easier and also experience better

workability which means that there is less compaction effort to obtain the appropriate density. Figure 2.5 illustrates the differences between round and angular-shaped aggregates. During construction, however, the ease of compaction is not sufficient as this can lead to rutting (Mamlouk & Zaniewski, 2006; Roberts et al., 1996).

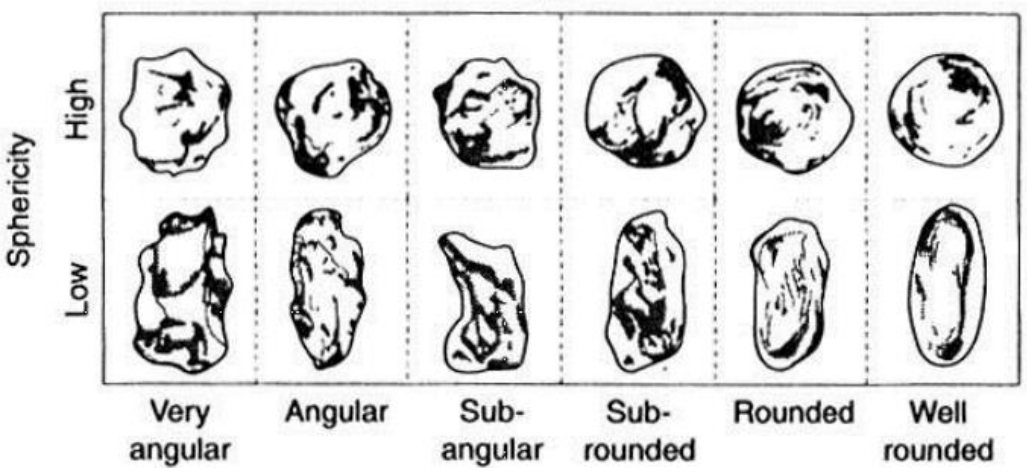

Figure 2.5 Visual Assessment of Particle Shape

Cleanliness is an important attribute when describing aggregates. Cleanliness is typically characterized by the absence of unwanted particles within aggregate mixtures. The more foreign materials there are in the HMA mixture, the more undesirable the mixture is. Some of the more typical unwanted materials are clay lumps, shale, wood, mica, vegetation, soft particles, and even excess dust from the aggregate crushing operation. Different tests, such as the sand equivalent test and plasticity index, can be used to characterize the quantity of harmful materials. Generally, there can be between 0.2 to 10 percent of deleterious particles in asphalt mixtures but the limiting value depends on the exact composition of the contaminant (Asphalt Institute, 2001; Roberts et al., 1996).

Durability is referred to as the ability for aggregates to resist weathering. Aggregates are exposed to extreme environmental conditions such as wetting, drying, freezing and thawing, and sulfate exposure. These aggregates need to be able to resist disintegration after being exposed to these

situations because strength is a huge concern when dealing with HMA mixtures. Most of the aggregates are covered with asphalt binder which prevents moisture getting inside the particles. However, moisture absorption is a key factor that can lead to deterioration so it is important to control and reduce moisture intake. Not only is weathering a big concern, but aging of the materials is also important. Over time, the aggregate particles experience large amounts of weathering so it is critical to account for aggregate stability in order to provide a longer service life. (Roberts et al., 1996).

Aggregate toughness is the ability to resist the damaging effects of loads. Through internal friction, aggregates must transmit, or transfer, the wheel loads from vehicle traffic down to the underlying layers. These aggregates are exposed to crushing, degradation, and disintegration during the stockpiling procedure and must be tough to resist these processes. When mixed with asphalt binder, these aggregates also need to be tough to resist the HMA pavers, rollers, and heavy truck mechanical degradation throughout the life cycle of the material. External vehicle forces have a large effect on the aggregates in HMA mixtures so it is critical for these materials to be able to resist such loads (Asphalt Institute, 2001; Mamlouk & Zaniewski, 2006; Roberts et al., 1996).

Absorption refers to ability for aggregates to capture and store water in the pores or surface voids. There are different moisture conditions of aggregates and these moisture conditions have a large effect on the aggregate properties. Aggregates can be completely dry (all pores empty), air dry (partially saturated but pores are partially filled), fully saturated surface dry (all pores full but no excess water), or wet (excess water) (Figure 2.6). In HMA mixtures, the aggregate absorption is critical because with saturated aggregates the bitumen is unable to act as a binder. Aggregates with higher absorption capabilities are undesirable and uneconomical because of larger amounts of added asphalt cement in these mixtures to bind the aggregates together. However, there also needs to be some asphalt absorption because this allows for proper bonding between the aggregates and asphalt.

Therefore, aggregates in asphalt mixtures should typically be low-absorbing aggregates (Domone & Illston, 2010; Mamlouk & Zaniewski, 2006).

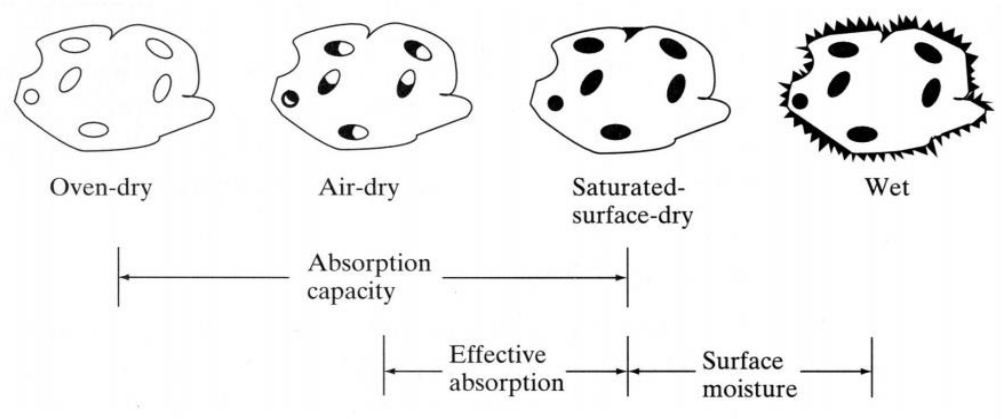

Figure 2.6 Moisture States of Aggregates

2.2.3 Aggregate Gradation

Gradation is referred to as the classification of aggregates based on different sizes. This classification scheme describes the particle size distribution of different aggregate blends. The three main aggregate sizes that are used in asphalt mixture characterization are coarse, fine, and mineral filler materials. In HMA mixtures, large aggregates can be advantageous and more economical because they can provide a better packing orientation and also have less surface area which reduces the amount of binder to coat the aggregates. However, HMA mixtures with large aggregates tend to require more compaction effort which means that they are more difficult to work into place. Therefore, when evaluating the aggregate gradation, it is vital to also evaluate construction considerations and equipment capabilities to ensure proper design (Mamlouk & Zaniewski, 2006).

The American Society for Testing and Materials (ASTM) characterizes aggregates as coarse, fine, and mineral fillers. These particle sizes are categorized based on size requirements. Gradation is evaluated by passing aggregates through different series of sieves and then assessing the aggregates that are either retained on, or passed through the specific sieve size (ASTM C136). The sieve retains

aggregates that are larger than that sieve size, and at the same time passes aggregates that are smaller than that specific sieve size opening. According to ASTM, the No. 4 sieve size (4.75 mm) separates the coarse and fine aggregates. Anything above the No. 4 sieve size (4.75 mm) is considered gravel, boulders, or cobbles, whereas anything below the No. 4 sieve size (4.75 mm) is considered either sand or mineral fillers. Mineral fillers are classified as the portion of the fine aggregates that pass the No. 200 sieve (0.075 mm). Aggregate classification is very important when determining the aggregates that are intended to be used in HMA mixtures.

Particle size distributions are used to classify aggregate mixtures. The different aggregate gradations that can be potentially used are gap-graded, continuously-graded, and uniformly-graded (Figure 2.7). Gap-graded mixtures typically represent aggregate blends that are missing one or more particle size fractions. Uniformly-graded mixtures are those that generally consist of one type of aggregate blend. The mixtures are composed of either small, medium, or large aggregates only. Lastly, continuously-graded aggregate blends have aggregates ranging from small to large in a consistant manner. Typically, continuous gradations produce the best densification arrangement of aggregates because these gradations provide all aggregate types. Using a gap-graded or uniformly-graded aggregate distribution can cause problems because the density and compaction requirements for asphalt mixtures can’t be achieved.

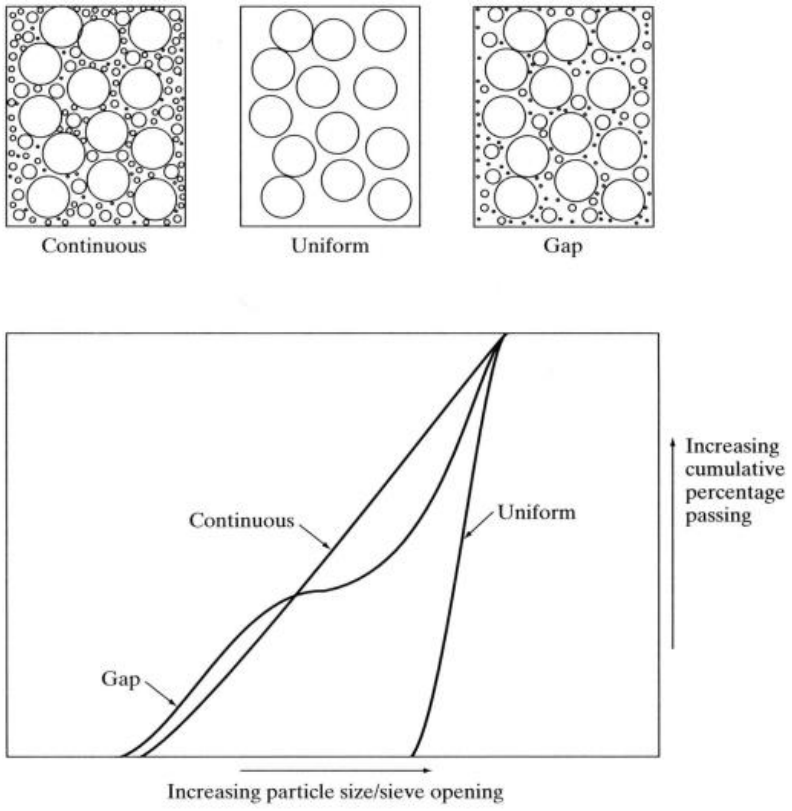

Figure 2.7 Aggregate Gradation Curves (Domone, P., & Illston, J., 2010)

Aggregate gradations in which the void space is a minium (i.e. maximum packing density) are important and these blends are based on continuously-graded mixtures. These type of mixtures develop high strength due to excellent aggregate interlock. Superpave® has developed gradation requirements to ensure that aggregate mixtures meet the specifications. Superpave® uses a 0.45 Power Curve (Figure 2.8) gradation which uses a graphic technique to show the cumulative particle size distribution of the aggregate blend. The vertical axis shows the percent passing of aggregetes and the horizontal axis shows the sieve size. The most important feature of the 0.45 Power Curve is that this curve represents the maximum density gradation achieved by compaction methods (which are different from geometrical random packings). This maximum density curve represents a gradation in which the aggregate particles combine in their densest possible arrangement and this is important to develop interlock and strength in the aggregate mixture (Asphalt Institute, 2001).

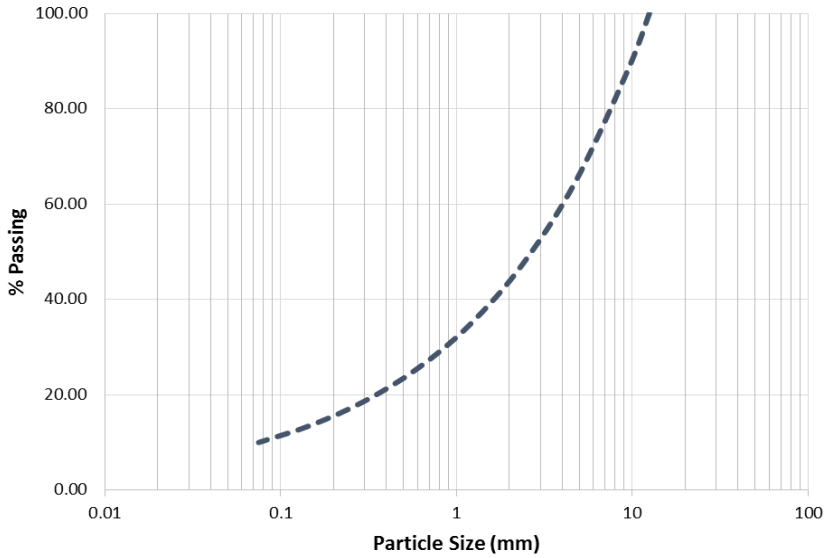

Figure 2.8 Representative 0.45 Power Curve

2.3 SUPERPAVE® ASPHALT MIXTURES

2.3.1 Mixture Behavior

Asphalt pavements cover nearly 93% of the 2 million miles of paved roads in the United States. Asphalt mixtures consist primarily of asphalt binder and aggregates. These two ingredients are mixed together at high temperatures and then compacted while the material is still hot. The asphalt binder acts as a binding material that holds the aggregate particles together. The asphalt mixture glues the aggregate particles into a dense configuration and also provides excellent waterproofing abilities. When the aggregates are combined with the asphalt binder, the aggregates act as a stone framework which provides strength and toughness to the structure. As mentioned before, the overall asphalt concrete performance depends entirely on the pavement design which includes the types of aggregates used as well as the type of asphalt binder that is selected. The objective of asphalt concrete is to provide the following properties (Roberts et al., 1996).

- Workability to reduce the effort of mixing, placing, and compacting

- Resistance to hardening or aging
- Stability and resistance to permanent deformation (rutting resistance) under traffic loads, especially at higher temperatures
- Fatigue resistance to prevent fatigue cracking under cyclic (repeated) loads
- Thermal-cracking resistance that can occur at lower temperatures due to the contraction of the material
- Resistance to moisture damage that can result in stripping of asphalt form aggregate particles

When wheel loads are applied to the pavement, the main stresses that act on the HMA pavement are vertical compressive stress and shear stress within the asphalt layer, as well as horizontal tensile stresses at the bottom of the asphalt layer. This means that the HMA material must be internally strong to resist the compressive and shear stresses to prevent permanent deformation. The material must also be strong in tension to withstand the stresses at the bottom of the asphalt layer as well as resisting cracking and fatigue failures. For cold climates, the material must also be able to resist freeze-thaw cycles which means that the HMA pavement needs to resist rapid decreasing and increasing temperatures. The individual components of HMA are important, but mixtures of HMA need to be analyzed to ensure that both the asphalt binder and the mineral aggregates act together (Asphalt Institute, 2001).

2.3.2 Asphalt Workability

The HMA mixtures are generally hot (115^{o}C-165^{o}C) during the production process which means that the overall viscosity is significantly lower than when the material is at normal (operating) temperatures. When the asphalt binder is mixed with aggregates, the mixture will only be compactable when the asphalt viscosity is within an optimum range. Being able to handle the

material is critical during the construction process. The material needs to be capable of mixing, placing, and compacting without excessive compaction effort. In HMA asphalts, the amount of air in the material is a critical part of evaluating the performance of the material. The optimum asphalt content has been defined by Superpave® as the asphalt content that produces 4 percent air voids at the final design. In general the target air void content is 8 percent which represents the density of the material at the completion of the construction of the asphalt layer. After the construction process, vehicle traffic generally continues to compact the material to some degree. Therefore, in terms of workability, it is critical to develop asphalt mixtures that are easy to mix, place, and compact, but at the same time have the ability to achieve appropriate values of air content (Roberts et al., 1996).

2.3.3 Age-Hardening Resistance

As previously mentioned, age-hardening resistance is a key factor when determining the quality of an HMA mixture. The asphalt material needs to be able to resist the effects of age-hardening which can be correlated to a longer service life. When evaluating the aging of an HMA material it is important to evaluate the mixture by examining both the asphalt binder, and the mineral aggregates acting together, since this is a more realistic approach to pavement analysis. The aggregates are capable of deteriorating throughout the production process, as well as during the life cycle of the HMA pavement. The asphalt binder also evolves during the service life by hardening due to oxidation. This process makes the material stiff and brittle, especially at low temperatures, so this results in crack formation and propagation. The hardening of the material also results in penetration reduction and an increase in the softening point. Reducing the rate at which the asphalt pavement ages also prevents unnecessary repair costs associated with cracking (Domone & Illston, 2010; Roberts et al., 1996).

2.3.4 High-Temperature Permanent Deformation (Rutting)

Rutting in HMA refers to the progressive movements of material under repeated loads which can occur from consolidation or through plastic flow. Rutting results from permanent distortion of the material due to wheel track loading, which is the most common form of permanent deformation. Permanent deformation is described by a surface cross section that is no longer in its original position or location. It is referred to as permanent deformation because this is an accumulation of small amounts of unrecoverable deformation that occur each time a load is applied (Roberts et al., 1996). Figure 2.9 (Asphalt Institute, 2001) and Figure 2.10 shows visual representations of the effects of rutting due to wheel track loading.

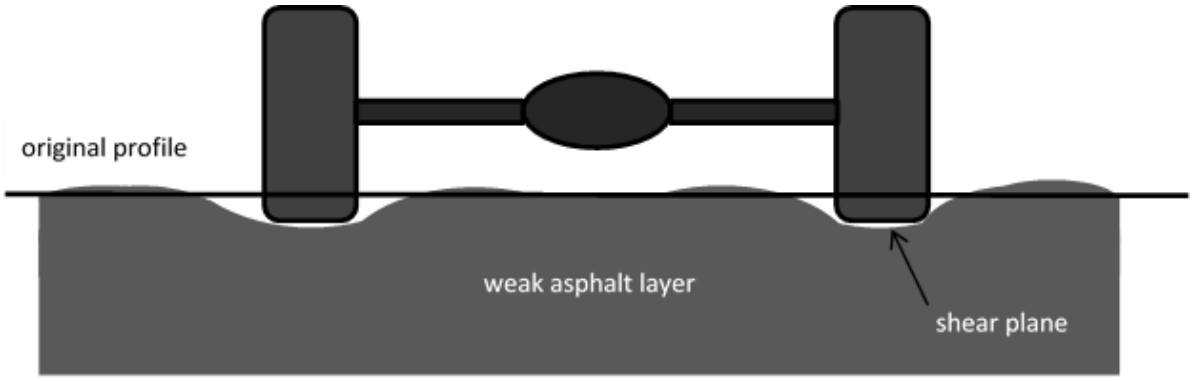

Figure 2.9 Rutting Characteristic of Asphalt Pavement due to Vehicle Loads

Generally, the deformation of the asphalt pavement is the type of rutting that is a major concern to mix designers. Rutting in the HMA layer results from an asphalt mixture with low shear strength required to resist the applied traffic loads. This response can be caused by using high amounts of added asphalt binder as well as poor compaction of the mixture. Using excessive amounts of asphalt binder in a mixture causes the loss of the internal friction between the aggregate particles, and this allows the particles to move more freely. By not compacting the HMA mixture properly, this allows for more air voids to deform during continuous traffic loads. At this point, the wheel loads are then

carried by the asphalt binder rather than the strong aggregate framework. This will result in small amounts of permanent deformations that will form a rut characterized by a downward and lateral movement of the pavement (Asphalt Institute, 2001; Roberts et al., 1996).

Figure 2.10 Rutting Damage Caused by Traffic Loads

In HMA pavement analysis, it is always critical to develop asphalt mixtures that reduce the ability to deform in terms of rutting. Mixtures should not deform when exposed to traffic loading. Rutting can be reduced by using larger aggregate sizes, and more angular and rough texture aggregates to increase particle friction. Stiffer asphalt binders can also be used to resist rutting at higher temperatures. At higher temperatures, when the material becomes less viscous, the resistance to permanent deformation becomes difficult. At this point, the primary strength is provided by the aggregate structure which means that the stone framework needs to be strong. Therefore, selecting appropriate aggregates (types and grades) is vital to the overall strength when it comes to rutting resistance. Binder selection is also important because stiffer asphalt binders can resist permanent deformations (Asphalt Institute, 2001; Roberts et al., 1996).

2.3.5 Intermediate-Temperature Fatigue Cracking

Fatigue cracking refers to failure due to repeated loads at intermediate temperatures. Under repeated cyclic loading, the asphalt pavement fractures under a fluctuating stress which is less than the maximum tensile strength of the material. Fatigue cracking occurs when the applied traffic loads overstress the asphalt material and then cracks form as a result. This damage associated with permanent deformation is typically due to shear distortion or volumetric changes (Perng, 1989). Intermediate longitudinal cracks in the wheel path are typically good indicators that fatigue cracking has occurred. Eventually, these cracks will then join with each other and more cracks will form (alligator cracking), weakening larger and larger sections of the pavement (Finn, Nair, & Hilliard, 1978). Figure 2.11 shows how fatigue cracking has propagated through a large asphalt pavement section.

Figure 2.11 Asphalt Fatigue (Alligator) Cracking

Fatigue cracking can be caused by a number of reasons and different factors depending on the conditions. Some of the factors that can affect fatigue cracking are the asphalt content, air void content, aggregate characteristics, temperature, and traffic (Hartman, Gilchrist, & Walsh, 2001). Asphalt cements that become hard during the aging process also develop poor fatigue characteristics

because these materials become brittle due to the excessive age-hardening. Thin pavement sections and pavement sections with weak underlying layers are vulnerable to fatigue cracking as well since these are exposed to higher deflections under heavy loads. These high deflections cause horizontal stresses at the bottom of the asphalt layer and this will result in fatigue-type failures (Shu, Huang, and Vukosavljevic, 2007).

Typically, fatigue cracking means that the asphalt pavement has sustained the designed amount of traffic loads, and this means the HMA section needs repair which is common. HMA mixtures should not crack when subjected to repeated, cyclic-type, loads over a long period of time but it is inevitable to prevent cracking forever. Fatigue cracking at the end of the pavement service life is expected, but fatigue cracking before the end of the pavement life means that the traffic loads were underestimated in the pavement design. In order to prevent fatigue cracking, designers should extensively evaluate the number of heavy loads during design, use thicker pavements, keep the subsurface dry, use pavement materials not excessively weakened by moisture, and use HMA that is resilient enough to withstand normal deflections. In order to overcome fatigue cracking, the HMA should act as a soft elastic material when loaded and unloaded in tension (Asphalt Institute, 2001).

2.3.6 Low-Temperature Thermal Cracking

A big concern to asphalt pavement designers is low-temperature thermal cracking. Thermal cracking is especially important to evaluate in climates with cold temperatures because these are non-load associated cracks. Thermal cracks are intermittent transverse cracks that are formed when the asphalt material shrinks or contracts due to low temperatures. The tensile stresses within the layer exceed the tensile strength of the material and then the asphalt layer cracks. These thermal cracks can form from a single-cycle of low temperatures or can develop from repeated freezing and thawing cycles (Kandhal, 1978). Figure 2.12 demonstrations the intermittent transverse cracks that were developed from low-temperature cycles.

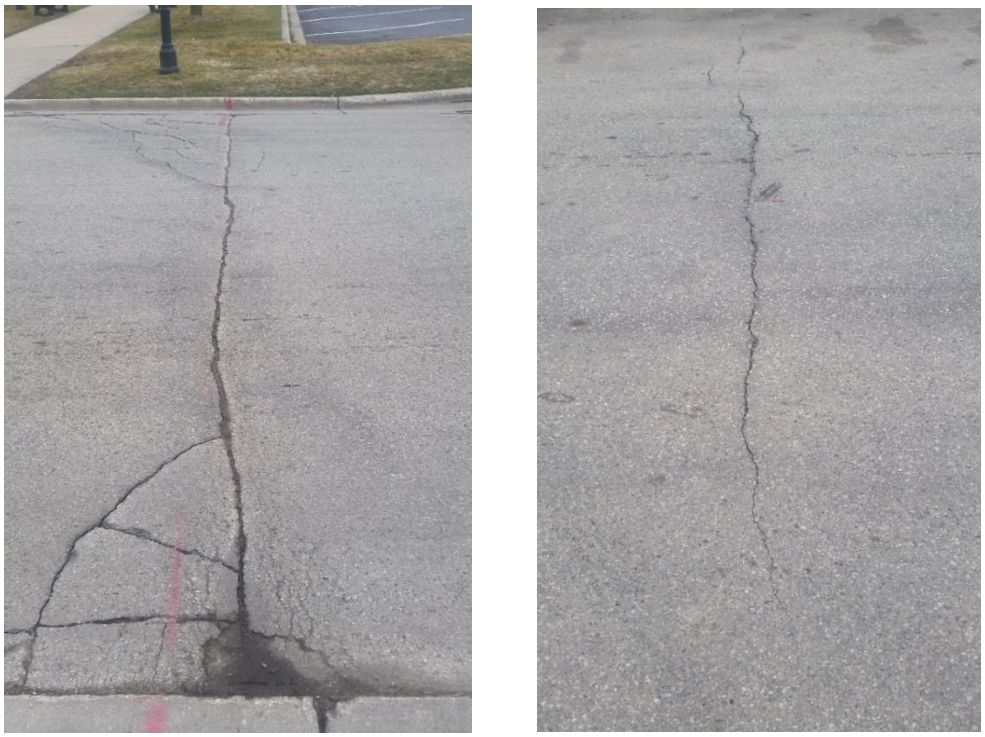

Figure 2.12 Low-Temperature Thermal Cracking

When performing an evaluation on low-temperature conditions, proper asphalt binder selection is the best way to resist thermal cracking. Researchers have recommended that limiting asphalt binder stiffness values in HMA mixtures will reduce the effects of thermal cracking (Fromm & Phang, 1971; Gaw, 1977; Kandhal, 1978, 1980). Asphalt binders that are harder tend to perform worse in low-temperature. Asphalt binders that are excessively aged also have poor performance at lower temperatures because these materials have developed age-hardening due to excessive oxidation. Therefore, mixtures should be designed with soft asphalt binders that are properly aged to minimize effects of low-temperature thermal cracking (Roberts et al., 1996).

2.3.7 Moisture Susceptibility

When exposed to moisture, some HMA mixtures lose the adhesion between the asphalt binder and the surface of the aggregate particles. Asphalt mixtures with high permeability tend to allow

excessive air and water into the material. Once the water is within the asphalt pavement, it can deteriorate the structure by destroying the contact zone with asphalt binder, aggregate particles, or both. Once the materials deteriorate, the bonding between the aggregate and the binder is compromised and the pavement starts to fail. After the bituminous material has been stripped from the aggregates, the overall strength is reduced and this strength loss can lead to rapid distresses. In some cases the asphalt binder can be stripped off the aggregate completely so that the only thing that remains is the bare aggregate particle. In most common cases, however, the strength progressively reduces over time and this strength reduction can lead to rutting and cracking in the wheel path (Domone & Illston, 2010; Mamlouk & Zaniewski, 2006).

There have been many different methods to reduce the moisture damage on asphalt pavements. Some of these methods include increasing the asphalt content, altering the aggregate gradation to reduce the void volumes, using clean the aggregates, and also using higher viscosity asphalt cement (Doyle, 1958; Mamlouk & Zaniewski, 2006). Increasing the asphalt content and altering the aggregate gradation can both reduce the void volume while providing more bituminous material that can bond to the aggregate particles. Additionally, cleaning the aggregates allows for better binding and higher viscosity asphalt resists the urge to strip from the aggregates. Moisture susceptibility is a significant variable when evaluating the overall life expectancy of the asphalt material and it is also essential in HMA design analysis.

2.4 COAL COMBUSTION PRODUCTS (CCPs)

2.4.1 Coal Combustion Product Production

Fly ash materials are the most commonly used pozzolan in civil engineering applications. Fly ash is a by-product of the coal combustion process. Carbon and most volatile materials are burned off by burning pulverized coal in electric power plants, however a significant amount of residual components

pass through the combustion chamber such as aluminosilicates, feldspar, and quartz, and. Upon coal combustion, these minerals fuse, and then the exhaust gases carry the fused materials (fly ash) out of the chamber. The fly ash material then cools down forming spherically shaped particles which can be either hollow or solid. Fly ash typically accounts for about 75 to 85% of the total coal ash, however the remainder of the material is collected as boiler slag or bottom ash. Fly ash can differ depending on the type of mineralogical composition of the coal, degree of coal pulverization, type of furnace and oxidation conditions, and the way the fly ash is collected and handled (Mamlouk & Zaniewski, 2006; Siddique & Iqbal Khan, 2011).

2.4.2 Chemical and Physical Properties

Fly ash particles have a diameter that ranges from 0.1 mm to 1 μm (70 to 90% of fly ash has a diameter less than 45 μm). Fly ash is a unique material in that the material particles are spherical in shape. The small spherical particles can improve the workability and reduce the porosity when mixed with other materials. Figure 2.13 shows a representative fly ash material under the Scanning Electron Microscope (SEM). Fly ash is primarily composed of silica (SiO_2), alumina (Al_2O_3), iron oxide (Fe_2O_3), and lime (CaO). There are different types of fly ash that are readily available. Class F fly ash is defined by ASTM C618 as a fly ash with pozzolan properties. Class C fly ash is defined as fly ash with pozzolan and cementitous properties. Class F fly ash typically has less than 5% CaO but sometimes has up to 10%. Class C fly ash has CaO contents ranging from 15 to 30% CaO (Mamlouk & Zaniewski, 2006).

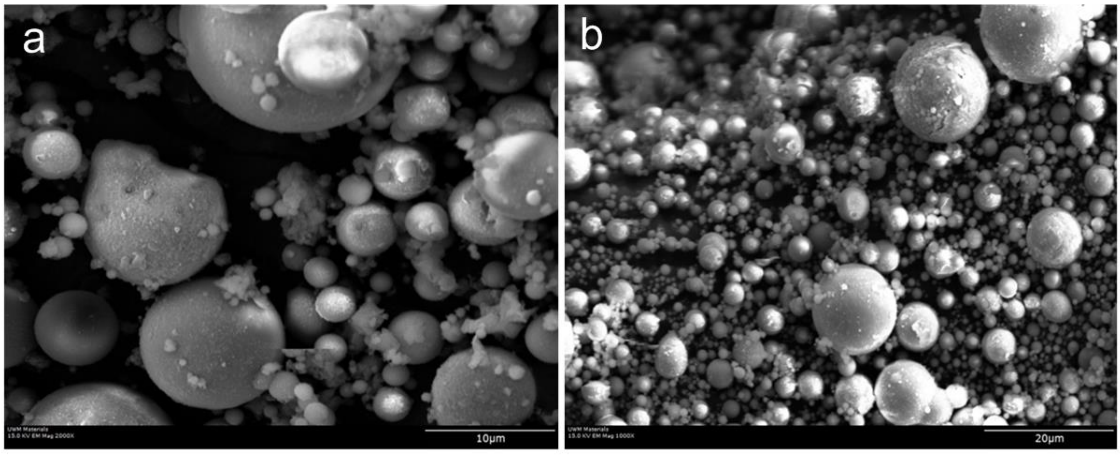

Figure 2.13 Scanning Electron Microscope of (a) Fly Ash F and (b) C (1000x Magnification)

2.4.3 Using Coal Combustion Products

As previously mentioned, Coal Combustion Products (CCPs) are by-products from the coal combustion process. These materials are sometimes disposed of in landfills. Fly ash has beneficial effects when used in certain engineering applications. Using these materials in concrete enhances certain properties such as increasing the overall compressive strength. The American Coal Ash Association (ACAA) came out with a report in 2006 and stated that there has been 72.4 million tons of coal ash produced. Surprisingly, only about 52,608 tons of fly ash was used as mineral fillers in asphalt applications. Other engineering applications that use CCPs can be observed in Figure 2.14 (American Coal Ash Association, 2006).

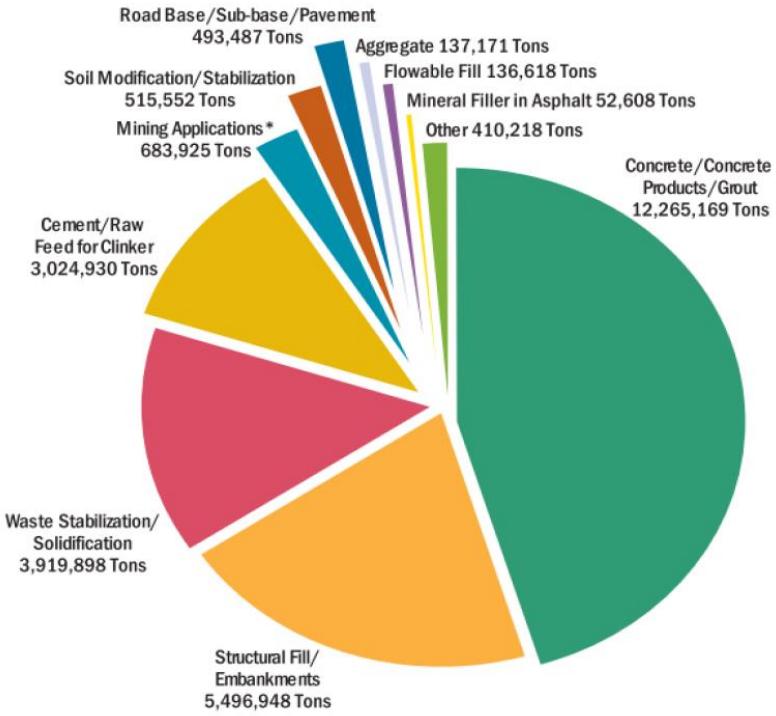

Figure 2.14 Uses of Fly Ash in Civil Engineering Applications

2.4.4 Effect of Fly Ash in Asphalt Mixtures

In the past, mineral fillers have been added to asphalt mixtures were found to improve certain characteristics of the mix. Mineral fillers are defined by ASTM as finely divided mineral matter such as rock dust, slag dust, hydrated lime, hydraulic cement, fly ash, loess, or other suitable mineral matter. In more recent years, CCPs, such as fly ash, was suggested as a mineral filler in asphalt mixtures. Fly ash was used in asphalt mixtures to reduce the asphalt content, increase stability, and improve bond strength between the asphalt binder and the aggregates (Brown, McRae, & Crawley, 1989). In other studies, fly ash was added to HMA mixtures to extend the material service life due to enhanced moisture resistance, rutting resistance, fatigue resistance, low-temperature thermal cracking resistance, aging resistance, and workability (Anderson, Brock & Tarris, 1982).

Adding fly ash to asphalt mixtures has been found to enhance moisture resistance. Resisting moisture damage is critical for asphalt as pavement retains strength when the voids are penetrated with water. In terms of moisture resistance, Carpenter (1952) found that by specimens with Class F fly ash retained great compressive strengths when immersed in water. Zimmer (1970) found that adding fly ash had resulted in improved strength when the specimens were immersed in water. Henning (1974) investigated these effects by using Class C fly ash in asphalt concrete. Adding 4% of fly ash resulted in higher stability and flow, lower air voids, and also improved stability after being immersed in water. Howell, Hudson, and Warden (1952) also found that fly ash was a great filling material in terms of mixing, compacting, material stability, and resistance to water damage.

Researchers have also found that adding fly ash to asphalt has improved the strength. Suheibani (1986) evaluated fly ash as an asphalt extender by using indirect tensile strength, creep and resilient modulus tests. An asphalt extender is a material that can replace asphalt and thus saves asphalt binder. It was found that adding Class F fly ash had improved fatigue life, rut depth resistance, and tensile strength. Goetz, Razi, and Tons (1983) had also evaluated the use of Class F fly ash as an asphalt extender. A full evaluation was developed on moisture damage, thermal cracking, rutting, fatigue life, and asphalt hardening in mixtures. The results of the experiment demonstrated improvements in density and tensile strength, moisture resistance, fatigue resistance, asphalt hardening resistance, and rutting resistance.

Mineral fillers such as fly ash have been found to enhance aging resistance in asphalt mixtures. Aging resistance, which can also be thought of as age-hardening resistance, is an important characteristic in asphalt mixtures because it retains desirable asphalt binder properties. Reducing the age-hardening reduces the stiffness of the material and this is necessary, especially when evaluating fatigue resistance and low-temperature thermal cracking. Faheem and Bahia (2009) performed a study on how aging affects the adhesion and cohesion properties between the asphalt binder and

aggregates. The study proved that adding mineral fillers to the asphalt mixture improved the overall bond strength between the binder and aggregates. Bianchetto, Martínez, Miró, and Pérez (2005) also evaluated aging of asphalt mixtures. By using a direct tension test, the results concluded that using the fillers in the study enhanced aging resistance.

Sobolev et al. (2013) studied the effects that Class C and Class F fly ash has on the performance of HMA mixtures. Workability and constructability were both evaluated by adding fly ash to a Standard Wisconsin mixture. Fly ash was added to different mixtures at quantities of 1 to 3% by weight and 10% by weight of the asphalt binder. Since asphalt binder is the most expensive ingredient in HMA mixtures, this study evaluated the ability of fly ash to extend the asphalt mixture. Sobolev found that adding fly ash to the mixture produced similar compaction efforts when compared to the control mixture, Figure 2.15. For all the mixtures, there were a similar number of gyrations to reach 8% air voids. This is an important result of the study because it proves that fly ash doesn't alter compaction. Therefore, fly ash can be added to asphalt mixtures and this can save money by reducing the binder content of the overall mixture.

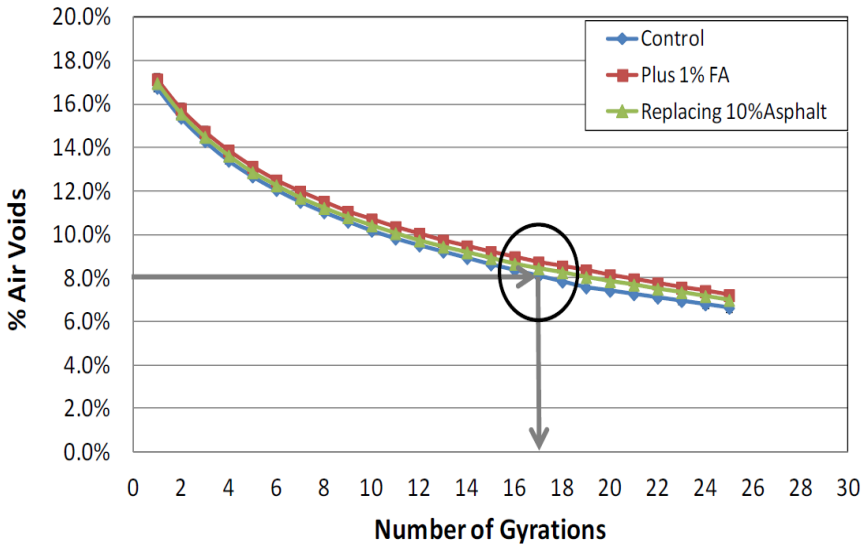

Figure 2.15 Comparison Curves for ASHphalt and HMA Mixtures

Bautista et al. (2015) studied the effects of Coal Combustion Products (CCPs) in asphalt mastics (mixture of asphalt binder and filler materials). The study evaluated different dosages (5, 10, 15, 25, and 40% by volume) of Class C, Class F, and SDA (Spray Dryer Absorber) materials in different Performance Graded asphalt binders. These ASHphalt mastics were then referenced with mastics composed of a limestone filler. Mastics were tested for shear using DSR (Dynamic Shear Rheometer), viscosity using Rotational Viscometer, aging resistance, rutting resistance using MSCR (Multiple Stress Creep Recovery), fatigue resistance using DSR, and thermal-cracking resistance using BBR (Bending Beam Rheometer). The experimental results demonstrated, for all Performance Grades, that many of the mastics performed better than the reference limestone filler. It was demonstrated that adding CCPs to asphalt mastics, especially at larger dosages, enhanced properties such as workability, rutting resistance, recovery, aging resistance, and low-temperature resistance.

CHAPTER 3.

PRELIMINARY STUDY

3.1 MATERIALS AND METHODS

For this research, a preliminary study was conducted to understand the performance of fly ash in asphalt mixtures. In addition to lab investigation, a field study was performed at the We Energies facility in Oak Creek, WI. This preliminary study helped to evaluate the test procedures and methods. This feasibility research evaluates the mix design aspects and compaction differences between a Control HMA mixture and an ASHphalt mixture with 10% binder substitution (by weight) of WE05 Class C fly ash. This section reviews the findings of this preliminary research.

For the preliminary testing, workability was the primary area of focus since constructability is very significant during the construction process. The more effort it takes to compact the asphalt material means the more energy required during the construction process. Since it is always important to evaluate the energy efficiency, the purpose, therefore, was to use a Superpave® Gyratory Compactor to see if substituting fly ash into an asphalt mixture could achieve a similar compaction effort as a Control mixture. Evaluating the densification curves was important to optimize the workability parameters.

3.1.1 Job Mix Formula (JMF)

Superpave® mix design methodology was used to design the JMF (Job Mix Formula) for the road in Oak Creek, WI which is listed in Figure 3.1. Superpave® mix design methodology evaluates binder selection and aggregate selection based on specific requirements to produce optimal asphalt

mixtures. Aggregate grading and asphalt binder performance requirements are necessary when evaluating the asphalt mix design. The JMF mix design specifies the asphalt binder, filler content, aggregate blends, by-product (e.g. RAP), mixing and compacting temperatures, and other miscellaneous volumetric data which will all be discussed individually in this section.

DESIGN NUMBER: 506809 JOB: 40023
PLANT: 40023 MIX TYPE: E-1 MIX TEMPERATURE: 145°C - 134°C
MIX SIZE: 12.5 mm Design ESAL Range (mil.): 0.3 to < 1

Compactive Effort: (Gyrations) Ni: 7 Nd: 60 Nm: 75

Binder Data: GRADE: PG 58-28 SOURCE: CRM Milwaukee Gb: 1.035 RAP Pb: 4.49

AGGREGATE SOURCE DATA

AGG	AGGREGATE	SOURCE	TEST#	LOCATION
AGG #1	FRAP	40023	8-B-09	
AGG #2	5/8" Chip	Prager	38-A-09	W1/2 S7 T4N R19E Racine Co.
AGG #3	3/8" Chip	Prager	39-A-09	W1/2 S7 T4N R19E Racine Co.
AGG #4	MFG'D Sand	Prager	40-A-09	W1/2 S7 T4N R19E Racine Co.
AGG #5	Natural Sand	Bloomfield	30-A-09	SW1/4 S1 and SE1/4 S2 T1N R19E Walworth Co.
AGG #6	Deg	Bloomfield	1	SW1/4 S1 and SE1/4 S2 T1N R19E Walworth Co.

AGGREGATE GRADATION

		Agg #1	Agg #2	Agg #3	Agg #4	Agg #5	Agg #6	JMF	SPECIFICATION MIN	SPECIFICATION MAX
% BLEND		20.0	16.0	12.0	14.0	37.7	0.3			
2	50.0 mm	100.0	100.0	100.0	100.0	100.0	100.0	100.0	0.0	0.0
1-1/2	37.5 mm	100.0	100.0	100.0	100.0	100.0	100.0	100.0	0.0	0.0
1	25.0 mm	100.0	100.0	100.0	100.0	100.0	100.0	100.0	0.0	0.0
3/4	19.0 mm	100.0	100.0	100.0	100.0	100.0	100.0	100.0	100.0	100.0
1/2	12.5 mm	99.4	85.2	100.0	100.0	100.0	100.0	97.5	90.0	100.0
3/8	9.5 mm	94.5	28.2	98.5	100.0	99.2	100.0	86.9	0.0	90.0
#4	4.75 mm	72.1	2.7	23.8	96.4	91.2	100.0	65.9	0.0	0.0
#8	2.36 mm	56.5	2.1	3.2	58.1	81.9	100.0	51.3	28.0	58.0
#16	1.18 mm	44.7	1.9	2.7	31.4	72.3	100.0	41.5	0.0	0.0
#30	0.60 mm	34.8	1.7	2.5	16.7	56.1	100.0	31.3	0.0	0.0
#50	0.30 mm	22.3	1.7	2.4	8.1	17.6	100.0	13.1	0.0	0.0
#100	0.15 mm	15.0	1.6	2.3	3.7	3.9	100.0	5.8	0.0	0.0
#200	0.075 mm	11.8	1.4	2.2	2.4	2.2	100.0	4.3	2.0	10.0
	FAA	42.7	0.0	0.0	47.2	40.5	0.0	42.4		
	Gsb	2.655	2.668	2.642	2.664	2.654	2.654	2.656		

AGGREGATE DATA FOR BLENDED DESIGN JMF

CRUSH 1F/2F: 95.9 / 93.3 Gsb: 2.656 Moist. Absorption: 1.4 L.A. WEAR: 0.0 (100) ELONGATED: 2.6 (5/1)
FAA: 42.4 Gsa: 2.759 Dust Proportion: 0.9 0.0 (500)
SE: 97 Gse: 2.713 Soundness: 0.0 Freeze-Thaw: 0.0

VOLUMETRIC DATA

Point	Added Pb	Total Pb	Gmm	Gmb	Va	VMA	VFB	Unit Wt.	%Gmm Ni	%Gmm Nm	TSR
A	4.0	4.9	2.513	2.365	5.9	15.3	61.4	2359			
B	4.5	5.4	2.495	2.385	4.4	15.1	70.9	2379			
C	5.0	5.9	2.476	2.404	2.9	14.8	80.4	2398			
JMF	4.6	5.5	2.491	2.391	4.0	14.9	73.2	2385	90.8	96.3	82.0
		Corr. Factor:	0.000								TSR N = 16
SPECIFICATION					4.0	14.0	65 - 78		90.5	98.0	

Figure 3.1 Job Mix Formula (JMF) for Feasibility Study in Oak Creek, WI

3.1.1.1 Asphalt Binder

The binder that was selected for this preliminary research was an unmodified PG58-28 binder. This means that this binder has the appropriate physical properties to withstand temperatures as high as 58°C and as low as -28°C. The design temperatures to select asphalt grades are the pavement temperatures rather than the air temperatures. Superpave® specifies the locations of the high temperatures to be at a location 20 mm below the pavement surface, and the low temperature to be at the pavement surface. Regardless, binder selection is always based on climate and traffic conditions in which the asphalt pavement is intended to serve. Most agencies specify the binder grade to be used which can be from the Long-Term Pavement Performance Program (LTPP) or the AASHTO Superpave® program. Since this We Energies project was conducted in Wisconsin, the appropriate Performance Grade was PG58-28 (Asphalt Institute, 2001). The total binder content was 5.5% for this project.

3.1.1.2 Aggregates

Superpave® design methodology specifies the aggregate selection based on combined gradation requirements. These requirements are necessary to ensure proper grading of the aggregates so that there is a more uniform distribution of particle sizes. Using a gap-graded or poorly-graded aggregate distribution can cause problems in some circumstances because the density requirements for the mixture can't be achieved. Other requirements are necessary for aggregate selection such as gradation control points and gradation restricted zones.

3.1.1.2.1 Sieve Analysis

The ASTM C136 is used for conducting a sieve analysis on aggregates. The basis of this test is to pass aggregates through different sieve sizes to determine the percentage of aggregates that were either retained on that specific sieve or that passed through that sieve size. The results are important

to determine the grading (particle size distribution, PSD) of the materials that are to be used in the aggregate blend. This test can be used to ensure that the particle size distribution fulfills the gradation requirements necessary for the specific job.

The procedure for this evaluation is very simple and well-established. The aggregates are first to be dried by being placed in an oven at 110 ± 5^{o}C and then cooled to room temperature. Appropriate sieve sizes are then selected in order to cover all the aggregate sizes in the aggregate blend (common sieve sizes are 37.5, 25, 19, 12.5, 9.5, 4.75, 2.36, 1.18, 0.6, 0.3, 0.15, and 0.075 mm). After recording the weights of each individual sieve, the sieve combinations should be stacked so that the largest opening is on the top and the smallest opening is on the bottom. Once the sieves are stacked, the top sieve should be covered and then all the sieves can be placed on the mechanical shaking machine, Figure 3.2. The criteria for sieving time is that after the completion, not more than 1% of the residue on any sieve will pass that sieve during 1 minute of continuous hand shaking. Once the mechanical sieve shaker has commenced, the weight of each sieve should be recorded and then the weight of the aggregates that were retained on each sieve can be calculated. The percent passing can be calculated from the percent retained. The total weight after sieving should also be compared with the original weight. If the amounts between the two weights differ by more than 0.3%, the results can't be used for acceptance purposes.

Figure 3.2 Mechanical Sieving Machine

For the road in Oak Creek, WI there were six different types of aggregates that were used in the asphalt mixture with the nominal maximum aggregate size of 12.5 mm. The six different types of aggregates used in this blend were Fractioned Reclaimed Asphalt Pavement (FRAP) (contained 0.9% asphalt binder), 5/8" Chip, 3/8" Chip, Manufactured (MFG'D) Sand, Natural Sand, and Baghouse Fines (BF); these are labeled Agg #1, Agg #2, Agg #3, Agg #4, Agg #5, Agg #6, respectively. A particle size distribution plot, Figure 3.3, was developed to understand the individual relationships related to these aggregates (the exact values from the aggregate distributions can be seen in Figure 3.1). This plot also displays the aggregate combination based on the JMF percentages and this combination is then compared to the 0.45 Power Curve. A 0.45 Power Curve is used to evaluate the maximum density gradation for aggregate mixtures. The JMF blend was determined by multiplying the individual components of each aggregate by a specific percentage (Figure 3.1) and then these percentages were

blended together to create a complete aggregate mixture which is represented by the JMF curve in Figure 3.3.

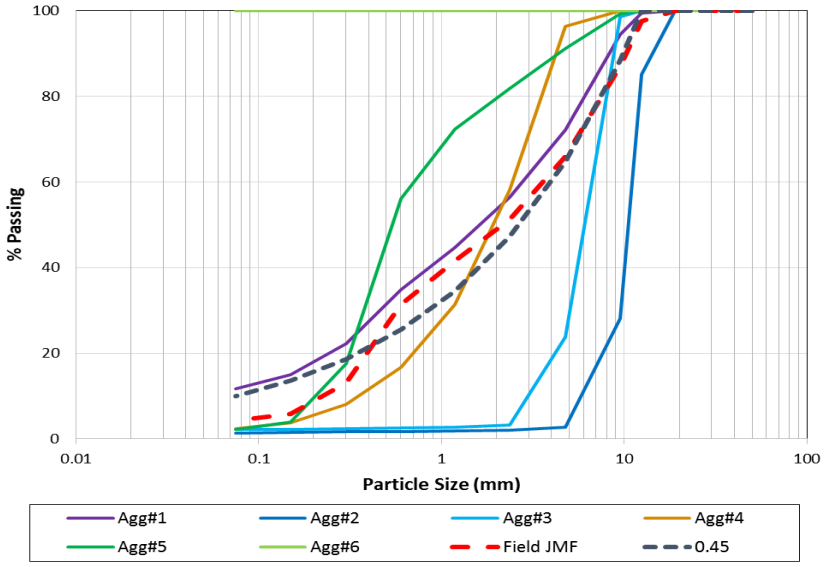

Figure 3.3 Particle Size Distribution for Aggregates Used in Preliminary Study

3.1.1.2.2 Gradation Requirements

Superpave® mix design methodology has established grading limitations for aggregate mixtures based on control points and restricted zones. These limitations are based on the maximum aggregate size and the nominal maximum aggregate size. The maximum aggregate size is defined as the aggregate that is one sieve size larger than the nominal maximum aggregate size. The nominal aggregate size, on the other hand, is defined as the aggregate that is one sieve size larger than the first sieve to retain more than 10 percent. For the investigated JMF blend, the maximum aggregate size is 19.0 mm and the nominal maximum aggregate size is 12.5 mm.

The grading limits can also be analyzed based on the maximum density gradation for the 12.5 mm nominal maximum aggregate size. As previously mentioned, Superpave® uses the 0.45 Power Curve to define the maximum allowable gradation for the aggregates being used. The x-axis corresponds to the sieve size (raised to the 0.45 power) whereas the y-axis comprises the percent passing on the specific sieve size. The maximum density curve, which is the linear line on the 0.45 power graph (Figure 3.4), is believed to represent the densest possible random arrangement of particles.

There are also individual control points (Table 3.1a) which are defined by Superpave® as the maximum and minimum boundaries for the given aggregate blend. These control points evaluate and control the nominal maximum size, an intermediate size, and the smallest size. The restricted zone (Table 3.1b) forms a band through which the gradation should generally not pass through. The restricted zone also prevents a gradation from following the maximum density line (Asphalt Institute, 2001). Since the JMF gradation satisfies the boundary limits, which can be seen in Figure 3.4, the aggregate mixture is a recommended blend.

Table 3.1 Superpave® Requirements for Gradation (a) Control Points (b) Restricted Zone Point

Control Points (% Passing)		
Sieve Size (mm)	12.5mm	
	Min.	Max
19	100	
12.5	90	100
9.5	-	90
4.75	-	-
2.36	28	58
0.075	2	10

(a)

Restricted Zone (% Passing)		
Sieve Size (mm)	12.5mm	
	Min.	Max
0.3	15.5	15.5
0.6	19.1	23.1
1.18	25.6	31.6
2.36	39.1	39.1
4.75	-	-

(b)

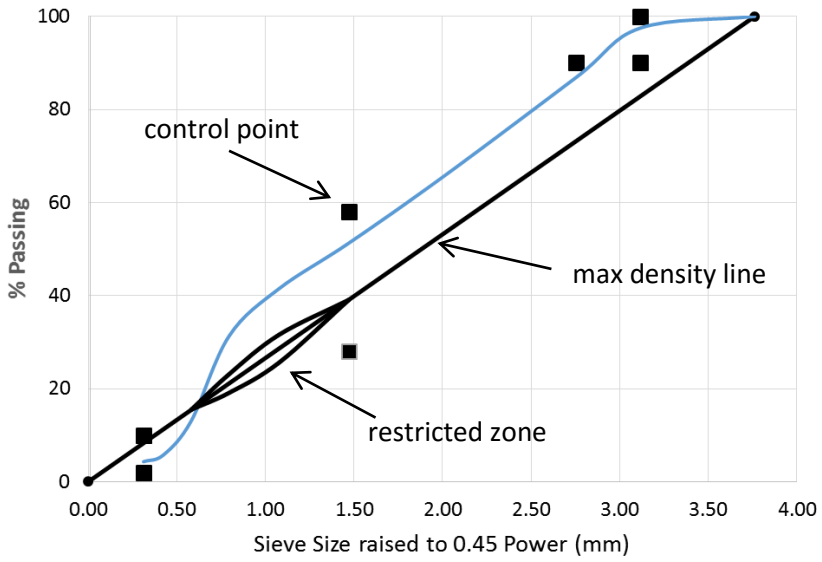

Figure 3.4 Superpave® Gradation Limits for Feasibility Study JMF Combination

3.1.2 Compaction

3.1.2.1 Superpave® Gyratory Compactor

The Strategic Highway Research Program (SHRP) developed the laboratory compaction method with several goals in mind. It was critical to develop a compaction method that was able to produce asphalt samples with realistic densities under realistic pavement climates and loading conditions. The method needed to be able to handle larger aggregate sizes and also be able to measure compactability so that compaction problems could be evaluated. The device needed to output parameters such as a vertically applied pressure, an angle of gyration, and a specimen height over time. The SHRP researchers then developed the Superpave® Gyratory Compactor (SGC) to handle all of these requirements, Figure 3.5.

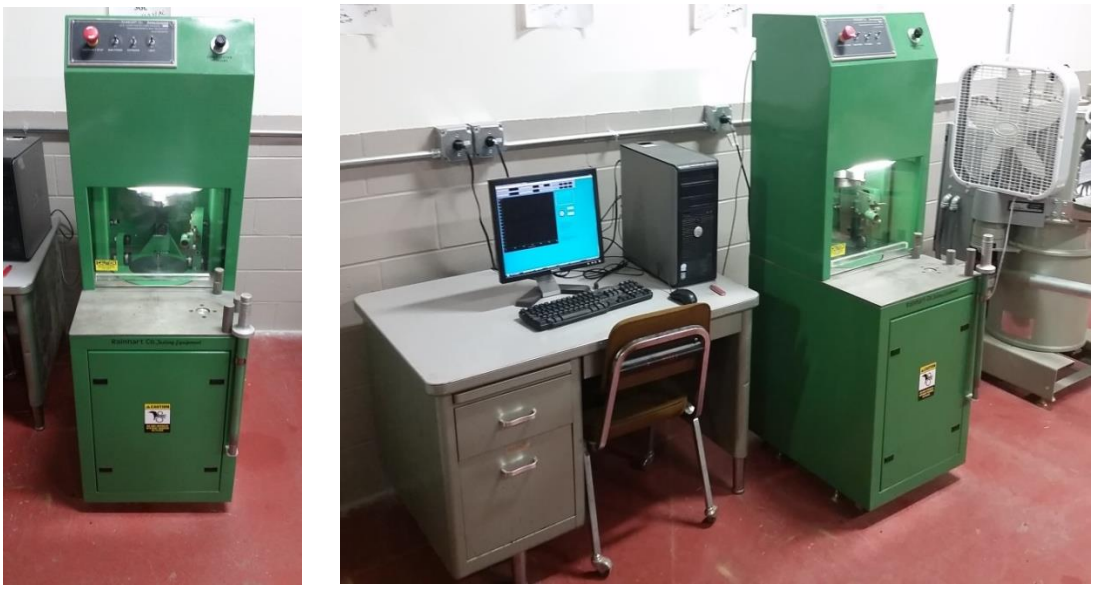

Figure 3.5 Superpave® Gyratory Compactor

The SGC is a piece of equipment that has a base that rotates at 30 rotations, or gyrations, per minute at an inclined angle of 1.25^{o}. The specimen is placed into a compaction mold, Figure 3.6, which is 150 mm in diameter. The loading system applies a load of 600 kPa of compaction pressure on the specimen while the base and compaction rotate together. The computer program then measures the gyration number, the angle, the pressure (kPa), and the specimen height (mm). The specimen height is important to record because the density can be calculated from the values. From these values, the percent air in the material after compaction can also be calculated which is a critical characteristic for asphalt pavements.

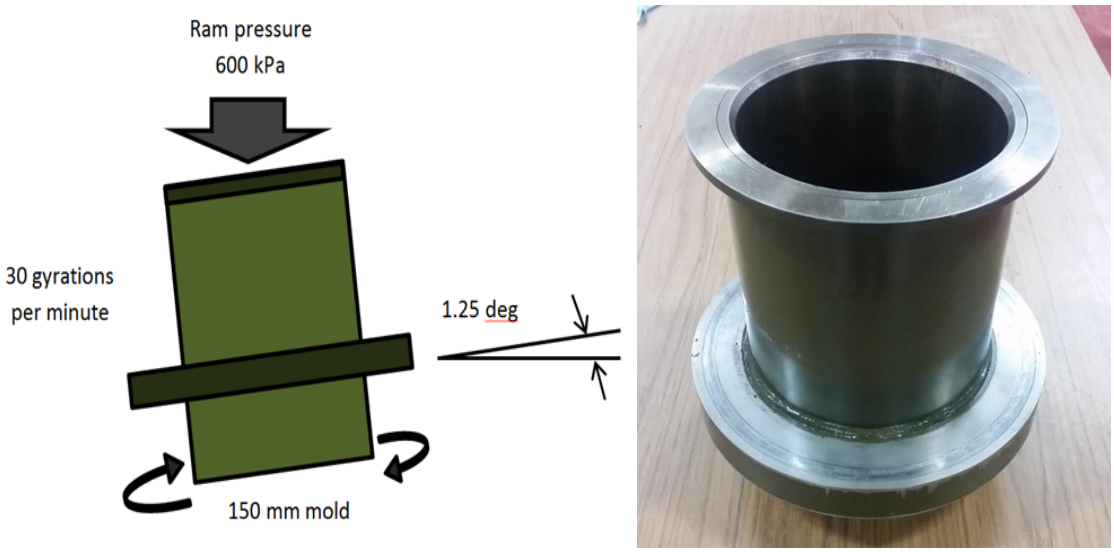

Figure 3.6 Superpave® Gyratory Compactor Mold

Asphalt mixtures are designed for a specific compaction effort. When using a SGC the compaction effort can be directly related to the number of gyrations necessary to achieve the appropriate amount of air voids. In Superpave® these variables can be expressed as the design number of gyrations, N_{des}. N_{des} is the design number of gyrations to achieve the specific compaction effort and a density of the asphalt mix that is expected in the field after the designed amount of traffic. Generally, after N_{des} gyrations, the compacted asphalt specimen will have 4 percent air voids.

The other gyration levels that are important are N_{ini} and N_{max}. N_{ini} is the initial number of gyrations and this is a measure of mixture compactibility. Tender mixtures tend to compact too quickly which is undesirable. At N_{ini} the compacted specimen should generally have about 11 percent air voids. The N_{max} is the maximum number of gyrations that should produce a density that should never be exceeded in the field. At N_{max}, the number of air voids should generally be less than 2 percent. Mixtures with less than 2 percent tend to be more prone to rutting and fracture (Roberts et al., 1996). All values of N_{ini}, N_{des}, and N_{max} are used in the design process as a function of traffic levels and this traffic level is represented by the design ESALs (Equivalent Single Axel Load).

Determining the number of wheel/axel loads a pavement will experience during its life-cycle can be difficult to estimate. The repeated loading and unloading of these wheel/axel forces cause damage to the pavement and there needs to be an estimation of traffic loads when analyzing pavement design. ESALs as used to convert ordinary daily traffic loads to magnitudes and repetitions to mimic a standard number of equivalent loads. A standard axel load of 80.0 kN is used to estimate the pavement performance over its lifetime.

The percentage of air voids is generally expressed in terms of $\%G_{mm}$. The $\%G_{mm}$ is the corrected relative density expressed as a percent of the maximum theoretical specific gravity. For most densification curves, the x-axis is represented by the number of gyrations while the y-axis is represented by $\%G_{mm}$. When evaluating $\%G_{mm}$ it is important to understand that the percentage of air voids ($\%V_a$) is basically 100 minus the $\%G_{mm}$ at that given point. So, if trying to achieve 4% air voids, the $\%G_{mm}$ would be 96%. Figure 3.7 visually represents a densification curve and where certain points such as N_{ini}, N_{des}, and N_{max} should be on the plot (46).

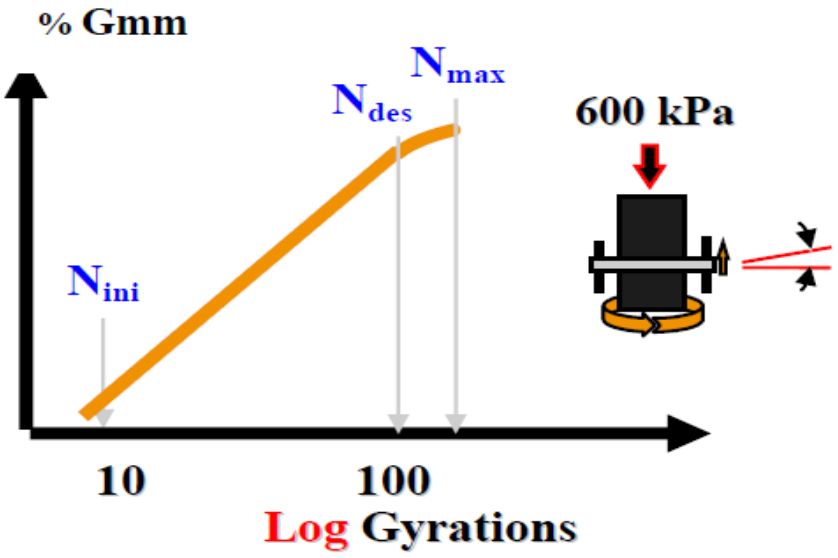

Figure 3.7 Maximum Theoretical Specific Gravity vs. Number of Gyrations (Faheem et al. 2008)

Table 3.2 summarizes the Superpave® compaction efforts and N_{des} characteristic values for different roadway applications. For the Oak Creek project, the number of ESALs that the roadway was designed for was 0.3 to < 1 (mil.), Figure 3.1. For this project N_i was 7, N_d was 60, and N_m was 75. This means that at the road application was designed for medium traffic.

Table 3.2 Superpave® Gyratory Compaction Parameters for Different Roadway Applications

Design ESALs (millions)	Compaction Parameters			Typical Roadway Applications
	N_{ini}	N_{des}	N_{max}	
< 0.3	6	50	75	Very light traffic (local/county roads; city streets where truck traffic is prohibited)
0.3 to < 3	7	75	115	Medium traffic (collector roads; mostly county roadways)
3 to < 30	8	100	160	Med. to high traffic (city streets; state routes; US highways; some rural interstates)
≥ 30	9	125	205	High traffic (most of the interstate system; climbing lanes; truck weighing stations)

The AASHTO T312-12 procedure was followed for compacting the asphalt samples using a Rainhart Co. Superpave Gyratory Compactor (SGC). The compaction mold and base plate were placed in the oven and preheated at the required compaction temperature for a minimum of 30 minutes prior to the beginning of the compaction. The Control mixtures and the ASHphalt mixtures were both compacted at 140^{o}C (all of the asphalt mixtures for the feasibility study came directly from the Oak Creek job site which means that these were industrial mixtures of aggregates, fillers, and asphalt binder). Approximately 4700 g of asphalt material was used for compaction and this was necessary when determining the bulk specific gravity. Approximately 1500 g of asphalt material was used as a loose mixture to determine the maximum specific gravity.

Once the compaction temperature was achieved, the mold and base plate were removed from the oven and a paper disk was placed at the bottom of the mold. The mixture was placed into the mold in one lift, then it was leveled, and then another paper disk was placed on top of the material inside the mold. The charged mold was placed into the gyratory compactor and centered beneath the ram. A pressure of 600 ± 18 kPa was applied to the specimen at an angle of 1.25°, while the rotating base spun at a constant 30 gyrations per minute. The Superpave Gyratory Compactor recorded the exact height, pressure, and angle of the compacted sample for each gyration (as these parameters are used for developing the compaction densification curve).

For the feasibility study, 60 gyrations were used to effectively analyze the entire compaction curve. Once the test was completed, the angle was removed from the mold as well as the ram pressure and then the ram was retracted from the mold. The specimens were then extruded from the mold and the paper disks were also removed. The same procedure was used when compacting the duplicate sample. The compacted specimen (Figure 3.8a) was important for evaluating the bulk specific gravity and the loose mixture (Figure 3.8b) was important for evaluating the maximum specific gravity.

(a) (b)

Figure 3.8 Representative Asphalt Samples for (a) Bulk Specific Gravity and (b) Max Specific Gravity

3.1.2.2 Asphalt Mixture Volumetrics

3.1.2.2.1 Aggregate Volumetrics

There are many different volumetric parameters of aggregates that are important to understand and evaluate asphalt mixtures. The basis of these calculations is reported in Figure 3.9 (13).

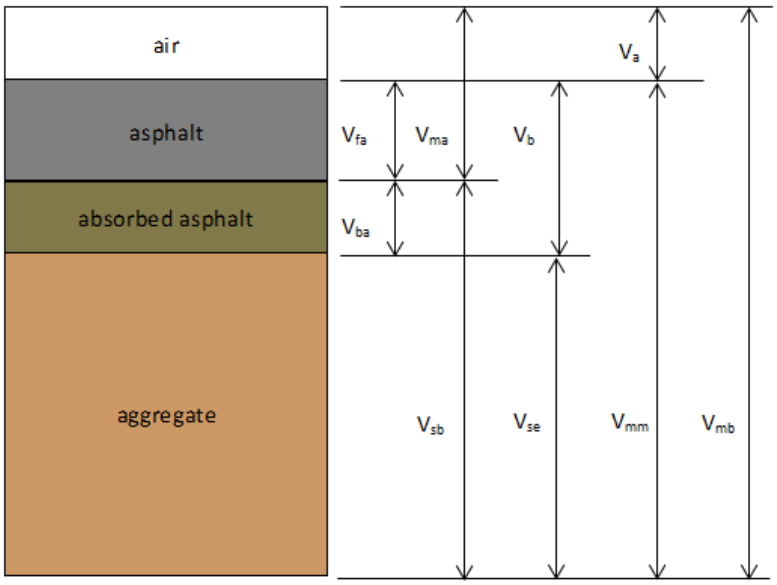

Figure 3.9 Component Diagram of Compacted HMA Specimen

%VMA = Volume of voids in mineral aggregate;

$\%V_{mb}$ = Bulk volume of compacted mix;

$\%V_{mm}$ = Voidless volume of paving mix;

%VFA = Volume of voids filled with asphalt;

$\%V_a$ = Volume of air voids;

$\%V_b$ = Volume of asphalt;

$\%V_{ba}$ = Volume of absorbed asphalt;

$\%V_{sb}$ = Volume of mineral aggregate (by bulk specific gravity);

$\%V_{se}$ = Volume of mineral aggregate (by effective specific gravity).

Aggregates in asphalt mixtures can absorb both water and asphalt binder. The most critical variables when evaluating aggregate and binder interactions is the volume of voids in the mineral aggregates, the volume of air voids in the mixture, and the volume of voids filled with asphalt. These parameters affect bonding strength as well as the coating film thickness and these are directly related to overall strength as well as moisture damage resistance.

3.1.2.2.2 Determination of G_{mm} and G_{mb}

The ASTM D6857/D6857M-11 procedure was used to determine the maximum specific gravity (G_{mm}) of the mixtures using a vacuum sealed material method and ASTM D6752/D6752M-11 specification was used to determine the bulk specific gravity (G_{mb}) of the mixtures using a vacuum sealed material method. After the asphalt mixtures were heated for both cases the samples were then cooled down for 16 ± 1 h at room temperature (AASHTO R30-02). Once the samples were cooled, the InstroTek CoreLok vacuum machine was used for the test, Figure 3.10.

Figure 3.10 InstroTek CoreLok Machine used to Determine G_{mm} and G_{mb}

For the maximum specific gravity, the loose rice samples were evenly spread out onto a pan and the particles were separated, taking care to avoid fracturing the aggregates. The particles of the fine

aggregate portion were broken up so that the aggregate size was not larger than 6.3 mm. The bags, along with the asphalt mixture, were weighed. The sample was then placed into the CoreLok machine and the air was vacuumed out. Once the machine stopped, the sealed sample was submerged in water and the sealed bag was then cut across the top for water to enter. The bags were opened by hand in order to allow water to enter the bags completely and then the sample was weighed again. By using the CoreLok computer program, the G_{mm} was calculated directly.

For the bulk specific gravity, once the compacted sample was cooled, it was then weighed. The sample was then placed into a bag and placed into the CoreLok machine in order to remove the air from the chamber and bag. The sealed sample was removed from the CoreLok machine once the test was completed and then the sealed sample was weighed underwater. After the scale stabilized the weight was recorded. It was important to reweigh the sample, without the bag, out of water to ensure that no water had entered the bag while it was submerged. By using the CoreLok computer program, G_{mb} was calculated directly.

Using both G_{mm} and G_{mb} values, the $\%G_{mm}$ could be calculated based on the equation below. With this calculation, it is important to understand that 100% minus the $\%G_{mm}$ is the percent air in the mixture. This is a very important relationship.

$$\%G_{mm} = \frac{G_{mb}h_m}{G_{mm}h_x} * 100\% \qquad \text{Eq. 3.1}$$

where:

$\%G_{mm}$ = corrected relative density expressed as a percent of the maximum theoretical specific gravity;

G_{mb} = bulk specific gravity of the extruded specimen;

G_{mm} = max specific gravity of the of the mix;

h_m = height of the extruded specimen (mm);

h_x = height of the specimen after x gyrations (mm).

3.1.2.2.3 Volumetric Calculations of Asphalt Mixtures

In order to properly analyze the compacted paving mixture it was important to evaluate and calculate volumetric parameters of the mixture. The equations below were used to evaluate the mixture based on Superpave® protocol.

3.1.2.2.3.1 Bulk Specific Gravity of Aggregates

$$G_{sb} = \frac{P_1 + P_2 + \cdots + P_N}{\frac{P_1}{G_1} + \frac{P_2}{G_2} + \cdots + \frac{P_N}{G_N}} \quad \text{Eq. 3.2}$$

where:

G_{sb} = bulk specific gravity for the total aggregate;

P_1, P_2, P_N = individual percentages by mass of aggregate;

G_1, G_2, G_N = individual (e.g. coarse, fine) bulk specific gravity of aggregates.

3.1.2.2.3.2 Effective Specific Gravity of Aggregate

$$G_{se} = \frac{P_{mm} - P_b}{\frac{P_{mm}}{G_{mm}} - \frac{P_b}{G_b}} \quad \text{Eq. 3.3}$$

where:

G_{se} = effective specific gravity of aggregate;

G_{mm} = maximum specific gravity of paving mixtures (no air voids);

P_{mm} = percent by mass of total loose mixture = 100;

P_b = asphalt content, percent by total mass of mixture;

G_b = specific gravity of asphalt.

3.1.2.2.3.3 Asphalt Absorption

$$\%P_{ba} = 100\% * \frac{G_{se}-G_{sb}}{G_{sb}*G_{se}} * G_b \quad \text{Eq. 3.4}$$

where:

$\%P_{ba}$ = absorbed asphalt, % by mass of aggregate;

G_{se} = effective specific gravity of aggregate;

G_{sb} = bulk specific gravity of aggregate;

G_b = specific gravity of asphalt.

3.1.2.2.3.4 Effective Asphalt Content

$$\%P_{be} = P_b - \frac{P_{ba}}{100} * P_s \quad \text{Eq. 3.5}$$

where:

$\%P_{be}$ = effective asphalt content, % by total mass of mixture;

$\%P_b$ = asphalt content, % by total mass of mixture;

$\%P_{ba}$ = absorbed asphalt, % by mass of aggregate;

$\%P_s$ = aggregate content, % by total mass of mixture.

3.1.2.2.3.5 Voids in Mineral Aggregate (VMA)

$$\%VMA = 100 - \frac{G_{mb}*P_s}{G_{sb}} \quad \text{Eq. 3.6}$$

where:

VMA = voids in the mineral aggregate, % of bulk volume;

G_{sb} = bulk specific gravity of total aggregate;

G_{mb} = bulk specific gravity of compacted mixture;

$\%P_s$ = aggregate content, % by total mass of mixture.

3.1.2.2.3.6 Percent Air Voids

$$\%V_a = 100 * \frac{G_{mm} - G_{mb}}{G_{mm}} \quad \text{Eq. 3.7}$$

where:

%Va = air voids in compacted mixture, % of total volume;

Gmm = maximum specific gravity of paving mixture;

Gmb = bulk specific gravity.

3.1.2.2.3.7 Voids in the Mineral Aggregate Filled with Asphalt (VFA)

$$\%VFA = 100 * \frac{VMA - V_a}{VMA} \quad \text{Eq. 3.8}$$

where:

%VFA = voids filled with asphalt, % of VMA;

%VMA = voids in the mineral aggregate, % of bulk volume;

%Va = air voids in compacted mixture, % of total volume.

3.1.2.2.3.8 Powder/Dust Proportion (Dust-to-Binder Ratio)

$$DP = \frac{P_{0.075}}{P_{be}} \quad \text{Eq. 3.9}$$

where:

$P_{0.075}$ = aggregate content passing the 0.075 mm sieve, percent by mass of aggregate;

P_{be} = effective asphalt content, percent by total mass of mixture.

After calculating these values, comparisons were then made with the Superpave® limitations in Table 3.3 (13). This table reports on limitations for the voids in the mineral aggregate (VMA), voids filled with asphalt (VFA), and a dust-to binder ratio. When evaluating the mixture, comparisons were evaluated by using a nominal maximum aggregate size of 12.5 mm.

Table 3.3 Superpave® Volumetric Mixture Design Requirements

Design ESALs (millions)	Required Density (% of Theoretical Maximum Specific Gravity			Voids-in-the Mineral Aggregate (Percent), minimum					Voids Filled With Asphalt (Percent)	Dust-to-Binder Ratio
				Nominal Maximum Aggregate Size, mm						
	N_{ini}	N_{des}	N_{max}	37.5	25.0	19.0	12.5	9.5		
< 0.3	≤ 91.5	96.0	≤ 98.0	11.0	12.0	13.0	14.0	15.0	70 - 80	0.6 - 1.2
0.3 to < 3	≤ 90.5								65 - 78	
3 to < 30	≤ 89.0								65 - 75	
≥ 30										
* Design ESALs are the anticipated project traffic level expected on the design lane over a 20-year period.										

3.2 RESULTS OF THE PRELIMINARY STUDY

The compaction results from the preliminary study demonstrated that the compaction effort for mixtures with 10% WE05 Class C fly ash was higher than the Control mixtures. Figure 3.13 reports on a visual representation of the densification curve for the Control mixtures and the ASHphalt mixtures. Since the ASHphalt mixtures had 10% (by weight) of the total asphalt binder substituted with fly ash, and at the same time the temperature was constant, these results make sense. More binder allows for better workability while also reducing the amount of air content.

Table 3.4 Preliminary Study Measured Volumetrics

Mixture	WE05 C 10% (140C)	CONTROL (140C)
Gmb	2.391	2.389
Gmm	2.497	2.483
Gmb/Gmm	0.958	0.962
Gsb	2.658	2.658
Gse	2.724	2.724
Gb	1.030	1.030
Pba (%)	0.939	0.939
Pb (%)	4.950	5.500
Ps (%)	95.050	94.500
Pbe (%)	4.058	4.613
VMA (%)	14.5	15.1
Va (%)	4.2	3.8
VFA (%)	70.9	74.9
Dust-to-Binder Ratio	1.0	0.8

Table 3.4 demonstrates the bulk specific gravity and the maximum specific gravity values for all the samples. The Maximum specific gravity of the ASHphalt mixtures was higher than the Control mixtures since fly ash has a higher specific gravity than asphalt binder. Even though the bulk specific gravity is similar, the ratio of G_{mb}/G_{mm} proves that the maximum densification is going to be less since G_{mb} is higher for ASHphalt mixtures (i.e. there will be more air voids for the ASHphalt mixture).

Table 3.4 also reports on the evaluation parameters that need to be compared to Table 3.3. Variables such as %VMA (voids in the mineral aggregate), %VFA (voids filled with asphalt), and the dust-to-binder ratio which are all compared to the Superpave® design requirements. Based on the 12.5 mm nominal maximum aggregate size, the %VMA for both mixtures is above 14%, the %VFA for both mixtures is between 65 and 78%, and the dust-to-binder ratio for both mixtures is between 0.6

and 1.2. All of the parameters correlate to the Superpave® design requirements which means that the JMF for the Oak Creek project was a very good mix design.

Figure 3.11 reports on the densification curve and it is obvious that the ASHphalt mixture with 10% WE05 Class C fly ash substitution needs more compaction effort to compact the material (i.e. the material is stiffer). The reason for this is due to the reduction in binder content. Interestingly enough, though, the plot demonstrates that the ASHphalt mixture requires less compaction effort at the beginning of the compaction process but then tapers off quickly and the densification curve related to the Control mixture passes the ASHphalt mixture. The final %Gmm for the Control mix was 96.21% Gmm (3.79% air voids) and was 95.77% Gmm (4.23% air voids) for the ASHphalt mix. These are very reasonable values in terms of compaction effort.

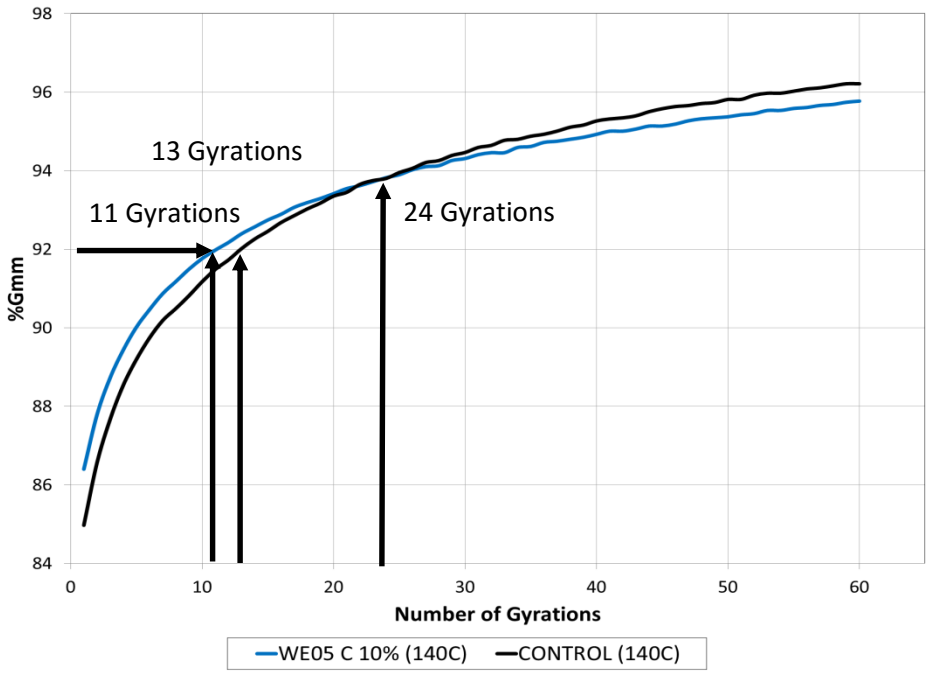

Figure 3.11 Preliminary Study Densification Curve

With the conclusion of the preliminary study, it seems realistic that adding 10% fly ash (by weight) to asphalt mixtures can allow for similar compaction efforts. In some cases, the compaction

temperature for the ASHphalt mixtures can be increased (making the material less viscous) to allow for improved compaction effects. Increasing the compaction temperature for the ASHphalt mixtures, while keeping the Control compaction temperature constant, could possibly provide better results for compaction. ASHphalt mixtures prove to be stiffer during compaction, but this could also provide for better resistance to fatigue and low-temperature testing. These parameters will all be evaluated in the thesis research study.

CHAPTER 4.

MATERIALS AND TESTING METHODS

The results of the laboratory feasibility study were obtained before this section to evaluate the workability performance of ASHphalt mixtures. The sections forth provide a full evaluation of a new mix design, different aggregate blends, new asphalt binder, and different fly ashes. The materials and methods are similar but not exactly the same unless verified. A more extravagant evaluation is developed based on different testing methods such as aggregate coating, workability performance, aging resistance, moisture damage resistance, fatigue resistance, and low-temperature thermal cracking resistance.

4.1 MATERIALS

4.1.1 Asphalt Binder

Asphalt binder selection was based on environmental conditions as well as traffic conditions which were similar to the We Energies project. The feasibility study used an unmodified PG58-28 asphalt binder. In this research, the asphalt binder that was used was also an unmodified PG58-28. Again, this means that the binder in this study possessed adequate physical properties up to at least 58^{o}C. This is the high pavement temperature that this binder can serve at. The second number refers to the low temperature grade which means that the binder used in this study could be used down to at least -28^{o}C. Figure 4.1 shows a representative bucket of PG58-28 binder that was used for this research.

Figure 4.1 PG58-28 Asphalt Binder

4.1.2 Aggregates

There were five different types of aggregates used in this blend: 12.5 mm (material retained on 12.5 mm sieve), 9.5 mm (material retained on 9.5 mm sieve), 4.75 mm (material retained on 4.75 mm sieve), Manufactured (MFG'D) Sand, and Natural (N) Sand. The maximum aggregate size is defined as 19.0 mm, and the nominal maximum aggregate size is 12.5 mm. The 12.5 mm, 9.75 mm, and 4.75 mm aggregates were separated by using larger sieves and manually shaking since this reduced sieving time by quite a bit. FRAP (Fractioned Reclaimed Asphalt Pavement) was not used in this aggregate blend because it was important to blend the existing aggregates together without reducing the asphalt binder content. By adding FRAP material, the total added asphalt binder content is reduced by 0.9% (the amount retained by the FRAP material). This study focused on comparing ASHphalt mixtures to Control mixtures rather than evaluating the complete mix design in too much depth. For this reason, FRAP material was not used. Figure 4.2 shows the five types of aggregates that were used in this study.

Figure 4.2 Aggregate Types Used in this Study

A particle size distribution plot, Figure 4.3, was developed in accordance with ASTM C136 to understand the individual relationships associated with these aggregates. This plot displays the 0.45 Power Curve as a representative curve, as well as the Field JMF curve which is the same as the Field JMF curve in the feasibility study. The objective was to combine the five aggregates, shown above, so that there was minimum deviation between the Combination curve and the Field JMF curve. The Field JMF particle size distribution used Superpave® protocol to develop the aggregate combination so it was critical to evaluate our mixtures based on the Field JMF curve.

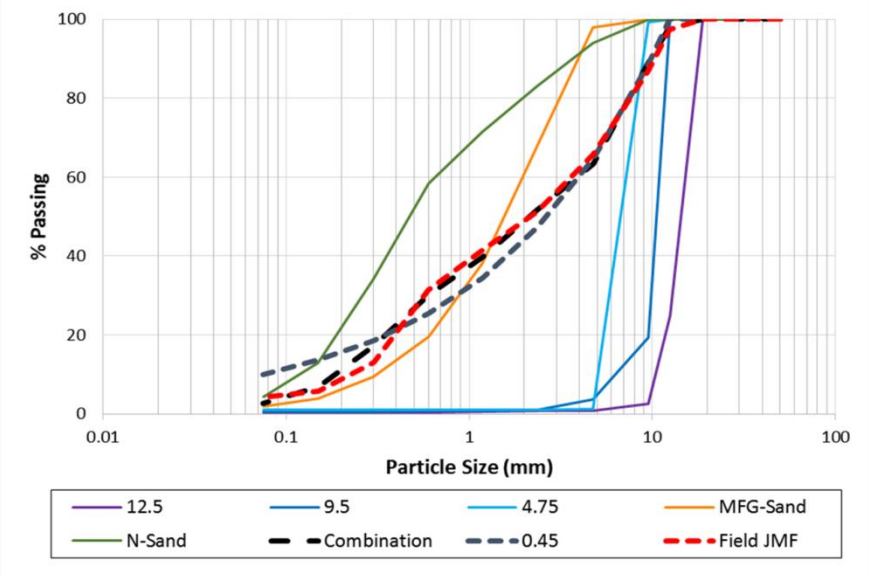

Figure 4.3 Particle Size Distribution Plots

By combining the five aggregates according to the blend percentages shown in Table 4.1, a very similar curve to the Field JMF curve was developed as shown by the Combination curve. Table 4.1 also shows the comparisons between the actual values from the Combination particle size distribution and the Field JMF particle size distribution. These two curves are very similar to each other, and this was important when evaluating the aggregate mix design.

Table 4.1 Aggregate Blend Evaluation based on Field JMF Combination

	Aggregate Type							
	12.5mm	9.5mm	4.75mm	MFG-Sand	Nat-Sand			
	Blend (%)							
Sieve Size (mm)	2.50	10.60	21.00	22.70	43.20	Combination	0.45	Field JMF
50	100.00	100.00	100.00	100.00	100.00	100.00	100.00	100.00
37.5	100.00	100.00	100.00	100.00	100.00	100.00	100.00	100.00
25	100.00	100.00	100.00	100.00	100.00	100.00	100.00	100.00
19	100.00	100.00	100.00	100.00	100.00	100.00	100.00	100.00
12.5	24.90	100.00	100.00	100.00	100.00	98.12	100.00	97.50
9.5	2.60	19.35	99.38	100.00	100.00	88.89	88.38	86.90
4.75	0.78	3.73	1.18	98.06	93.93	63.50	64.70	65.90
2.36	0.75	1.05	1.10	68.10	83.10	51.72	47.23	51.30
1.18	0.68	0.71	1.10	38.21	71.42	39.85	34.57	41.50
0.6	0.25	0.71	1.10	19.67	58.44	30.02	25.50	31.30
0.3	0.25	0.68	1.10	9.34	34.22	17.21	18.67	13.10
0.15	0.25	0.65	1.10	3.82	13.02	6.80	13.67	5.80
0.075	0.25	0.61	0.98	1.87	4.40	2.60	10.00	4.30

Even though the Combination particle size distribution looked similar to the JMF Field particle size distribution and has little deviation, it was still critical to evaluate the Superpave® gradation limits. Figure 4.4 shows the gradation limits with the Combination particle size distribution. As seen from this figure, the 0.45 Power Curve represents the maximum density line where the particles fit together in the densest possible arrangement. The Combination particle size distribution line is within all the control points which is required since the control points function as extreme ranges through which gradation must pass. Lastly, the Combination curve does not pass through the restricted zone which

means that the mixture is not over-sanded. This also means that the gradation veers from the 0.45 Power Curve which allows the asphalt mixture sufficient room for durability and adequate VMA.

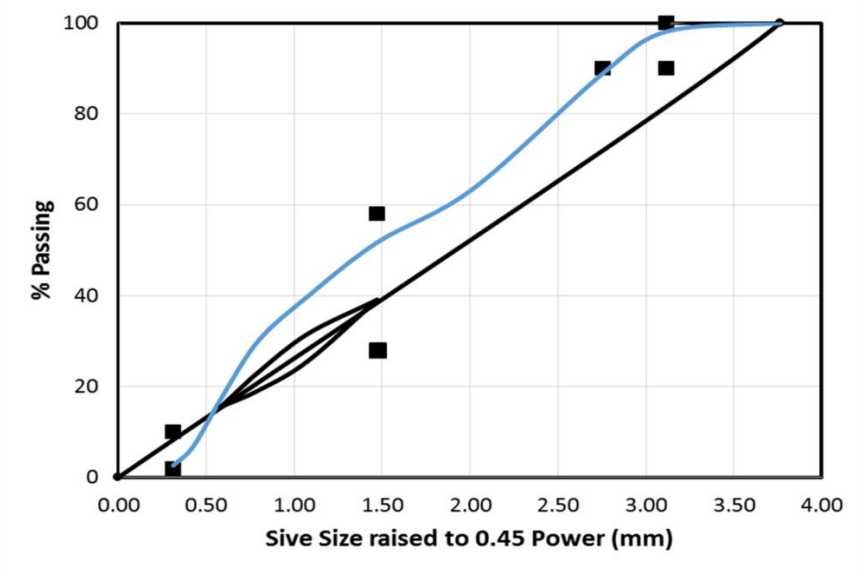

Figure 4.4 Superpave® Gradation Limits

4.1.3 Coal Combustion Products (CCPs)

In this research there were four types of representative Coal Combustion Products (CCPs) that were used: WE05 Class C, TA11 Class F, LG14 Class F, and SF15 SDA (Spray Dryer Absorber). These materials were evaluated based on physical and chemical properties which are important when differentiating them. ASTM D5550 was followed to determine the specific gravity by using the Helium Pycnometer, ASTM D4464 was followed to determine the particle size distribution, surface area, and fineness modulus by using Laser Light Scattering equipment, and ASTM E986 was followed to determine the particle shape by using the Scanning Electron Microscope (6).

4.1.3.1 Physical Properties

As previously mentioned there are four types of Coal Combustion Products (CCPs) used in this research, Figure 4.5. These fly ashes range in physical type, color, and even size. The most important

physical properties, though, are the particle size distributions, specific gravity, surface area, and the fineness modulus. These physical characteristics were all analyzed to evaluate which had the largest effect on the results.

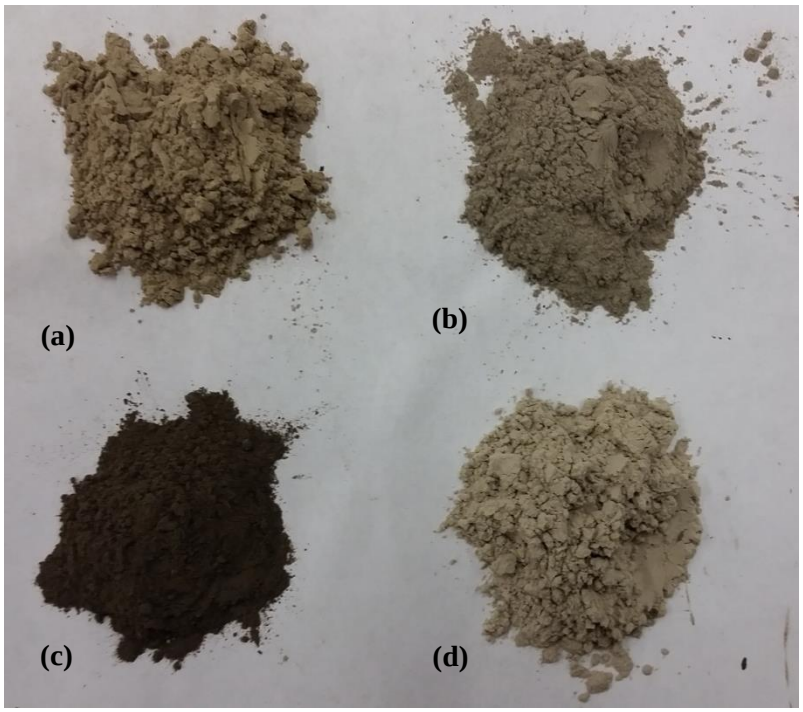

Figure 4.5 Fly Ash Samples (a) WE05 (b) TA11 (c) LG14 (d) SF15

The particle size distribution, fineness modulus, surface area, and fineness modulus were all evaluated by using Laser Light Scattering equipment in accordance to ASTM D4464. As seen from the particle size distribution, Figure 4.6, the WE05 Class C fly ash had the smallest particle size (maximum size range of 30 to 50 µm) which means that the surface area is the largest (925.13 m^2/kg). On the other hand, the TA11 and LG14 Class F fly ashes had the largest particles (TA11 maximum size range of 150 to 200µm and LG14 maximum size range of 50 to 60µm) and this means that the surface area for these particles is the smallest (466.18 and 267.48 m^2/kg). The SF15 SDA material had an overall average particle size distribution (maximum size range of 25 to 35 µm) which provided an average

surface area (610.30m^2/kg). After developing the particle size distribution plots, fineness modulus values were calculated along with D10, D50, and D90 values which can be seen in Table 4.2.

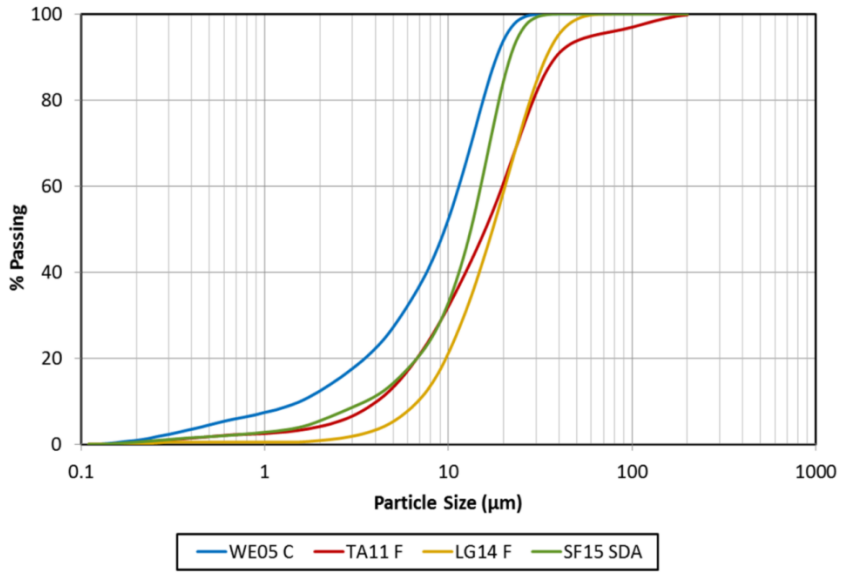

Figure 4.6 Particle Size Distributions of Coal Combustion Products (CCPs)

Specific gravity was determined by following the procedure in ASTM D5550 by using the Helium Pycnometer test. The specific gravity for the different CCPs can be seen in Table 4.2. It can be determined that the specific gravity of WE05 (C) was 2.71, TA11 (F) was 2.62, LG14 (F) was 2.50, and SF15 (SDA) was 2.33. This means that if all the CCPs were converted to a mass from a constant volume, the WE05 material would weigh the most, while the SDA material would weigh the least. These parameters will be important when evaluating the maximum specific gravities.

Table 4.2 Physical Properties of Coal Combustion Products (CCPs)

Materials ID	Class	Specific Gravity	Surface Area (m^2/kg)	Fineness Modulus	D10, (µm)	D50, (µm)	D90, (µm)
WE05	C	2.71	925.13	4.75	1.87	9.55	18.43
TA11	F	2.62	466.18	3.32	4.08	15.91	38.56
LG14	F	2.50	267.48	4.31	6.82	17.42	34.08
SF15	SDA	2.33	610.30	3.61	3.55	13.27	21.90

4.1.3.2 Chemical Properties

Chemical properties were evaluated in accordance to ASTM C618. This standard categorizes different pozzolan materials based on Al_2O_3, CaO and SiO_2 contents. The ASTM limitations require that the SAF (sum of SiO_2, Al_2O_3, Fe_2O_3) content is a minimum of 50.0% for Class C fly ashes and 70.0% for Class F fly ashes. For Class C and Class F fly ashes, the SO_3 content can be a maximum of 5.0%, the moisture content can be a maximum of 3.0%, and the loss of ignition (LOI) can be a maximum of 6.0%. According to Table 4.3, WE05 Class C, TA11 Class F, and LG14 Class F all meet the ASTM C618 requirements. The SDA material, however, does not meet the requirements since the SAF content is below the minimum requirements and also because the SO3 content is above the maximum limitations. A visual representation can also be evaluated from the ternary diagram in Figure 4.7.

Table 4.3 Chemical Properties of Coal Combustion Products (CCPs)

Materials ID	Class	Al_2O_3 (%)	CaO (%)	Fe_2O_3 (%)	SiO_2 (%)	SO_3 (%)	SAF (%)	LOI (%)
WE05	C	22.3	24.6	5.4	32.9	1.8	60.6	0.3
TA11	F	24.5	13.0	9.0	42.9	2.0	76.4	1.9
LG14	F	26.0	2.8	16.9	46.3	1.5	89.2	2.0
SF15	SDA	17.5	28.1	4.4	25.2	14.2	47.1	2.7

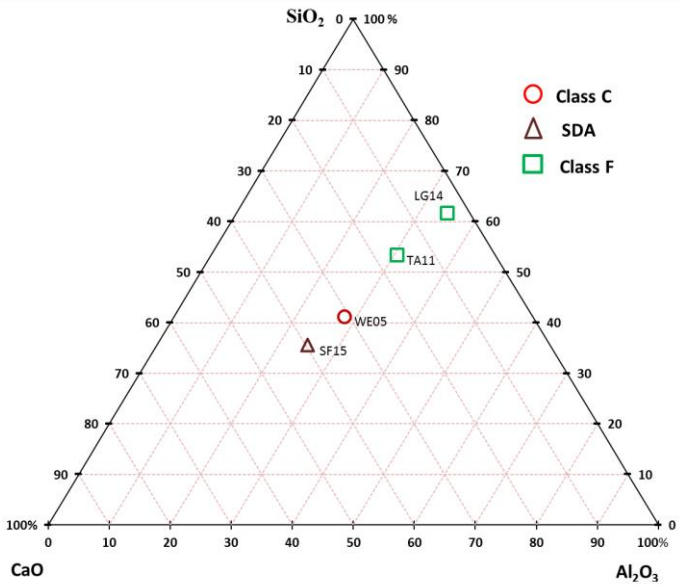

Figure 4.7 Ternary Diagram of WE05 Class C, TA11 Class F, LG14 Class F, and SF15 SDA

Other parameters that have been found to have effects on ASHphalt mixtures are the CaO content and SO_3 content. It has been discovered that increasing the CaO content can increase the filler reactivity when mixed with asphalt mixtures (Faheem & Bahia, 2010; Wang et al., 2011). When increasing the SO_3 content, it has been found that the stiffness may also increase (DeFoe, 1983; Wu, 2009).

4.2 TESTING METHODS

4.2.1 Experimental Testing Plan

This section explains the experimental testing matrix for both the Control asphalt mixtures and the ASHphalt mixtures in terms of aggregate coating, workability, aging resistance, moisture damage resistance, fatigue-cracking resistance, and low-temperature thermal-cracking resistance. Table 4.4 presents the experimental testing matrix for the entire project along with the materials used for this

project. For all of these tests, at least two samples were tested and averages were determined. For the aggregate coating, workability, and aging comparison, six replicates were produced and compared. For the moisture damage resistance, fatigue cracking resistance, and thermal cracking resistance, two replicates were produced and tested. The experimental testing methods are described in detail in the next sections.

Table 4.4 Experimental Research Testing Matrix

Test	Measured Indicator		Aging	CCPs	CCP Dosage	Replicates per Test	Total
Aggregate Coating	Asphalt Binder Film Thickness		Short-Term	1. WE05 2. TA11 3. LG14 4. SF15 5. Control	10% of Binder by **MASS**	6	30
Workability	Number of Gyrations to Compact to 92%Gmm		Short-Term			6	30
Aging Comparison			Long-Term			6	30
Moisture Damage	Tensile Strength Ratio	Dry	Long-Term			2	10
		Saturated				2	10
		Conditioned				2	10
Fatigue	Number of Cycles Drop in E* using IDT	Intermediate Temperature	Long-Term			2	10
Thermal Cracking	Fracture Energy	Low Temperature	Long-Term			2	10
						Total	**140**

4.2.2 ASHphalt Mix Design and Production Procedure

4.2.2.1 Quantity Preparation

For this research there were two different types of mix designs: Control and ASHphalt. The Control mixtures used a total added binder content of 5.50% (similar to the preliminary study). The ASHphalt

mixtures had 10% (by mass) of CCP in bitumen which means that the total added binder content was reduced to 4.95%. The aggregate quantities were constant throughout all the mixtures to allow for a more even comparison between the two different mixture types. The total mass of the mixtures as well as the added binder mass are shown in the equations below:

$$Total\ Asphalt\ Mixture\ Mass = \frac{Aggregate\ Mass}{1-Pb} \quad \text{Eq. 4.1}$$

$$Added\ Binder\ Mass\ (P_b) = \left[\frac{Aggregate\ Mass}{1-Pb}\right] - Aggregate\ Mass \quad \text{Eq. 4.2}$$

where:

Aggregate Mass = Total mass of aggregates (4700 g or 1500 g);

P_b = added binder content.

The total mixture mass and added binder mass for a batch both depend on the specific test that the mixtures were used for. The mass of all the aggregates was 4700 g when compacting to determine the bulk specific gravity. The mass of all the aggregates was only 1500 g for the batch used to determine the maximum specific gravity. These quantity requirements are specified by ASTM D6857/D6857M-11 procedure for determining the maximum specific gravity (G_{mm}) and in ASTM D6752/D6752M-11 for the bulk specific gravity (G_{mb}).

Table 4.5 provides the specific aggregate quantities as well as the quantity of binder that was added to the Control and ASHphalt mixtures. The total asphalt in the mixtures was kept at 5.50% for the Control mixes whereas the total added binder was reduced to 4.95% for the ASHphalt mixes. The total weights of each mixture type remained constant which also reduced any unnecessary deviations. The blend percentages are the same as those in Table 4.1. These percentages were simply multiplied by the total mass of the aggregate (either 4700 g or 1500 g) and then individual weights were calculated for each aggregate type. Once these weights were calculated an aggregate splitter was used

to achieve a more uniform representation of the aggregates. The aggregates were then weighed and mixed together according to the mix design. For ASHphalt mixtures, fly ash was weighed out and mixed with the aggregates before mixing.

Table 4.5 Quantities for Control and ASHphalt Mixtures

Blend (%)	Aggregate Type	CONTROL Mix Quantities (g)		ASHphalt Mix Quantities (g)	
		4700.00	1500.00	4700.00	1500.00
2.5%	12.5	117.50	37.50	117.50	37.50
10.6%	9.5	498.20	159.00	498.20	159.00
21.0%	4.75	987.00	315.00	987.00	315.00
22.7%	MFG-Sand	1066.90	340.50	1066.90	340.50
43.2%	NAT-Sand	2030.40	648.00	2030.40	648.00
Added Pb (5.5%)		273.54	87.30	246.19	78.57
Added Fly Ash (10% Pb)		0.00	0.00	27.35	8.73
Total Weight		4973.54	1587.30	4973.54	1587.30

4.2.2.2 Mixing Procedure

The asphalt mixing method that was used was in accordance to AASHTO T312-12. Once all the materials were weighed out, the aggregates were then mixed thoroughly, and then put in the oven to warm up to the designated temperature. As a reminder, for the ASHphalt mixtures, the fly ash was added to the mixed aggregates prior to being placed in the oven. All Control mixes were mixed at 145^{o}C and then compacted at 140^{o}C, whereas all mixes with fly ash were mixed at 150^{o}C and then compacted at 145^{o}C. The compaction temperatures were lowered from the mixing temperatures to mimic the temperature loss during delivery which is typically experienced in real-world applications. The appropriate amount of asphalt binder was also warmed up to the mixing temperature. When all

the materials reached the mixing temperature, the aggregates were placed into a hot mixing bucket and a crater was formed in the center of the bucket. The asphalt material was weighed into the mixture to achieve the desired batch weight. The mixing bucket was then placed into the Humboldt Asphalt Mixer (Figure 4.8) and mixed for 3 minutes at 60 RPMs. It was noted that all the aggregates were thoroughly coated once the mixing was completed.

Figure 4.8 Humboldt Mechanical Mixer

4.2.2.3 Short-Term Aging

Short-term aging conditioning was performed in accordance to AASHTO R30-02. Short-term aging is supposed to mimic the short-term effects that result from HMA mixtures being produced, placed, and compacted. After mixing the aggregates and asphalt binder together, the material was placed in a pan and spread to an even thickness ranging between 25 and 50 mm. This mixture was then placed into a forced-draft oven for 2 h ± 5 min at a temperature equal to the mixture's compaction temperature ± 3^{o}C to simulate a short term aging. The mixture was stirred after 60 ± 5 min to maintain

a uniform conditioning. After the 2 h ± 5 min, the mixture was removed from the forced-draft oven and ready for compaction.

4.2.2.4 Compaction

The AASHTO T312-12 procedure was used to evaluate workability by compacting the asphalt mixtures with the Superpave Gyratory Compactor (SGC), from Rainhart Co. As previously mentioned in Section 3.1.2.1 the compaction mold and base plate were placed in the oven and preheated at the required compaction temperature for a minimum of 30 minutes prior to the beginning of the compaction. After short-term aging, the mixtures were then ready to be compacted. The Control mixtures were compacted at 140^{o}C and the ASHphalt mixtures were compacted at 145^{o}C. The reason the ASHphalt mixtures were compacted at higher temperatures was because these mixtures demonstrated higher compaction efforts in the preliminary study. Increasing the temperature reduced the viscosity and made the compaction and densification more comparable.

During the compaction, a pressure of 600 ± 18 kPa was applied to the specimen at an angle of 1.25^{o}, while the rotating base spun at a constant 30 gyrations per minute. The Superpave Gyratory Compactor recorded the exact height, pressure, and angle of the compacted sample for each gyration. For short-term aged materials, 100 gyrations were used to analyze the entire compaction curve. Once the test was completed, the angle was removed from the mold as well as the ram pressure and then the ram was retracted from the mold. The specimens were then extruded from the mold and the paper disks were also removed.

4.2.2.4.1 Determining Volumetric Properties

The ASTM D6857/D6857M-11 procedure was used to determine the maximum specific gravity (G_{mm}) and ASTM D6752/D6752M-11 specification was used to determine the bulk specific gravity

(G_{mb}). For both cases the samples were cooled down after heating for 16 ± 1 h at room temperature before testing (AASHTO R30-02). The InstroTek CoreLok machine was used for vacuuming out the air. The volumetric analysis calculations are the same as those is Section 3.1.2.2.2.

4.2.2.5 Long-Term Aging

The long-term aging procedure that was used was in accordance to AASHTO R30-02 and methods adapted by Elwardany, Rad, Castorena, & Kim (2010). These methods evaluate the aging of mixtures with either compacted specimens or loose mixtures and the methodology mimics a 5 to 10 year aging process. After the short-term aged samples were compacted to 100 gyrations, these were then tested to find G_{mb}. Once the bulk specific gravity was determined, the cores were then re-melted by being placed into a force-draft oven for approximately 1 h at the compaction temperature. The samples were then melted and broken up so that the mixture became loose. After this point, the loose mixtures were then placed into the force-draft oven for 120 ± 0.5 h at a temperature of 85 ± 3^{o}C. After 120 ± 0.5 h the specimens were then heated back up to the compaction temperature and then re-compacted to 92% G_{mm} (8% air voids) based on the existing volumetrics. This material was re-compacted to 92% G_{mm} because this represents the density of the material after the construction of the asphalt layer has been completed. Figure 4.9 shows the stacked asphalt mixtures after being melted and Figure 4.10 shows the covered asphalt mixtures in the oven for long-term aging. The compacted samples were the only samples that were long-term aged.

Figure 4.9 Compacted Asphalt Material after being Melted

Figure 4.10 Long-Term Aging Setup

4.2.3 Aggregate Coating

Aggregate coating was evaluated based on physical observations as well as calculated parameters. Pictures were taken to make the side-by-side comparisons between the Control samples and the

ASHphalt samples. Since the total binder content for the Control mixtures was 5.50%, whereas the total binder content for the ASHphalt mixtures was only 4.95%, it was important to evaluate aggregate coating to ensure proper performance.

The percent of asphalt, as well as the diameter, particle size distribution, and surface area of the aggregate particles, have an effect on the thickness of the asphalt film. The asphalt film thickness decreases when the average diameter of the aggregate particle decreases because the surface area increases. For this reason, surface area factors (Table 4.7) can be used to evaluate, or estimate, the total aggregate surface area in a given asphalt mixture. This assumes that all of the particles are rounded, however it serves as a good approximation. The surface area can be calculated by multiplying the surface area factor by the percent passing that specific sieve size. The units of the results are square feet per pound of aggregate (9).

Table 4.6 Surface Area Factors

Sieve Size	Surface Area Factors
Percent Passing Maximum Sieve Size	2
Percent Passing No. 4	2
Percent Passing No. 8	4
Percent Passing No. 16	8
Percent Passing No. 30	14
Percent Passing No. 50	30
Percent Passing No. 100	60
Percent Passing No. 200	160

Once the surface area of the aggregates is determined (converted to m^2/kg), a volumetric analysis needs to be evaluated in order to find the film thickness. The equations below show the necessary steps to calculate the variables needed to find film thickness:

$$Total\ volume\ P_{bv} = \frac{(total\ weight\ \ of\ mixture)*(P_b)}{G_b} \quad \text{Eq. 4.3}$$

$$P_{ba} = \frac{G_{se}-G_{sb}}{G_{sb}*G_{se}} * G_b \quad \text{Eq. 4.4}$$

$$P_{baw} = (P_{ba}) * (total\ weight\ of\ mixture * (1 - P_b)) \quad \text{Eq. 4.5}$$

$$P_{bav} = \frac{Weight\ of\ absorbed\ asphalt}{G_b} \quad \text{Eq. 4.6}$$

$$P_{bev} = 100\% * \frac{G_{se}-G_{sb}}{G_{sb}*G_{se}} * G_b \quad \text{Eq. 4.7}$$

P_{bv} = total volume of asphalt cement, by total mass of mixture (mL);

P_b = asphalt content, by total mass of mixture;

P_{ba} = absorbed asphalt content, by total mass of mixture;

G_{se} = effective specific gravity of aggregate;

G_{sb} = bulk specific gravity of aggregate;

G_b = specific gravity of asphalt;

P_{baw} = weight of absorbed mixture (g);

P_{bav} = volume of absorbed asphalt (mL);

P_{bev} = effective volume of asphalt (mL);

After these variables are determined, the film thickness can then be calculated using the equation below:

$$T_F = 1000 * \frac{V_{asp}}{SA*W} \quad \text{Eq. 4.8}$$

where:

T_F = Average film thickness (microns);

V_{asp} = Effective volume of asphalt cement (liters);

SA = Surface area of the aggregate (m^2 per kg of aggregate);

W = weight of aggregate (kg).

With this equation it is important to understand that when the surface area estimations were made, the units need to be converted from square feet per pound to m^2 per kg of aggregate. Once these units are converted, the equation can be used.

4.2.4 Workability

Workability performance was evaluated by comparing the short-term aged ASHphalt mixtures with the short-term aged Control mixtures. Using the Superpave® Gyratory Compactor, it could be determined how easily the mixtures are compacted based on the compaction effort. Lower compaction efforts allowed the densification curve to reach higher values of $\%G_{mm}$, or lower $\%V_a$. The purpose of this testing was to evaluate the compactability of the ASHphalt mixtures. If the ASHphalt mixtures reached higher values of $\%G_{mm}$, then the workability is said to be reduced which is desired. This is an important evaluation because if the compaction effort is reduced for the ASHphalt mixtures, then this supports the original hypothesis and research objectives.

4.2.5 Aging Resistance

Aging resistance was measured as a comparison in compaction efforts between the long-term aged materials and the short-term aged materials. As the material ages the material becomes stiffer. Since the experimental matrix required that the long-term aged materials be re-compacted to 92% G_{mm}, a comparison was made between the two different aging conditions. The number of gyrations to reach 92% G_{mm} was evaluated and compared to calculate aging index. Therefore, the aging index represents the ratio of the number of gyrations required for the long-term aged materials to reach 92% G_{mm} as compared to the short-term aged materials. Lower aging indexes demonstrate higher

aging resistance. If the aging index is low, this means that the material resists the stiffening effects of age-hardening. Therefore, the aging index is calculated using the equation below:

$$Aging\ Index = \frac{N_{LT}}{N_{ST}} \quad \text{Eq. 4.9}$$

where:

N_{LT} = Number of gyrations to reach 92% G_{mm} for long-term aged materials;

N_{ST} = Number of gyrations to reach 92% G_{mm} for short-term aged materials.

4.2.6 Moisture Damage

4.2.6.1 Specimen Conditioning

This testing procedure is in accordance to AASHTO T283-07. Moisture damage is the result from water or air damaging the bond between the aggregate particles and the asphalt binder. It is required that the compacted asphalt mixtures resist this damage to a certain degree when saturated with water. Specimens were therefore prepared and conditioned to evaluate proper moisture damage resistance. Duplicate samples were tested for each situation.

After the asphalt mixtures were long-term aged and compacted to 92% G_{mm}, these were then core drilled and saw cut to a 101.6 ± 2.0 mm diameter and a 50.8 ± 2.0 mm thickness (Figure 4.11a shows the core drilling method and Figure 4.11b shows the resulting cored drill/saw cut specimen). Typical core drilling procedures were followed as well as saw cutting. Two specimens were collected (after core drilling and saw cutting) from each compacted sample. The samples from the compacted cores were randomly chosen for each testing procedure.

(a)

(b)

Figure 4.11 Methods for Core Drilling (a) Core Drill (b) 101.6 mm diameter by 50.8 mm Thick Specimen

After the 101.6 ± 2.0 mm diameter by 50.8 ± 2.0 mm thick specimens were produced, the samples were separated into subsets and then the subsets were placed under three different environments: dry, saturated, and conditioned. The dry samples were placed into a leak-proof plastic bag and then placed in a water bath at 25 ± 0.5^{o}C for 2 hr ± 10 min with a minimum of 25 mm of water above the surface of the specimen. The specimens were then ready to be tested with the Indirect Tension Machine.

The saturated and conditioned specimens were submerged in a water container with a minimum of 25 mm of water above their top surface, and with also 25 mm of water below the bottom surface (a perforated spacer was used to raise the specimen off the base of the water container). Using the InstroTek Corelok machine (Figure 4.12), the samples were then vacuumed to remove the air, and thus insert the water into the void spaces. After the machine completed the cycle, the samples were left in the water bath for approximately 5 to 10 minutes. After this time period the samples were

taken out of the water bath and the degree of saturation (S') was calculated by using the equations below:

$$S' = \frac{100 * J'}{V_a} \quad \text{Eq. 4.10}$$

$$V_a = \frac{P_a * E}{100} \quad \text{Eq. 4.11}$$

$$J' = B' - A \quad \text{Eq. 4.12}$$

where:

V_a = volume of air voids (cm^3);

P_a = air voids, (percent);

E = volume of the specimen, (cm^3).

J' = volume of absorbed water, (mL);

B' = mass of the saturated, surface-dry specimen after partial vacuum saturation, (g);

A = mass of the dry specimen in air, (g).

A requirement from AASHTO T283-07 is that all of the saturated and conditioned specimens need to have a degree of saturation between 70 and 80%. If the degree of saturation is less than 70% the specimen needs to be vacuumed so that the degree of saturation increases. If the degree of saturation is higher than 80%, the specimen must be discarded due to excessive damage. The degree of saturation is important because this presents an allowable range where the asphalt pavement is not excessively damaged, but at the same time demonstrates realistic water penetration. This procedure is critical to evaluate the bonding between the asphalt binder and the aggregate particles. If the bond between these materials is significantly damaged due to water penetration, the materials will separate and the mixture becomes weak which is undesirable.

Figure 4.12 Vacuum-Saturated Method

After all the saturated specimens reached the appropriate range between 70 and 80%, the specimens were then placed into a water bath at 25 ± 0.5°C for 2 hr ± 10 min with a minimum of 25 mm of water above the surface of the specimen. The specimens were then ready to be tested with the Indirect Tension Machine. After the conditioned specimens were saturated, they were then placed in a water bath at 60 ± 1°C for 24 ± 1 h (Figure 4.13). The specimens were submerged so that at least 25 mm of water was above the top surface of the asphalt specimen. After 24 ± 1 h, the specimens were removed from the water bath and then placed into a different water container that was 25 ± 0.5°C for 2 hr ± 10 min with at least 25 mm of water above the top surface. Maintaining the temperature for this water bath was critical since the samples were warmer than 25 ± 0.5°C. Once this time had elapsed, the specimens were then removed from the water bath and then tested using the IDT.

Figure 4.13 Humboldt Water Bath set at 60°C.

4.2.6.2 Indirect Tensile Test (IDT)

The Humboldt Indirect Tensile Machine (IDT), Figure 4.14, was used to evaluate the moisture damage resistance in accordance to ASTM D4123. This machine uses a single compressive load that acts parallel to the vertical plane of the specimen. As the vertical compressive load pushes down on the specimen (at a rate of 50 mm/min.), horizontal tensile forces begin to develop. The specimen then fails by splitting in half along the vertical plane that the load acts on (Figure 4.15). The required thickness of the loading strip for a 101.6 mm diameter asphalt specimen is 12.7 mm and this was used for this study. This specific thickness provides a uniform loading condition which produces a nearly uniform stress distribution.

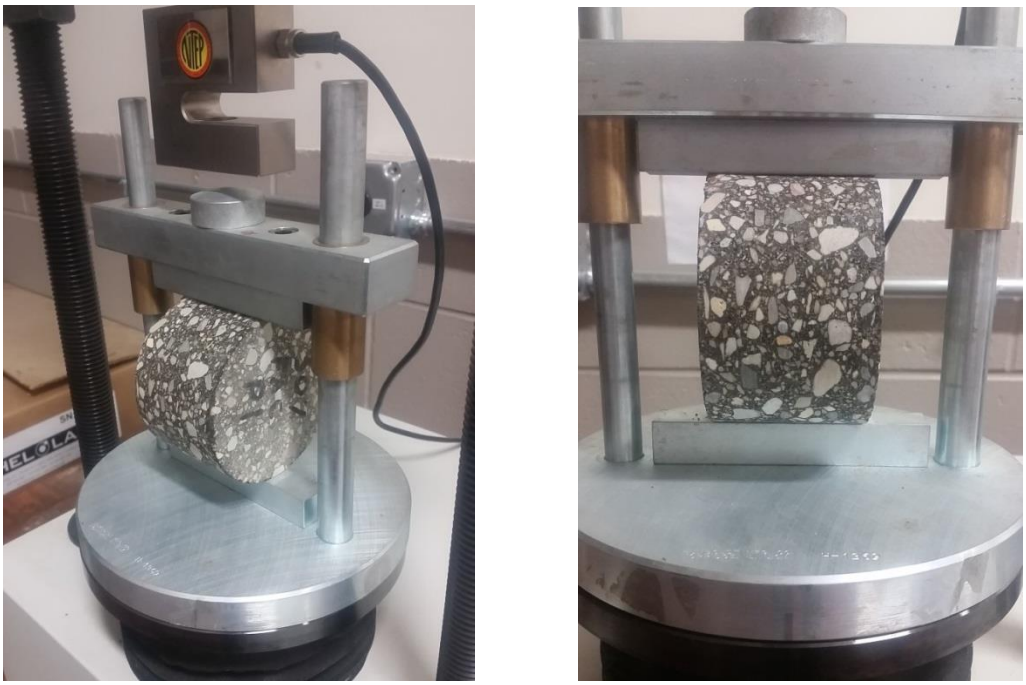

Figure 4.14 Humboldt Indirect Tensile Machine Setup

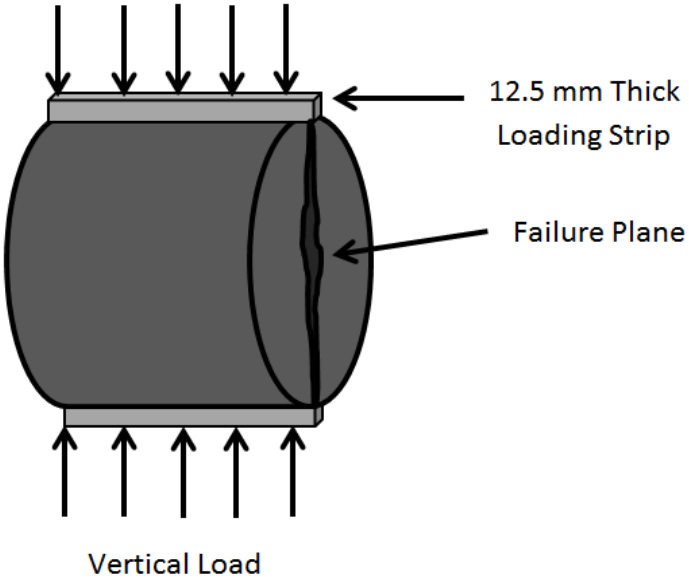

Figure 4.15 Indirect Tension Test at Failure

The IDT provides two important properties that are very useful in HMA mixture analysis: moisture damage resistance and tensile strain at failure. For moisture damage resistance, the tensile strength of

a dry compacted asphalt sample is compared to that of a water-conditioned, or vacuum-saturated, compacted asphalt sample. This value can be expressed as a Tensile Strength Ratio (TSR). The higher the value for the TSR, the better the mixture performed in terms of moisture damage resistance. A lower value indicates poor performance of the specimen. AASHTO T283-07 requires a TSR of at least 80%. The other beneficial variable that can be calculated from the IDT is the tensile strain at failure which can help predict the cracking potential. Mixtures that are able to resist cracking generally can tolerate higher strains at failure which is beneficial to the asphalt pavement.

Equations for tensile stress and tensile strain have been developed (Anagnos & Kennedy, 1972; Hadley, Hudson & Kennedy, 1970, 1972) and are shown below:

$$\sigma_x = \frac{2P}{\pi dt} \quad \text{Eq. 4.13}$$

$$\sigma_y = \frac{6P}{\pi dt} \quad \text{Eq. 4.14}$$

where:

σ_x = horizontal tensile stress at center of specimen, (MPa);

σ_Y = vertical tensile stress at center of specimen, (MPa);

P = applied load, (N);

d = diameter of specimen, (mm);

t = thickness of specimen, (mm).

$$\varepsilon_f = 0.52x_t \quad \text{Eq. 4.15}$$

where:

ε_f = tensile strain at failure (mm/mm);

xt = horizontal deformation across the specimen (in.).

$$TSR = \frac{S_s}{S_d} \quad \text{Eq. 4.16}$$

where:

S_s = average tensile strength of conditioned specimen (dimensionless);

S_d = average tensile strength of dry, or saturated, specimen (dimensionless).

The methods explained in this section were used to convert loads and deflections to stresses and strains. Moisture damage resistance was also calculated and evaluations have been made.

4.2.7 Fatigue-Cracking Resistance

Fatigue testing was performed to evaluate the effects of fatigue-cracking resistance in ASHphalt mixtures. Fatigue cracking is a result of repeated loads at intermediate temperatures. Over the life-cycle of the asphalt pavement, the material begins to deteriorate due to cyclic loading. As traffic loading overstresses the asphalt material, the pavement begins to crack. The factors affecting fatigue cracking are the asphalt content, air void content, aggregate characteristics, temperature, and traffic. Also, asphalt binders that become stiffer during aging also develop poor fatigue characteristics. Ideally, asphalt materials should act as a soft, elastic material when loaded and unloaded. Since fatigue cracking is an undesirable characteristic of asphalt pavements, it was vital to evaluate this parameter and potential contribution of CCPs.

Figure 4.16 demonstrates a typical fatigue testing curve. The horizontal axis represents the number of cycles and the vertical axis represents the displacement of the material. As seen from Figure 4.16 there are different zones within this type of fatigue curve. The most critical section of this curve that is evaluated in this research is the secondary fatigue section and the point where the tertiary fatigue section starts. During the secondary fatigue stage, the material undergoes a constant cyclic loading and the material deforms at a constant rate. The slope of this line represents the

constant deformation per cycle in which the material is deforming. This is important because it demonstrates perfect elastic deformation over time. The tertiary portion represents the point at which the material is failing. This section was important to understand where the material fails (N_f). Even though the curve continues in the tertiary fatigue section, the material was considered to have failed when the tertiary fatigue section started.

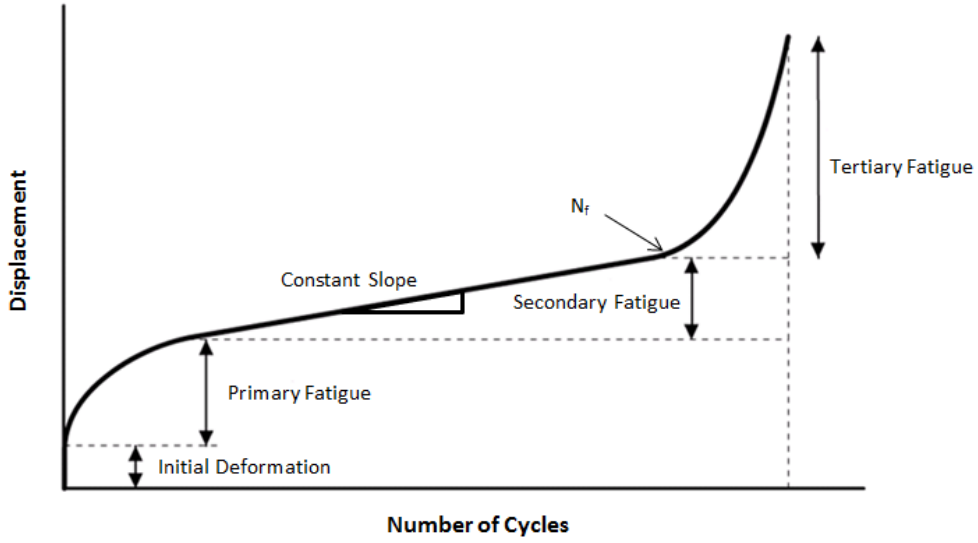

Figure 4.16 Typical Fatigue Curve

The Complex Modulus, E*, represents the storage and loss moduli of a viscoelastic material. The complex modulus is a complex number that shows the relationship between the stress and strain and this can be modeled from the equation below:

$$E^* = E' + iE" \qquad \text{Eq. 4.17}$$

where:

E = storage modulus or elastic component of the complex modulus (MPa);

E" = loss modulus or the viscous component (MPa).

The Complex Modulus can also be determined by evaluating the stress and strain rate at different locations. By calculating the ratio of the stress amplitude and the strain-rate from the cyclic test, the dynamic modulus is represented as:

$$E^* = \frac{\sigma_o}{\varepsilon_o} \quad \text{Eq. 4.18}$$

where:

σ_o = stress amplitude (MPa);

ε_o = strain-rate (mm/cycle).

Since the amplitude of the load cycle remains constant (i.e., stress remains constant), the deformation (i.e., strain) is the only variable changing. E* remains constant over the secondary fatigue section since the stress is constant and the strain-rate is increasing at a constant rate. Therefore, it is actually critical to evaluate the number of cycles till E* drops in magnitude and this is represented by N_f which is where the tertiary fatigue starts. Since E* is a function of stress and strain, the strain rate influences E* since stress is considered constant. The E* finally reduces as the strain rate increases (since it is the denominator of the function). When the tertiary fatigue section starts, the strain rate increases and thus E* decreases. In this research evaluation, Nf is used to determine the point at which E* drops.

Fatigue testing was performed as a modified test from AASHTO T322-03, AASHTO T342-11, and methods adapted by Shu, Huang, & Vukosavljevic (2007). In these procedures, fatigue is evaluated by using different parameters such as loading curve, temperature, load amplitude, and a frequency in which the load is applied. For this study, fatigue was evaluated by using a sine wave loading condition, a test temperature of 20 ± 1^{o}C, a 2% pre-loading condition, a 20% ultimate loading condition, and a frequency of 10 Hz (Figure 4.17). For all specimens, the same loading condition was used to directly

compare the specimens. The loading conditions were calculated based on the ultimate loads obtained from the dry specimens tested in IDT.

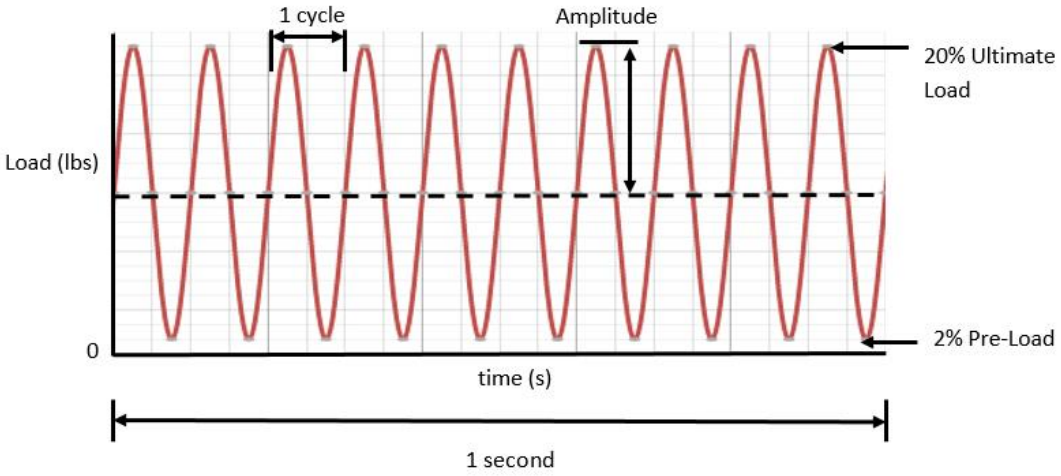

Figure 4.17 10 Hz Sine Wave Representation of Fatigue Test

A sine wave was used to represent a cyclic loading condition to the specimen as it was tested in fatigue. The equation that was used to represent the loading cycle is shown below:

$$y(t) = A * \sin(2\pi f t + \varphi) \qquad \text{Eq. 4.19}$$

where:

A = Amplitude (peak from the reference line) (N);

f = frequency (number of oscillations, or cycles, per second) (Hz);

t = time (s);

$\varphi =$ phase (where the oscillation is at t = 0) (radians).

To evaluate the fatigue cracking resistance, a MTS 858 Mini Bionix II loading frame was used with a MTS 651 Environmental Chamber (Figure 4.18). This environmental chamber was connected to a temperature controller to ensure the temperature in the chamber was accurate. The chamber was also insulated to ensure the appropriate temperature did not fluctuate dramatically throughout

testing. The same testing frame from the IDT, with a 12.7 mm loading strip, was also attached to the MTS frame (Figure 4.18). This equipment recorded data by using MTS data acquisition software.

Figure 4.18 MTS Environmental Chamber with IDT Testing Frame

The samples that were used for fatigue testing were 101.6 ± 2.0 mm diameter by 50.8 ± 2.0 mm thick with duplicates tested. An important aspect of this type of testing was to evaluate both the horizontal and vertical displacements. The applied load and vertical displacement were both recorded directly from the MTS testing frame. Horizontal displacement was recorded by using an LVTD displacement sensor. This sensor was attached to the specimens and then recorded through the MTS computer program. Figure 4.19 and Figure 4.20 explain the test setup and LVDT configuration.

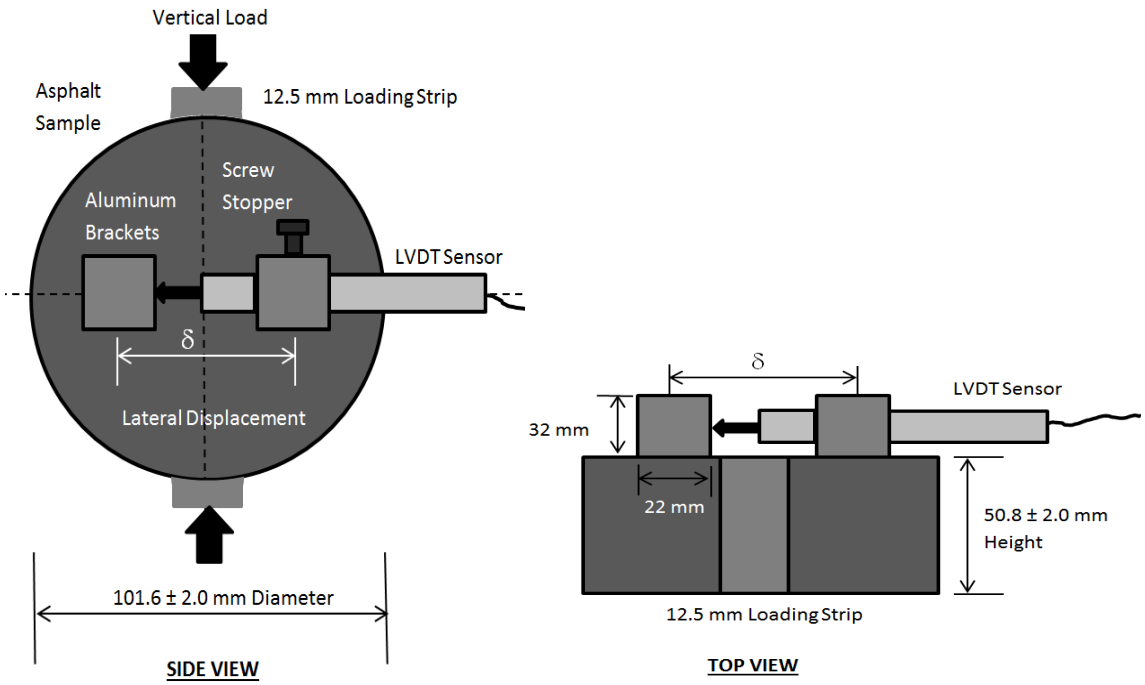

Figure 4.19 Asphalt Sample LVDT Configuration

Figure 4.20 Asphalt Sample Assembly for Fatigue Testing

The LVDT sensor was connected to the sample and then the sample was loaded into the environmental chamber. After the sample was loaded, it was then tested according to specified protocol using the MTS software. Figure 4.21 shows the specimen being tested in fatigue.

Figure 4.21 Complete Testing Setup for Fatigue

4.2.8 Thermal-Cracking Resistance

Thermal-cracking resistance was used as a parameter to evaluate the low-temperature response of fly ash based asphalt mixtures. Thermal cracking is an important parameter to evaluate in climates with cold weather because these types of cracks are directly related to low temperatures. Reducing the asphalt mixture stiffness can reduce the effects of thermal cracking and this is critical for low-temperature evaluations. Stiffer asphalt mixtures usually perform worse in lower temperatures whereas asphalt binders that are soft typically perform better. Asphalt binders that are excessively aged also have poor performance in lower temperatures because the binder has been exposed to higher amounts of age-hardening due to excessive oxidation.

Low-temperature thermal cracking resistance was evaluated by using the Semi-Circular Bending Test (SCB). The SCB is a 3-point bending test using semi-circular specimens, with a notch cut in the bottom, at lower temperatures to evaluate Fracture Energy (G_f), Fracture Toughness (K_{IC}), and

Stiffness (S). The Fracture Energy, G_f (J/m^2), is the energy required to create a unit surface area of a crack. This is obtained by dividing the work of fracture (area under the load vs. load line displacement curve, Figure 4.22) by the ligament area (ligament length and thickness of specimen). The Fracture Toughness, K_{IC}, (Pa*m$^{0.5}$) is the ability of the asphalt sample to resist fracture due to material toughness. The Stiffness, S (kN/mm), is the slope of the linear portion of the load-line displacement curve (Figure 4.23).

$$G_f = \frac{W_f}{A_{lig}} \quad \text{Eq. 4.20}$$

$$W_f = \int Pdu = W + W_{tail} \quad \text{Eq. 4.21}$$

$$A_{lig} = (r - a) * t \quad \text{Eq. 4.22}$$

$$\frac{K_{IC}}{\frac{P}{2rt}*\sqrt{\pi * a}} = Y_{I(0.8)} \quad \text{Eq. 4.23}$$

$$Y_{I(0.8)} = 4.782 + 1.219\left(\frac{a}{r}\right) + 0.063\exp\left(7.045\left(\frac{a}{r}\right)\right) \quad \text{Eq. 4.24}$$

where:

$W_f = \int Pdu = W + W_{tail}$, work of fracture (J);

P = applied load (N);

u = load line displacement (m);

A_{lig} = ligament area (m^2);

r= specimen radius (m);

a = notch length (m);

t = specimen thickness (m);

Y_I = the normalized stress intensity factor (dimensionless).

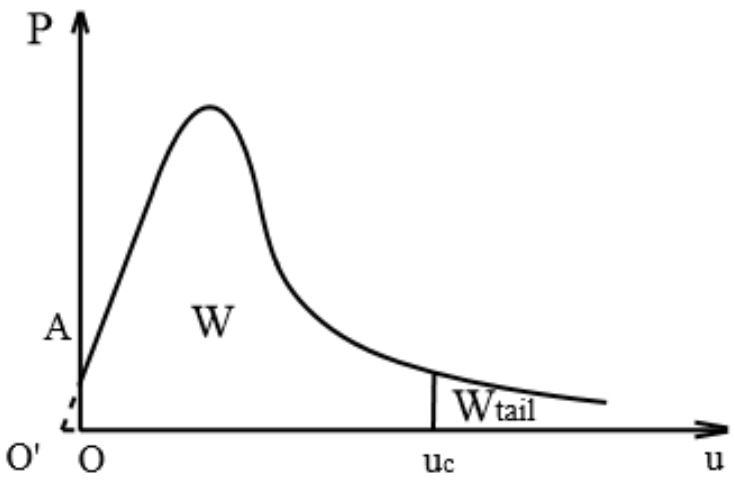

Figure 4.22 Low-Temperature Load vs. Load-Line Displacement Representation

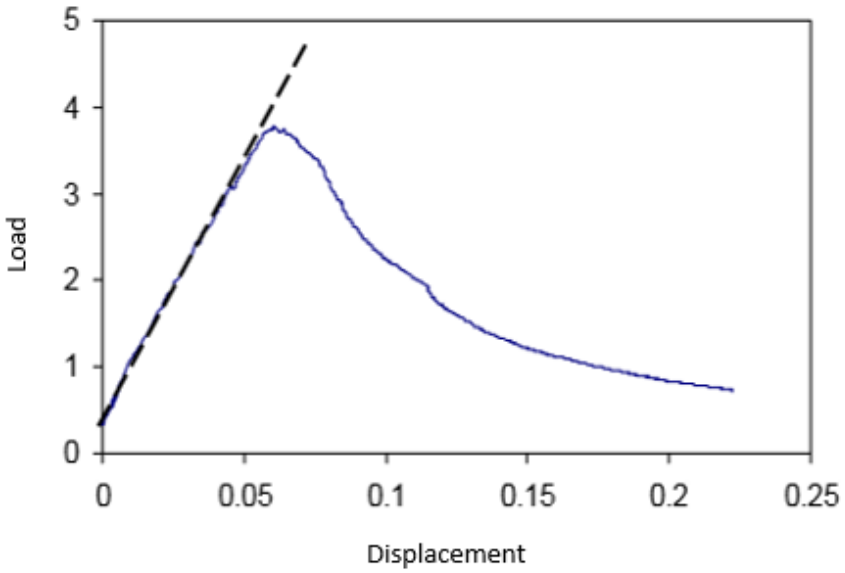

Figure 4.23 Stiffness (S) Determination of Low-Temperature Testing

Samples were cut in half (laterally) and then cut to a 25.4 ± 2.0 mm thickness. The test temperature was set to -18 ± 1°C and the loading rate was 0.03 mm/min. The samples were conditioned for 2 ± 0.2 hrs at -18 ± 1°C prior to testing (duplicates were tested). The dimensions of the samples and the testing setup can be seen in Figure 4.24 and Figure 4.25. For all specimens, the same loading condition was used to directly compare the specimens.

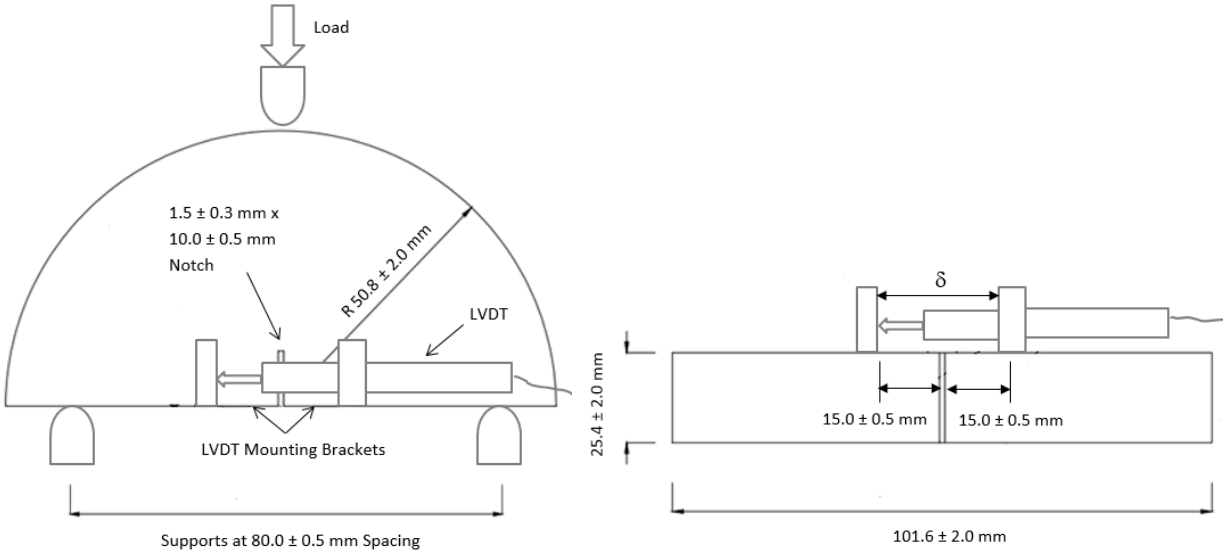

Figure 4.24 SCB Dimensions

Figure 4.25 Asphalt Sample Assembly for SCB

The SCB test was performed using the MTS 858 Mini Bionix II loading frame, the MTS 651 Environmental Chamber, and a 3 point-testing frame, Figure 4.26. The test was done once the load dropped below 0.5 kN. This machine was used to evaluate both the vertical load and the vertical load-line displacement. The horizontal deformation was measured by a LVDT sensor and this represented the crack propagation. The LVDT sensor was attached to the specimens and then recorded through the MTS computer program.

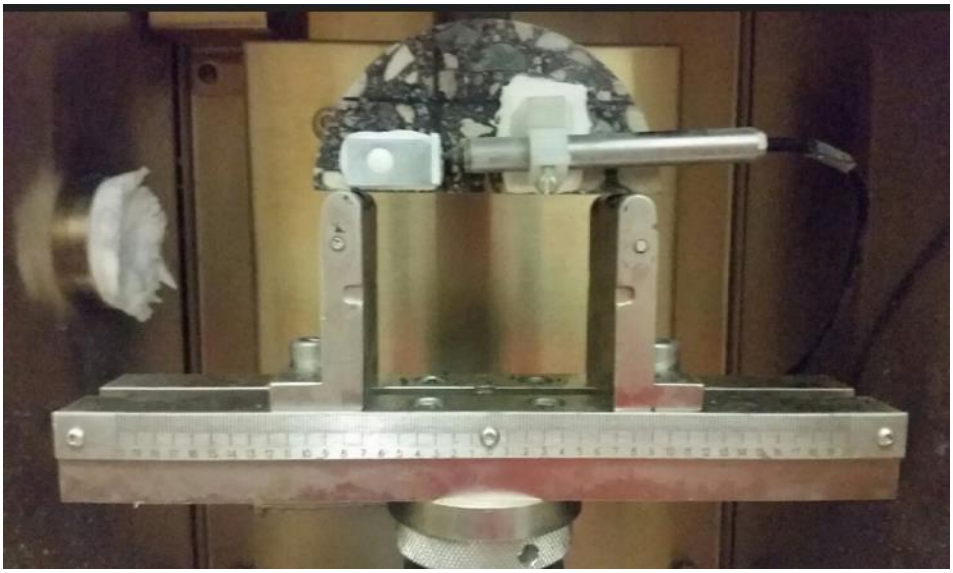

Figure 4.26 Complete Testing Setup for SCB

CHAPTER 5.

RESULTS AND ANALYSIS

5.1 AGGREGATE COATING

Asphalt film thickness was used to evaluate proper aggregate coating for both Control and ASHphalt mixtures. This parameter was important to calculate since the ASHphalt had 10% (by mass) binder replacement with fly ash and this means less binder is available to coat the aggregates. The calculated asphalt film thickness represents the average thickness of the asphalt that surrounds the aggregate particle and this has been related directly to durability. If the asphalt film thickness is too thin, air can enter the compacted HMA more rapidly and this will oxidize the asphalt binder which can cause the HMA to become brittle and fracture by cracking. Also, if the film thickness is too thin, water can enter through the binder and penetrate the aggregate particles which can cause moisture damage and this can lead to rutting, raveling, freeze-thaw damage, and bleeding.

Asphalt film thickness is not directly considered as a Superpave® design requirement, however evaluating aggregate coating is critical. It has been found that average values for asphalt film thickness should typically be between 6 to 8 µm (Hmoud, 2011). This thickness range has been found to establish a thick enough coating around the aggregate particles which will prevent rapid oxidation, and even prevent moisture damage.

Table 5.1 reports the surface area factors, percent passing of the asphalt mixtures, and also the surface area of aggregates. From this table it can be seen that the total surface area of the aggregates used in the Control mixtures was approximately 5.35 m^2/kg and the aggregates used in the ASHphalt mixtures was approximately 5.53 m^2/kg (this increase in surface area is due to the added fly ash).

Table 5.1 Calculated Surface Area of Aggregates

Sieve Size	Surface Area Factors	Percent Passing (%)		Surface Area (ft^2/lb)		Surface Area (m^2/kg)	
		Control	ASHphalt	Control	ASHphalt	Control	ASHphalt
Max (19.00mm)	2	100.00	100.00	2.00	2.00	0.41	0.41
No.4 (4.75mm)	2	63.50	63.50	1.27	1.27	0.26	0.26
No.8 (2.36mm)	4	51.72	51.72	2.07	2.07	0.42	0.42
No.16 (1.18mm)	8	39.85	39.85	3.19	3.19	0.65	0.65
No.30 (0.6)	14	30.02	30.02	4.20	4.20	0.86	0.86
No.50 (0.3)	30	17.21	17.21	5.16	5.16	1.06	1.06
No.100 (0.15)	60	6.80	6.80	4.08	4.08	0.84	0.84
No.200 (0.075mm)	160	2.60	3.15	4.16	5.04	0.85	1.03
SUM				26.13	27.01	5.35	5.53

The surface area was then used to calculate the film thickness which is shown in Table 5.2. From this table it is seen that the film thickness of the Control mixtures was 9.03 µm and the film thickness of the ASHphalt mixtures was 7.66 µm. This makes sense that the film thickness of the ASHphalt mixtures was less than the Control mixtures because 10% (by mass) of asphalt binder was substituted with fly ash in the ASHphalt mixtures. It is also important that both mixture types were either within the recommended range of 6 to 8 µm or above this range as this is critical for durability.

Table 5.2 Asphalt Film Thickness for Control and ASHphalt Mixtures

Mixture	Control	ASHphalt
Surface Area of Aggregates (ft^2/lb)	26.13	27.01
Surface Area of Aggregates (m^2/kg)	5.35	5.53
Bulk Specific Gravity of Aggregate	2.656	2.656
Effective Specific Gravity of Aggregate	2.713	2.713
Asphalt Specific Gravity	1.035	1.035
Asphalt Content (%)	5.50%	4.95%
Total Weight (g)	4700.0	4700.0
Asphalt Volume (mL)	249.76	224.78
Asphalt Absorbed (by weight of aggregate)	0.819	0.819
Weight of Absorbed Asphalt (g)	36.36	36.58
Volume of Absorbed Asphalt (mL)	35.13	35.34
Effective Volume of Asphalt (mL)	214.62	189.44
Film Thickness (Tf) (microns)	9.03	7.66

After the film thickness was calculated it was also important to visually inspect the coating of the aggregates. During the mixing process, there were no problems observed in terms of aggregate coating. The asphalt binder seemed to coat the aggregates at the same rate for both the Control mixtures and ASHphalt mixtures. Figure 5.1 shows representative aggregates for each mixture type. From this figure it is clear that no major differences can be reported.

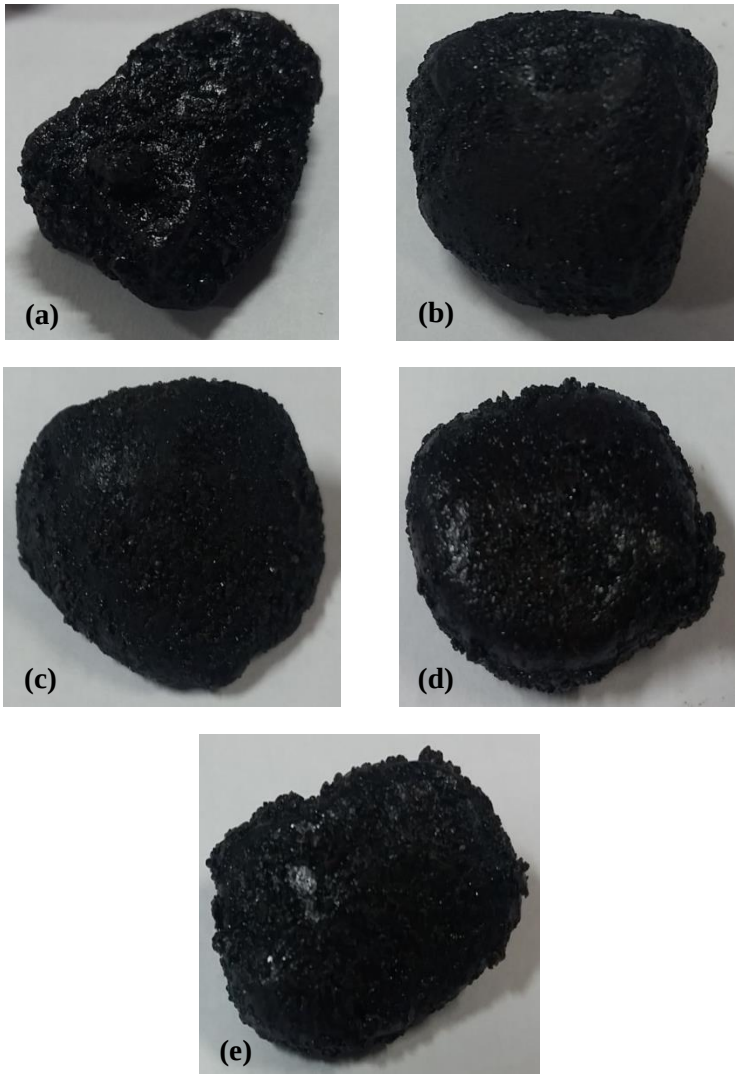

Figure 5.1 Aggregate Coating (a) Control (b) WE05 C (c) TA11 F (d) LG14 F (e) SF15 SDA

5.2 WORKABILITY

Workability was evaluated by comparing the densification curves of the Control mixtures and ASHphalt mixtures. All compaction comparisons for workability were evaluated for short-term aged materials because this demonstrates the physical condition in which the material is mixed, placed, and compacted. Lower compaction efforts demonstrated better workability properties. For all evaluations, the Control mixtures were compacted at 140°C and the ASHphalt mixtures were compacted at 145°C. As seen by the preliminary study results, the ASHphalt mixtures required more compaction effort. To eliminate these differences, temperature was increased (making the material less viscous) to allow for improved compaction efforts.

Figure 5.2 demonstrates the workability results for Control and ASHphalt mixtures. Every mixture was compacted to 100 gyrations to understand the material behavior over a wide range of gyrations. It can be seen that every specimen was compacted to approximately 96% G_{mm} (4% air voids) and this is a critical parameter to evaluate in terms of Superpave® compaction efforts (as previously discussed). Every mixture developed similar curves which proved that compacting the ASHphalt mixtures at higher temperatures reduced the compaction effort. Increasing mixing and compaction temperatures was necessary since there was less binder (10% of bitumen was replaced with CCP) and at the same time the addition of particulate matter increased mastic viscosity. Therefore, the ASHphalt materials experienced a reduction in viscosity due to being compacted at 145°C rather than 140°C. This proves that the ASHphalt mixture in the preliminary study could have potentially reduced the compaction efforts if heated to higher temperatures.

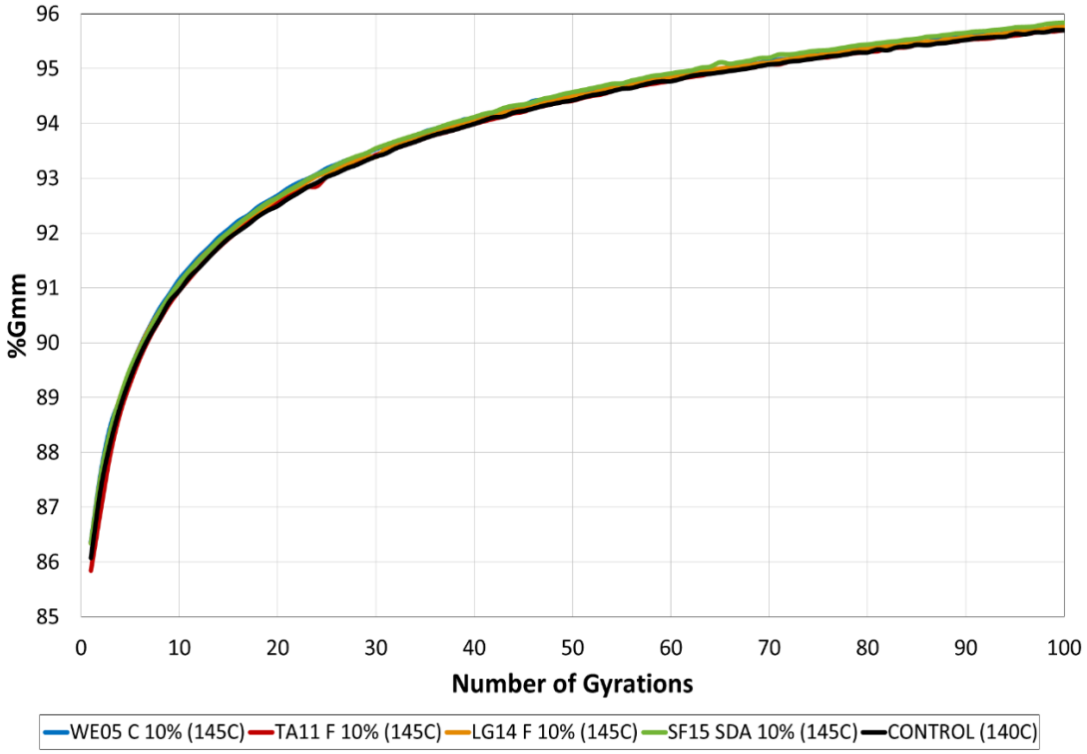

Figure 5.2 Densification Curve for 100 Gyrations

Figure 5.3 reports on the densification curves when the materials reach 92% G_{mm}. This section of the curve is critical because this represents the density of the material after the construction of the asphalt layer has been completed. Figure 5.3 demonstrates that WE05 (C) mixtures compacted with the least amount of compaction effort. LG14 (F) and SF15 (SDA) mixtures also exhibited a reduction in compaction effort when compared to the Control mixture. The TA11 (F) mix on the other hand, demonstrated similar compaction efforts as the Control mixture which means that the viscosity of the material must be relatively high since the increase in temperature still did not reduce the compaction effort to the level sufficient enough to surpass the Control mixture.

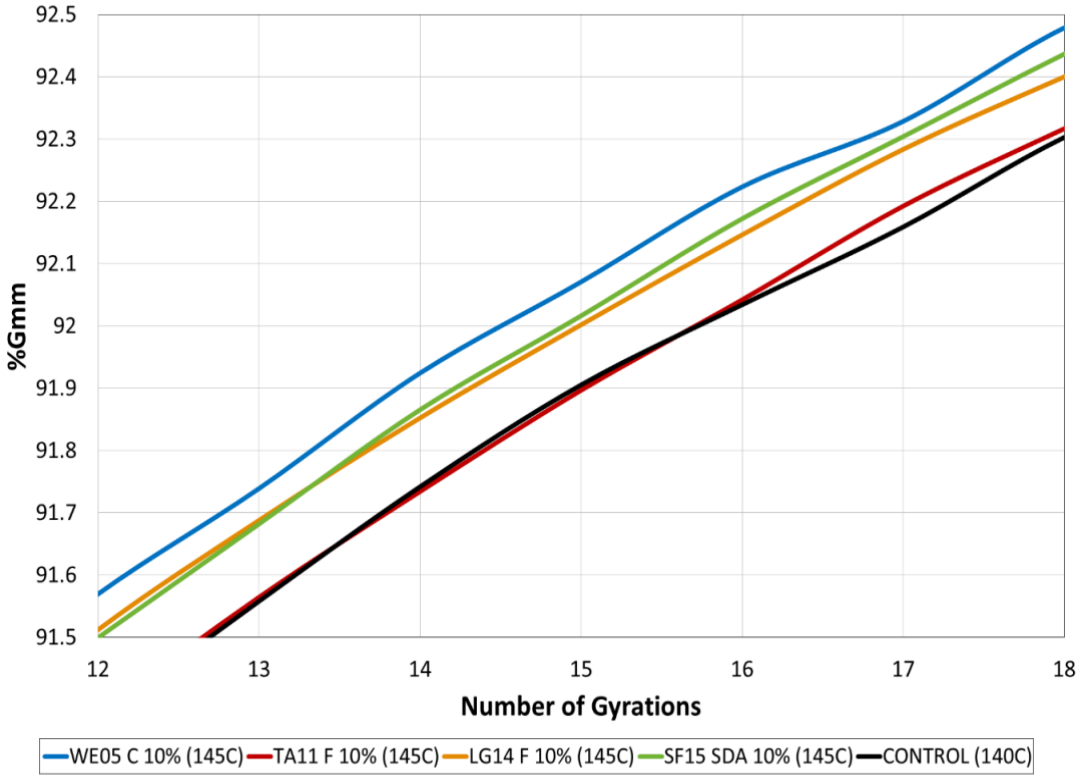

Figure 5.3 Densification Curve at 92% G_{mm}

Figure 5.4 evaluates the differences in densification curves from 95 to 100 gyrations. This section of the densification curve is important because it evaluates the final gyrations that the compacted specimens had encountered. This section of the curve is also important because it demonstrates the long-term compaction response of the materials. Comparing Figure 5.3 and Figure 5.4 it can be seen that WE05 (C) mix had an increase in compaction effort since this densification curve got closer to densification curve of the Control mixture. The SF15 (SDA) mix experienced a long-term reduction in compaction effort since the material performed the best in terms of workability. TA11 (F) and LG14 (F) mixtures did not experience any long-term compaction alterations. Regardless, every ASHphalt mixture was compacted at 145°C to the same $\%G_{mm}$, or better, than the Control mixture at 140°C.

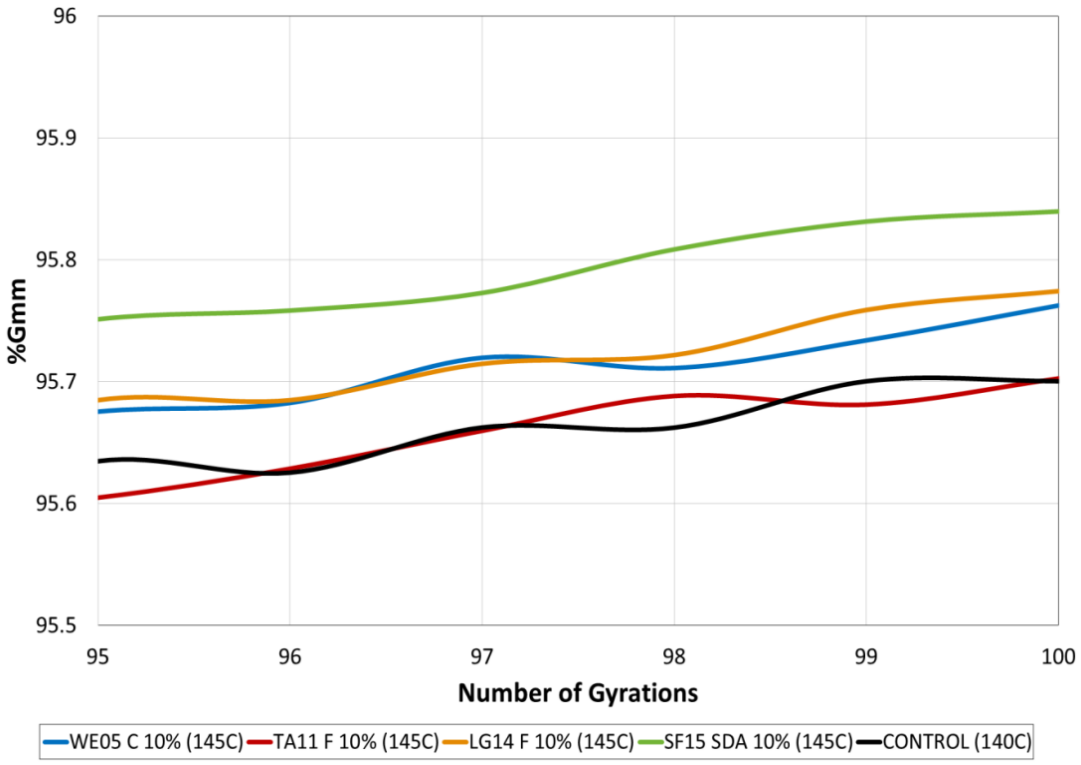

Figure 5.4 Densification Curve at 100 Gyrations

The compaction volumetrics were evaluated to understand the differences between the Control and ASHphalt mixtures. Table 5.3 shows the difference in mixture volumetrics for all mixture types. From this table it can be seen that the bulk specific gravity (G_{mb}) and the maximum specific gravity (G_{mm}) both increased due to the addition of CCPs. The reason for this increase is because the specific gravity of the CCPs (WE05 C, 2.71; TA11 F, 2.62; LG14 F, 2.50; SF15 SDA, 2.33) were higher than the specific gravity of asphalt binder (1.035). Since 10% of binder was being replaced with fly ash (by weight), the bulk and max specific gravities increased due to the proportional increase in the aggregate quantities. The results also demonstrate higher maximum specific gravities for the fly ashes with higher specific gravities such as WE05 (C) and TA11 (F).

Other volumetrics that demonstrate the differences are the added binder content (P_b), aggregate content (P_s), effective asphalt content (P_e), voids in the mineral aggregate (VMA), air voids (V_a), voids

filled with asphalt (VFA), and the dust-to-binder ratio. Since 10% (by mass) of asphalt content was being replaced with fly ash, the added binder content, effective asphalt binder content, voids in the mineral aggregate, and the voids filled with asphalt were all reduced as a result. The reduction in these parameters can be corellated directly to the asphalt film thickness because the film thickness was reduced as well for ASHphalt mixtures (i.e., less binder contents). However, considering that more fly ash dust (material that passes the No. 200 sieve) was added to the ASHphalt mixtures, the dust-to-binder ratio increased to 0.8 as compared to the Control mixture with 0.6 (Table 5.3).

Table 5.3 ASHphalt and Control Mixture Volumetrics

Mixture	WE05 C 10% (145C)	TA11 F 10% (145C)	LG14 F 10% (145C)	SF15 SDA 10% (145C)	CONTROL (140C)
Gmb	2.422	2.420	2.421	2.423	2.404
Gmm	2.529	2.529	2.528	2.528	2.512
Gmb/Gmm	0.958	0.957	0.958	0.958	0.957
Gsb	2.656	2.656	2.656	2.656	2.656
Gsa	2.759	2.759	2.759	2.759	2.759
Gse	2.713	2.713	2.713	2.713	2.713
Gb	1.035	1.035	1.035	1.035	1.035
Pba (%)	0.819	0.819	0.819	0.819	0.819
Pb (%)	4.950	4.950	4.950	4.950	5.500
Ps (%)	95.050	95.050	95.050	95.050	94.500
Pbe (%)	4.172	4.172	4.172	4.172	4.726
VMA (%)	13.3	13.4	13.3	13.3	14.5
Va (%)	4.2	4.3	4.2	4.2	4.3
VFA (%)	68.2	67.9	68.3	68.7	70.3
Dust-to-Binder Ratio	0.8	0.8	0.8	0.8	0.6

When evaluating the Superpave® volumetric mixture design requirements it was noted that the VMA needs to be above 14% (based on a nominal maximum aggregate size of 12.5 mm), the VFA needs to be between 65 and 78% (0.3 to < 3 ESALs in millions) or 65 and 75% (3 to < 30, 30 ≤ ESALs in millions), and the dust-to-binder ratio needs to be between 0.6 and 1.2. Evaluating the mixture volumetrics in Table 5.3 it can be observed that for the Control mixtures all of these parameters are

satisfied. For the ASHphalt mixtures however, even though all of the requirements are fulfilled, the VMA is less than 14%. Findings from this research, though, could be used to implement new evaluations on mix designs and this is a possible objective.

5.3 AGING RESISTANCE

The aging resistance was evaluated by comparing the aging index of all the mixtures. The aging index is the ratio of the number of gyrations to reach 92% G_{mm} for long-term aged materials versus the number of gyrations to reach 92% G_{mm} for short-term aged materials. The short-term aging procedure used in this research mimics the aging due to mixing, placing, and compacting whereas the long-term aging procedure used in this research represents 5 to 10 years of aging in the field. Comparing the material in these different aging conditions was critical because resisting the effects of age-hardening could potentially increase the life expectancy of the material since it would become stiffer at a slower rate.

Figure 5.5 displays the percentage of air for both the short-term and long-term compacted specimens at 8 gyrations (N_{ini}). Age hardening increases the stiffness of the material which means the compaction effort needs to increase. Figure 5.5 visually demonstrates this hardening effect due to aging. From this figure it is important to understand that mixtures with similar percentages of air at 8 gyrations resist the effects of aging. Materials with poor aging resistance reveal higher deviations in percentages of air at different aging conditions. Since there is more air in the long-term aged mixtures at 8 gyrations, these materials demonstrate age-hardening due to the increase in compaction effort.

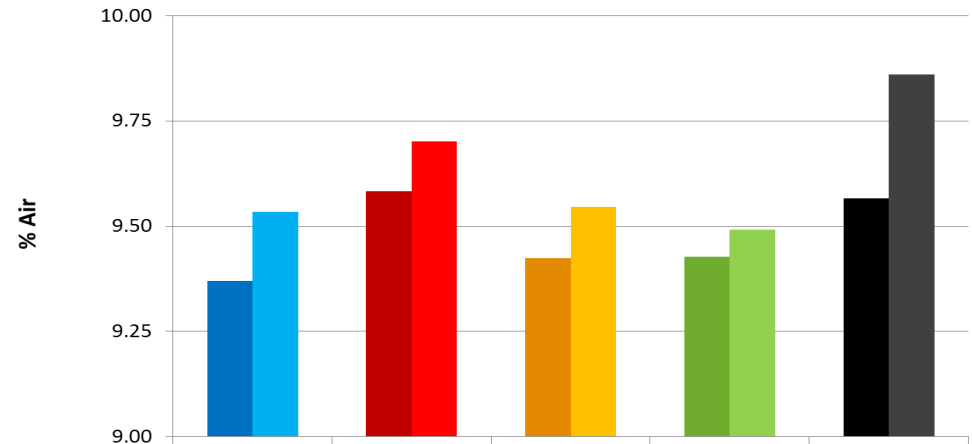

	WE05 C 10% (145C)	TA11 F 10% (145C)	LG14 F 10% (145C)	SF15 SDA 10% (145C)	CONTROL (140C)
Short-Term Aging	9.37	9.58	9.42	9.43	9.57
Long-Term Aging	9.53	9.70	9.55	9.49	9.86

Figure 5.5 Percent Air at 8 Gyrations for Short-Term and Long-Term Aged Mixtures

Table 5.4 and Figure 5.6 show the results of the aging resistance testing. Table 5.4 shows the compaction differences by comparing the average number of gyrations for long-term aged materials to reach 92% G_{mm} as compared to the short-term aged materials (i.e. the extra gyrations needed for long-term aged materials to reach 92% G_{mm}). It can be seen that all long-term aged materials needed extra gyrations to reach 92% G_{mm} which was expected. Lower values are desirable as this demonstrates better age-hardening resistance since the material does not stiffen at a fast rate over time. Figure 5.6 shows the comparisons in aging index. In this case, a lower aging index represents a material that resists age hardening. It can be seen that the SF15 (SDA) mixture performed the best with an aging index of 1.04. The LG14 (F) mix also demonstrated a better aging index of 1.06 than the Control mixture with 1.07. WE05 (C) and TA11 (F), on the other hand, revealed that these materials aged slightly worse than the Control mixture.

Table 5.4 Compaction Differences for Short-Term and Long-Term Aged Mixtures

Mixture	Gyrations to 92% G_{mm}		Difference
	Short-Term Aged	Long-Term Aged	
WE05 C 10% (145C)	14.5	15.8	1.3
TA11 F 10% (145C)	15.5	16.7	1.2
LG14 F 10% (145C)	15.0	15.8	0.8
SF15 SDA 10% (145C)	14.9	15.5	0.6
CONTROL (140C)	15.7	16.8	1.1

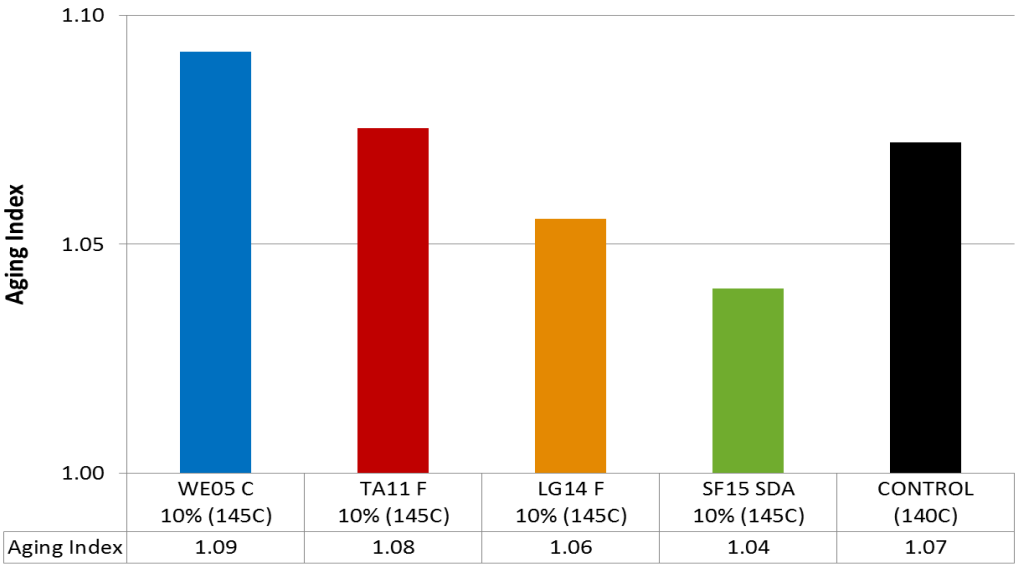

Figure 5.6 Aging Index for Control and ASHphalt Mixtures

5.4 MOISTURE DAMAGE

Moisture damage was used as a parameter to evaluate the durability of asphalt pavements. Asphalt specimens were tested under different conditions to understand the effects of moisture damage. The samples that were tested were dry, saturated, and conditioned. The dry samples were placed into a leak-proof plastic bag and then placed in a water bath at 25 ± 0.5°C for 2 hr ± 10 min and

then tested with the IDT. The saturated and conditioned specimens were both vacuum-saturated to a degree of saturation of 70 to 80%. The saturated specimens were then placed into a water bath at 25 ± 0.5°C for 2 hr ± 10 min and then tested with the IDT. The conditioned samples were placed in a water bath at 60 ± 1°C for 24 ± 1 h, then placed in a water bath at 25 ± 0.5°C for 2 hr ± 10 min and then tested with the IDT. The amount of absorbed water, as well as the degree of saturation for the saturated and conditioned samples can be seen in Table 5.5.

Table 5.5 Degree of Saturation for Control and ASHphalt Mixtures

Sample		Air Voids (%)	Air Voids (cm^3)	Absorbed Water (mL)	Degree of Saturation (%)
Saturated	WE05 C 10%	7.98	32.87	25.80	78.50
	TA11 F 10%	7.995	32.93	25.20	76.53
	LG14 F 10%	7.96	32.78	25.30	77.17
	SF15 SDA 10%	7.98	32.87	26.00	79.11
	Control	8.04	33.11	25.10	75.80
Conditioned	WE05 C 10%	7.99	32.91	24.95	75.82
	TA11 F 10%	8.02	33.01	24.95	75.59
	LG14 F 10%	7.98	32.87	25.70	78.19
	SF15 SDA 10%	7.98	32.87	25.00	76.08
	Control	7.92	32.62	25.25	77.41

The results of the Indirect Tensile Test (IDT) for dry, saturated, and conditioned samples can be seen in Table 5.6. These results demonstrate that all the ASHphalt mixtures developed higher strengths when compared to the Control mixture, however, flow (displacement) was reduced in most cases. For dry samples, the TA11 (F) mix had the highest ultimate strength of 12.21 kN whereas the Control sample only had an ultimate load of 11.50 kN. SF15 (SDA) mix had the highest flow (displacement) of 3.39 mm and WE05 (C) had the lowest flow. Load and displacement can be correlated as an inverse relationship in this case. As the maximum load increased, the maximum flow of the sample decreased.

For saturated samples it is interesting to see that the maximum load increased in certain situations as compared to the dry samples even though the samples had a degree of saturation between 70 and 80%. TA11 (F), LG14 (F), and SF15 (SDA) mixtures all demonstrated higher strength when they were saturated and then tested. The TA11 (F) and Control mixtures also experienced higher maximum flow (mm). These results have to be investigated further to understand the contribution of CCP filler.

Table 5.6 Moisture Damage Load and Flow Results

Condition	Sample	MAX Load (kN)	MAX Flow (mm)
Dry	WE05 C 10%	11.97	2.98
	TA11 F 10%	12.21	3.02
	LG14 F 10%	11.54	3.19
	SF15 SDA 10%	11.65	3.39
	CONTROL	11.50	3.23
Saturated	WE05 C 10%	11.88	2.96
	TA11 F 10%	12.34	3.29
	LG14 F 10%	11.70	2.93
	SF15 SDA 10%	11.85	3.23
	CONTROL	11.12	3.64
Conditioned	WE05 C 10%	10.39	2.84
	TA11 F 10%	10.92	2.77
	LG14 F 10%	10.65	2.90
	SF15 SDA 10%	10.72	3.14
	CONTROL	9.47	3.19

Figure 5.7 shows different samples that underwent dry testing and conditioned testing. Figure 5.7a shows the dry sample and Figure 5.7b shows the moisture damaged specimen. Samples that experience excessive moisture damage have large amounts of aggregate exposed due to the stripping of the asphalt binder. This result demonstrates minimal moisture damage if not any since there are few aggregates exposed. The resistance for these specimens to resist moisture damage is critical and from this result there seems to be minimum moisture damage which is an excellent outcome.

Figure 5.7 Representative Sample Exposed to (a) Dry Condition (b) Moisture Damage

Figure 5.8 demonstrates the horizontal tensile stress and Figure 5.9 demonstrates the vertical tensile stress of the ASHphalt and Control samples. These results give a visual correlation to the maximum load results represented in Table 5.5. From these figures it can be seen that the maximum vertical and horizontal stresses for ASHphalt samples were higher than the Control samples. For dry samples, TA11 (F) had the highest maximum horizontal stress of 1.51 MPa and a maximum vertical stress of 4.52 MPa. The Control mixtures only had a maximum horizontal stress of 1.42 MPa and a vertical stress of 4.25 MPa which is lower than all ASHphalt samples.

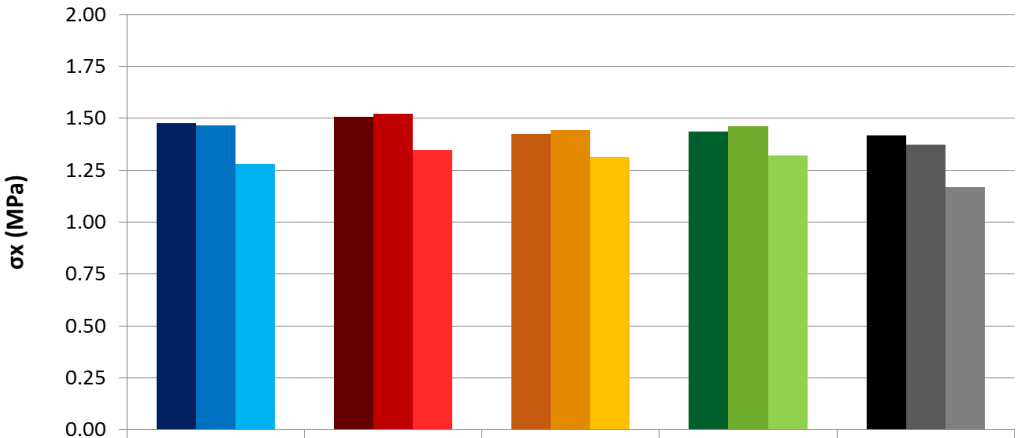

	WE05 C 10%	TA11 F 10%	LG14 F 10%	SF15 SDA 10%	CONTROL
Dry	1.48	1.51	1.42	1.44	1.42
Saturated	1.46	1.52	1.44	1.46	1.37
Conditioned	1.28	1.35	1.31	1.32	1.17

Figure 5.8 Horizontal Tensile Stress at Center of Specimen

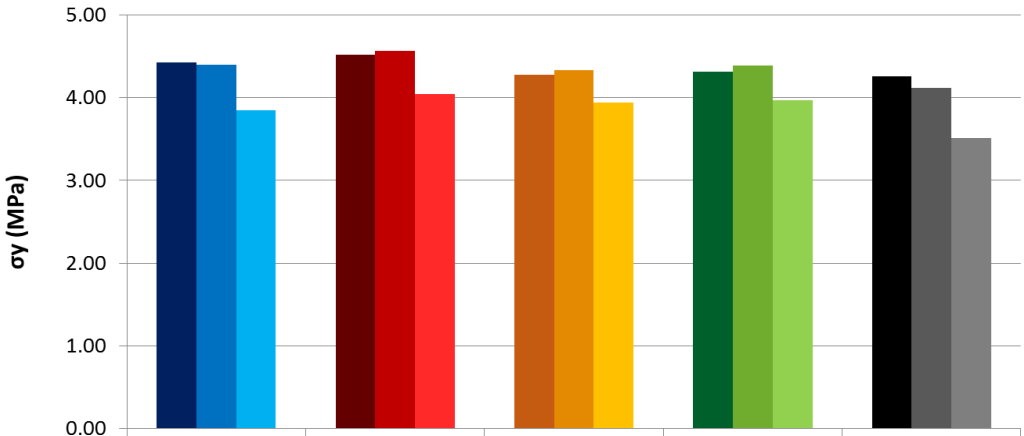

	WE05 C 10%	TA11 F 10%	LG14 F 10%	SF15 SDA 10%	CONTROL
Dry	4.43	4.52	4.27	4.31	4.25
Saturated	4.39	4.57	4.33	4.39	4.12
Conditioned	3.84	4.04	3.94	3.97	3.51

Figure 5.9 Vertical Compressive Stress at Center of Specimen

Figure 5.10 shows the tensile strain at failure for the ASHphalt and Control specimens. These results give a visual representation of the maximum flow (displacement) results represented in Table 5.5. This figure demonstrates the effects of moisture damage on the ability for asphalt pavements to deform. For conditioned specimens the strain at failure is reduced in all cases. It is interesting to see

that the ultimate strain (related to flow) increases for the saturated TA11 (F) and Control specimens. The SF15 (SDA) mixtures experienced the highest strain at failure of 0.0694 mm/mm for the dry samples and WE05 (C) experienced the lowest strain at failure of 0.0611 mm/mm for the dry samples.

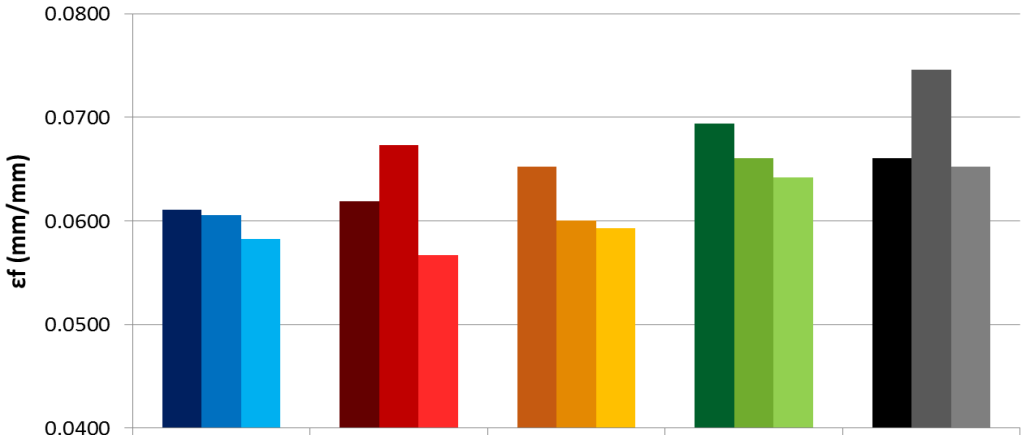

	WE05 C 10%	TA11 F 10%	LG14 F 10%	SF15 SDA 10%	CONTROL
Dry	0.0611	0.0619	0.0653	0.0694	0.0660
Saturated	0.0606	0.0673	0.0601	0.0660	0.0746
Conditioned	0.0582	0.0567	0.0593	0.0642	0.0653

Figure 5.10 Tensile Strain at Failure

The Tensile Strength Ratio (TSR) was calculated and compared for conditioned and dry samples (Figure 5.11), as well as for conditioned and saturated samples (Figure 5.12). The TSR values are required to be at or above 80%; the results demonstrate that all mixtures fulfilled this requirement. Higher values of TSR are desired as this indicates a better performance in terms of moisture damage resistance. It can be observed that all ASHphalt mixtures enhanced the moisture damage resistance when compared to the Control mixture. When comparing the conditioned samples with the dry samples, LG14 (F) performed the best since the TSR was 0.923 and the Control performed the worst with a TSR of 0.824. When comparing the conditioned samples with the saturated samples LG14 (F) also performed the best with a TSR of 0.911 and the Control samples performed the worst with a TSR of 0.852.

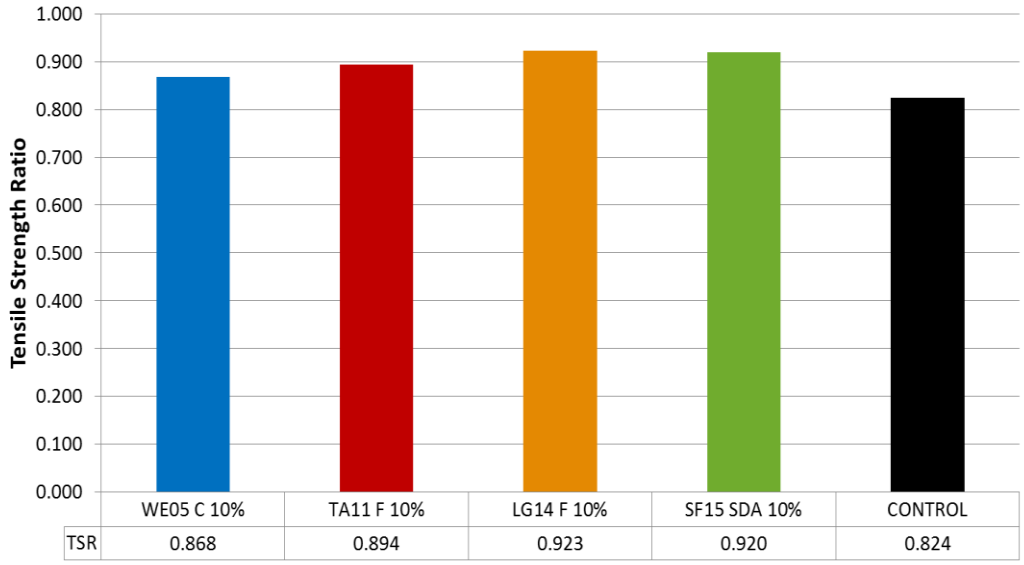

Figure 5.11 TSR Conditioned Samples Compared with Dry Samples

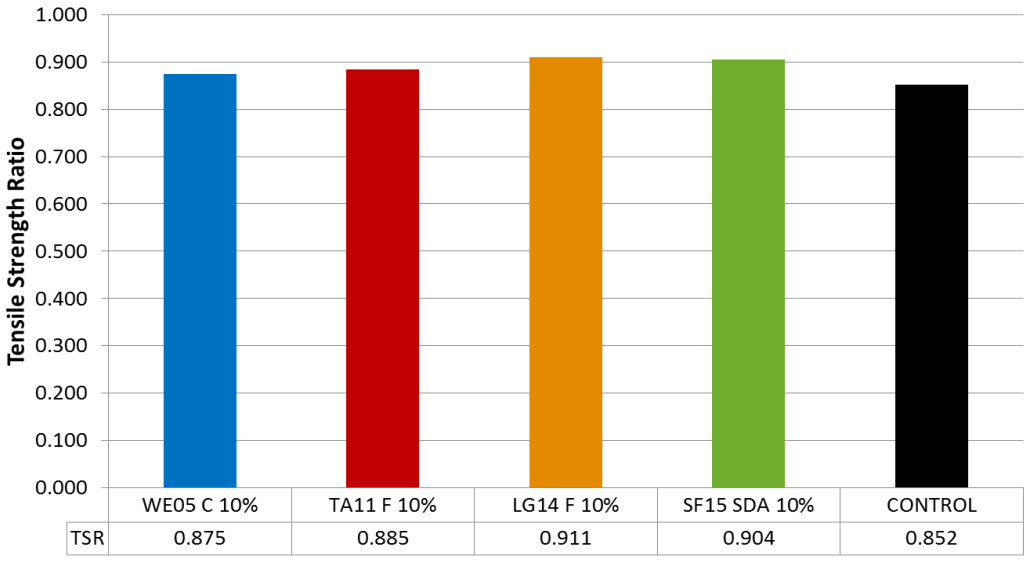

Figure 5.12 TSR Conditioned Samples Compared with Saturated Samples

In terms of moisture damage resistance it can be concluded that ASHphalt mixtures resisted the effects of moisture damage better than the Control mixtures. The results proved that adding CCPs to asphalt mixtures enhanced the moisture damage resistance. The ASHphalt mixtures also demonstrated higher strengths in IDT which is an important parameter.

5.6 FATIGUE RESISTANCE

Fatigue cracking resistance was evaluated to understand the number of cycles each specimen can withstand till failure. The fatigue test that was used evaluated the slope of the secondary fatigue section as well as the failure point (N_f) which is where the tertiary fatigue section started. It was determined that at this point, the Complex Modulus (E*) started to decrease since the slope of the deformation (strain) line increased. Asphalt pavements that demonstrated smaller deformation rates, as well as demonstrated higher amounts of cycles till failure were considered to be desired.

For this study, fatigue was assessed by using a sine wave loading condition, a test temperature of 20 to 25^{o}C, a 2% pre-loading condition, a 20% ultimate loading condition, and a frequency of 10 Hz. After evaluating the IDT results for the dry samples it was decided to use an ultimate load of 11.0 kN. Using this ultimate load resulted in a 20% ultimate load of 2.2 kN, a 2% pre-loading of 0.2 kN, an amplitude of approximately 1.0 kN (reference line was at 1.2). The fatigue test was ran until the material failed. Figure 5.13 shows a WE05 (C) sample being tested and a fatigue crack propagating in the center of the sample. Figure 5.14 shows a representative sample that failed due to fatigue cyclic loading.

Figure 5.13 Fatigue Crack Propagating for a WE05 C 10% Sample

Figure 5.14 Representative Sample Failed in Fatigue

The results of the fatigue testing can be seen in Figure 5.15 and Figure 5.16. These results demonstrate the performance of duplicate samples that were tested in fatigue. These figures show the results for the initial deformation, primary, and secondary fatigue phases (tertiary phase was removed). As seen from these figures, all the ASHphalt samples performed better than the control

mixtures because the samples were able to withstand much more cycles than the Control samples. The slopes of all ASHphalt samples in the secondary fatigue sections were also lower than the Control samples which means that there was a slower rate of deformation due to loading. This decrease in deformation rate is critical because it is a characteristic of an elastic material that can recover from deformation and this parameter is directly related to fatigue cracking resistance.

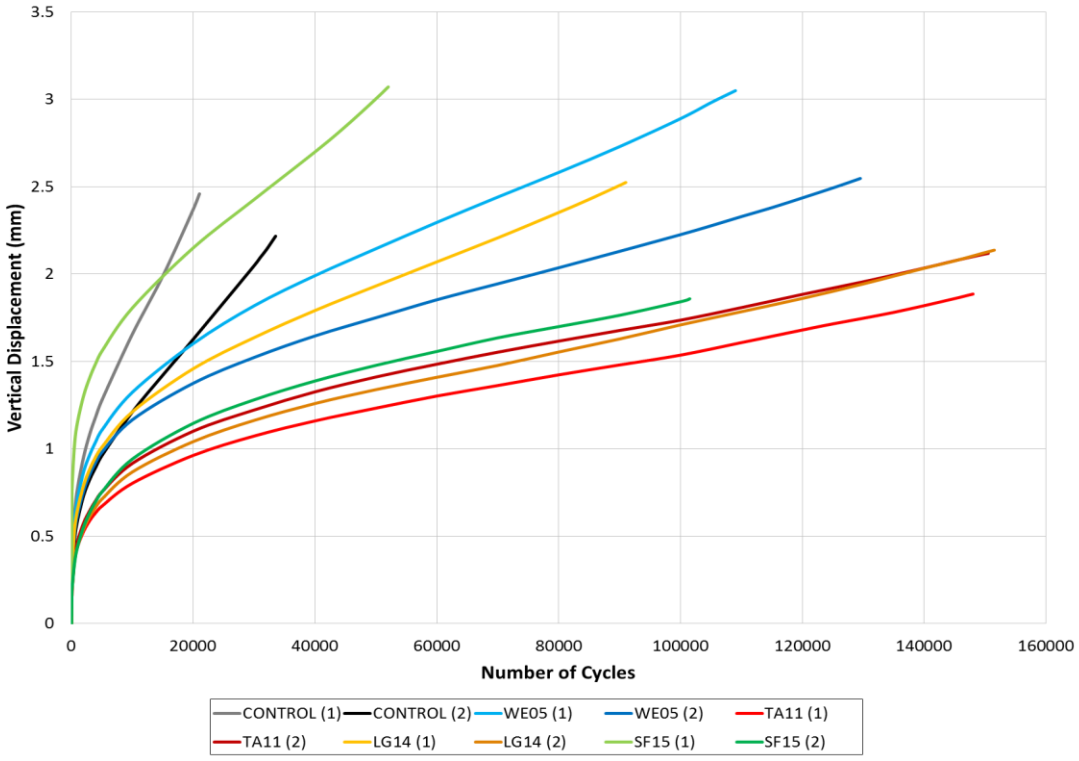

Figure 5.15 Fatigue Vertical Displacement vs. Number of Cycles

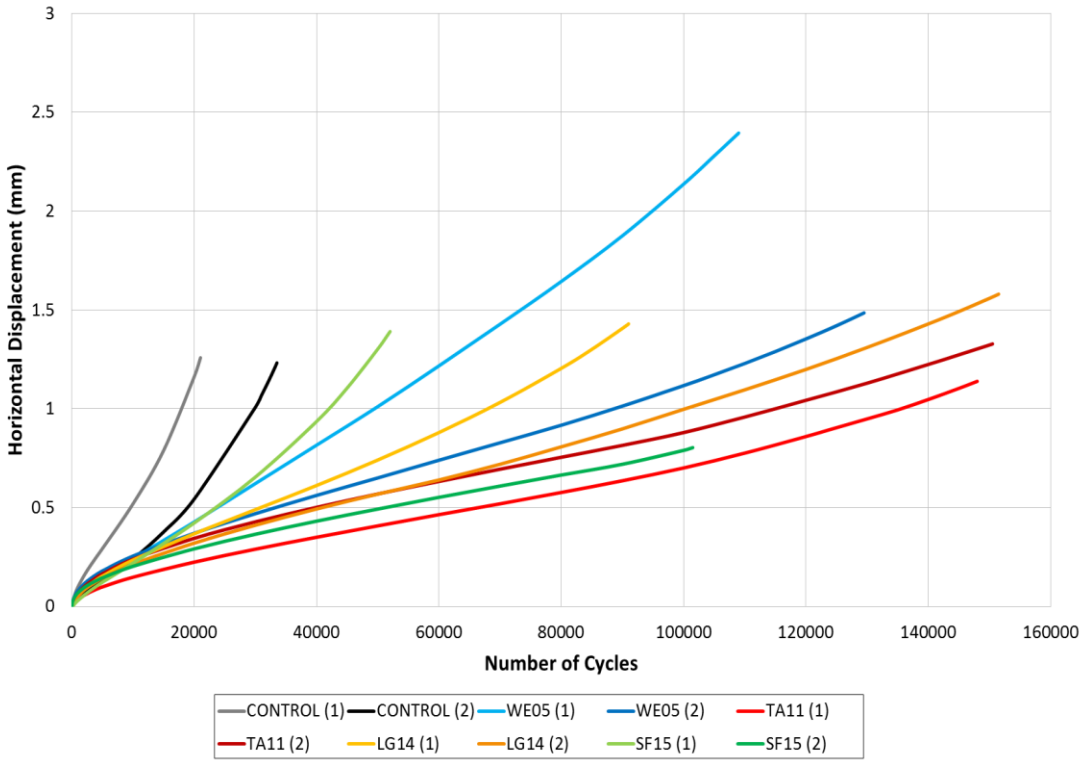

Figure 5.16 Fatigue Horizontal Displacement vs. Number of Cycles

Figure 5.17 and Figure 5.18 display the actual vertical and horizontal deformation fatigue slopes (from the secondary fatigue sections) of the materials. The gage lengths for measured deformations were different for the vertical and horizontal displacements which is why these values are not the same for most cases. Regardless, both displacement results show similar trends. The TA11 (F) mixture demonstrated the lowest deformation rate of 6.52E-06 mm/cycle in the vertical direction and 6.95E-06 mm/cycle in the horizontal direction. The Control samples performed the worst as these samples deformed at a rate of 5.72E-05 mm/cycle in the vertical direction and 5.70E-05 mm/cycle horizontal directions. The remaining ASHphalt samples still performed much better than the Control samples and this is a significant discovery.

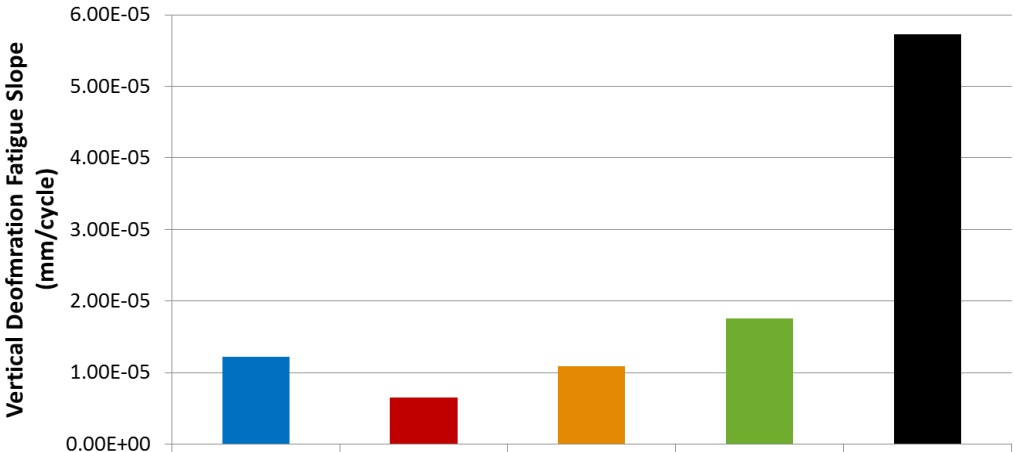

	WE05 C 10%	TA11 F 10%	LG14 F 10%	SF15 SDA 10%	CONTROL
Vertical Deformation Slope (mm/cycle)	1.22E-05	6.52E-06	1.09E-05	1.76E-05	5.72E-05

Figure 5.17 Vertical Deformation Fatigue Slope

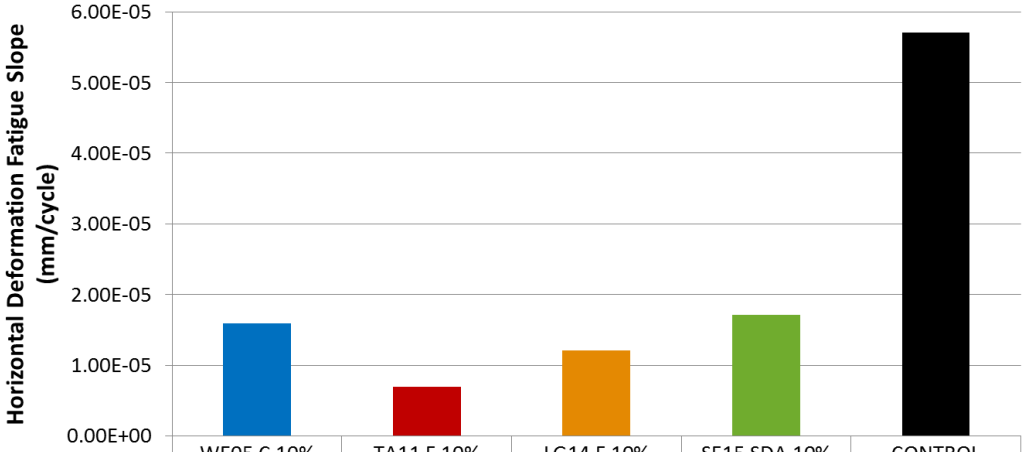

	WE05 C 10%	TA11 F 10%	LG14 F 10%	SF15 SDA 10%	CONTROL
Horizontal Deformation Slope (mm/cycle)	1.59E-05	6.95E-06	1.21E-05	1.71E-05	5.70E-05

Figure 5.18 Horizontal Deformation Fatigue Slope

Figure 5.19 demonstrates the number of cycles that the samples could withstand till there was a drop in E* (Complex Modulus). This drop in E* is directly correlated to N_f as this is the defined point of failure. The results demonstrate that TA11 (F) mixtures performed the best since this mixture type lasted for 149,250 cycles in fatigue without a decrease in E*. As seen from previous results, the

Control samples performed the worst since these were only able to withstand 27,250 cycles till failure. These results can be correlated to the IDT results in that the samples with higher ultimate strengths and flow could last longer. The TA11 (F) mixtures demonstrated superior strengths in IDT and average flow properties and it was seen in this case that this material had performed the best. Specimens like SF15 (SDA) and Control samples had excellent flow but relatively weak strength and this resulted in lower number of cycles till E* dropped. Regardless, every ASHphalt sample was able to endure more loading cycles before the failure than the Control samples and this is an important find.

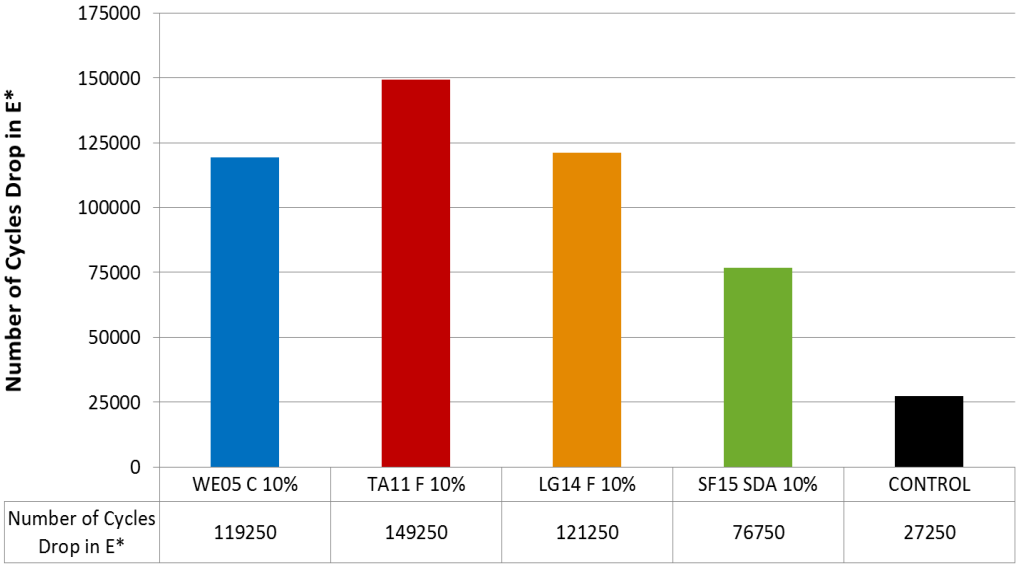

Figure 5.19 Number of Cycles Drop in E*

Figure 5.20 and Figure 5.21 demonstrate the total vertical and horizontal deformations at failure. These results are interesting in that they do not correlate directly to the maximum flow (deformation) results obtained from IDT testing. As seen from these results, WE05 (C) mixtures were able to deform the most vertically with 2.8 mm and horizontally with 1.94 mm till failure. In the dry IDT testing, the WE05 (C) specimens only deformed 2.98 mm which was the lowest deformation for IDT testing. This correlation needs to be investigated further to develop conclusions.

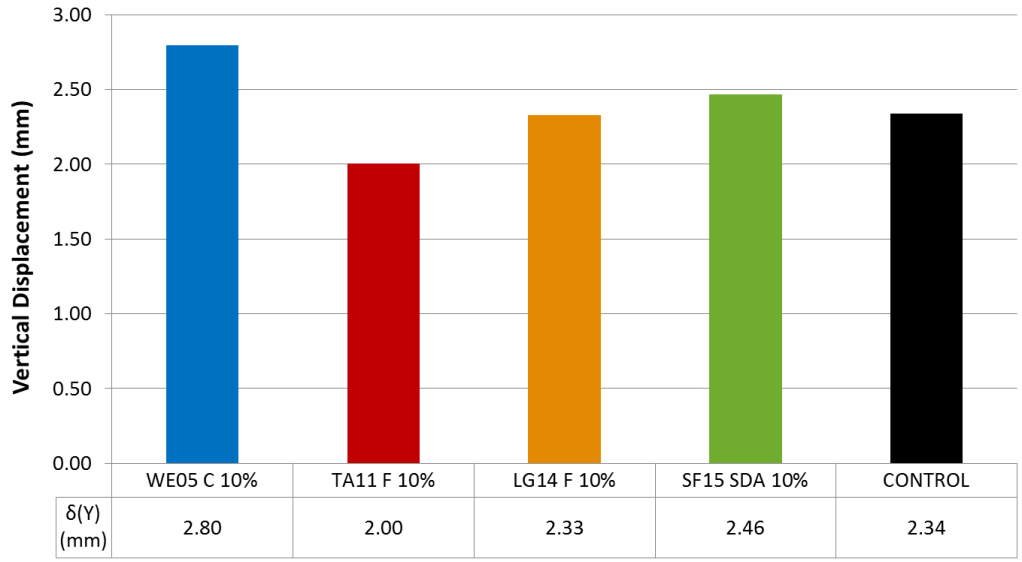

Figure 5.20 Vertical Displacement at Failure (N_f)

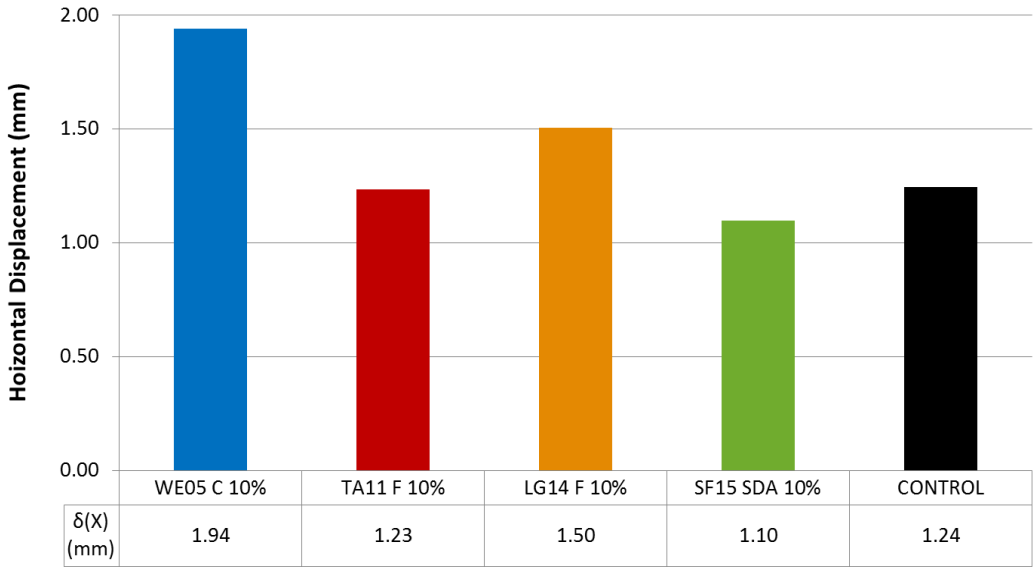

Figure 5.21 Horizontal Displacement at Failure (N_f)

The results of this study prove that ASHphalt mixtures perform better in respect to intermediate-temperature fatigue cracking resistance. Every ASHphalt mixture demonstrated smaller deformation fatigue slopes, and these mixtures were all able to withstand more loading cycles till failure.

5.7 THERMAL-CRACKING RESISTANCE

The Semi-Circular Bending (SCB) test was used to determine the low-temperature (-18°C) properties such as Fracture Energy (G_f), Fracture Toughness (K_{IC}), and Stiffness (S). Asphalt mixtures become brittle at low temperatures and when the developing thermal stresses become too large, the pavement cracks as a result. Therefore, asphalt materials that are too brittle at low temperature are undesirable whereas materials that are more elastic perform better since these are able to recover from the emerging stresses. For this testing, higher values of both G_f and K_{IC} are desirable as this demonstrates larger amounts of energy that is necessary to crack the specimen. On the other hand, lower stiffness values are desirable as this demonstrates a more ductile material that can recover from the stresses that are developed due to traffic loads.

Figure 5.22 shows a representative sample that failed in the SCB test. This figure is a perfect example of how asphalt pavements become brittle and then crack due to lower temperatures. It can be seen that the shear forces directly severed the aggregate particles and also created large stresses in the mixture which eventually resulted in failure.

Figure 5.22 Representative Sample Failed in SCB

The SCB test is performed at -18°C by applying a vertical load on the specimen at a rate of 0.03 mm/min and the test is done once the load decreases to 0.5 kN. Table 5.7 and Figure 5.23 show the results from the SCB testing. From these results it can be seen that the LG14 (F) was the only ASHphalt mixture that had higher ultimate strengths than the Control mixture. The SF15 (SDA) mix was the only sample that achieved a higher horizontal displacement (δ(X)) than the Control mixture. At the same time, all ASHphalt mixtures were able to achieve higher load-line displacements (δ(Y)). The load-line displacement curves also demonstrate the rapid brittle failure of all asphalt mixtures.

Table 5.7 SCB Testing Results

Sample	Ultimate Load (kN)	δ(Y) @ 0.5 kN (mm)	δ(X) @ 0.5 kN (mm)
WE05 C 10%	2.41	0.33	0.11
TA11 F 10%	2.47	0.50	0.14
LG14 F 10%	2.99	0.57	0.09
SF15 SDA 10%	2.20	0.43	0.16
CONTROL	2.50	0.32	0.15

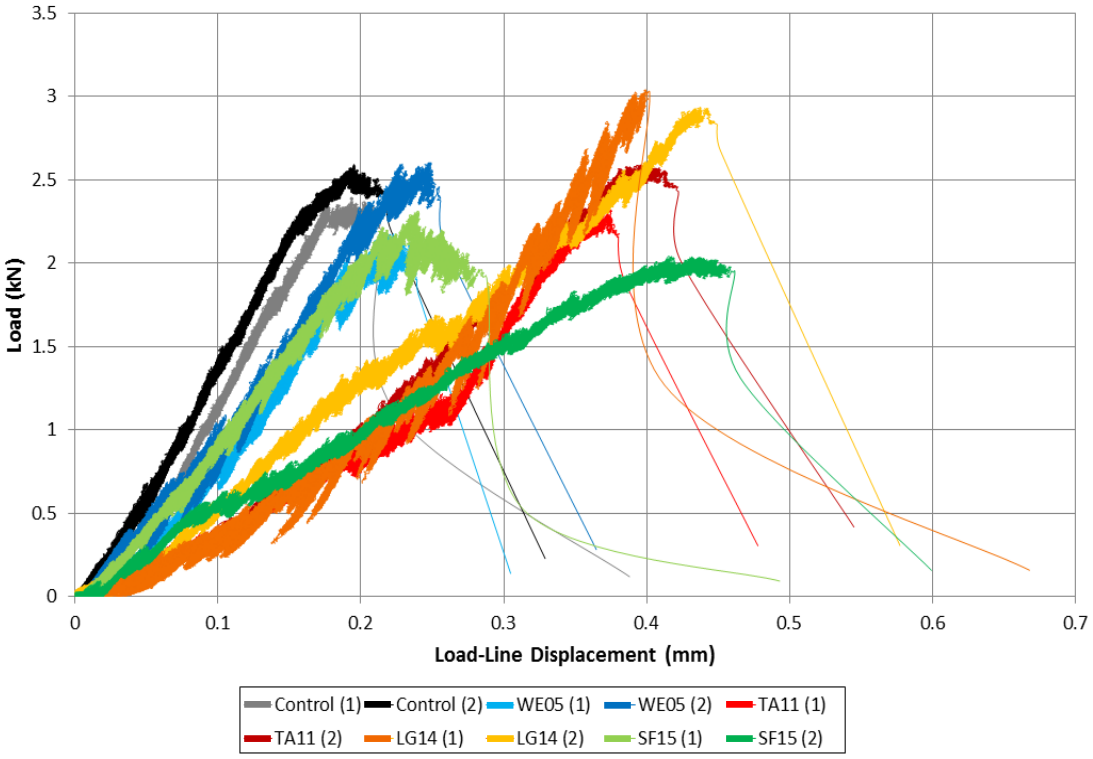

Figure 5.23 Load vs. Load-Line Displacement Curves

Figure 5.24 demonstrates the Fracture Energy (G_f) of investigated asphalt materials. As previously mentioned, larger values of G_f are desirable as this demonstrates larger energy required to create a unit surface area of crack. This is obtained by dividing the work of fracture (area under the load vs. load line displacement curve) by the ligament area. From the results it can be seen that all ASHphalt mixtures performed better than the Control mixture in terms of G_f. The LG14 (F) mix performed the best as this mixture was able to achieve a G_f value of 1.25 J/m^2. These results are extremely significant since this demonstrates improved performance of ASHphalt mixtures at low temperature.

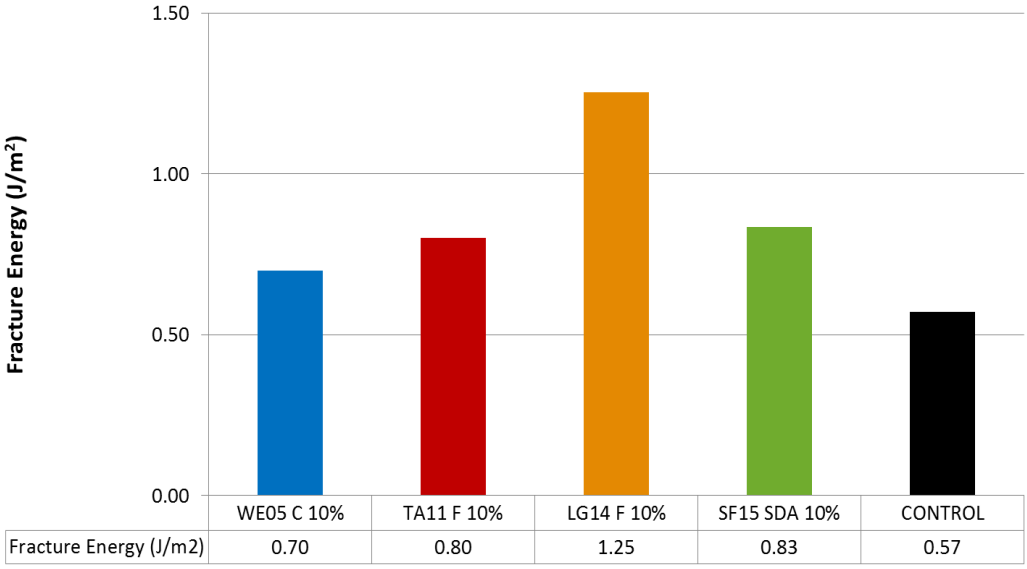

Figure 5.24 Fracture Energy (G_f) Results

The Fracture Toughness (K_{IC}) is the ability of the asphalt sample to resist fracture due to material toughness. Larger values of K_{IC} are desirable as this demonstrates larger ultimate loads upon material failure. From Figure 5.25 it can be seen that LG14 (F) achieved the highest K_{IC} value of 1.22 Pa*m$^{0.5}$. In contrast, SF15 (SDA) had the lowest KIC value of 0.90 Pa*m$^{0.5}$. Since K_{IC} is directly related to ultimate strengths (Table 5.7), these results make sense. As strengths increase, the fracture toughness increases.

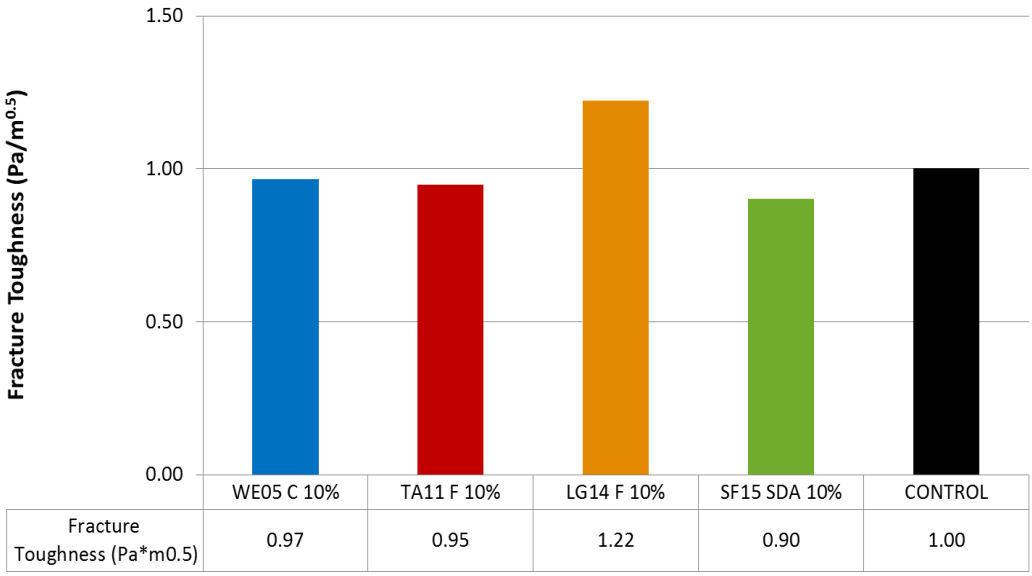

	WE05 C 10%	TA11 F 10%	LG14 F 10%	SF15 SDA 10%	CONTROL
Fracture Toughness (Pa*m0.5)	0.97	0.95	1.22	0.90	1.00

Figure 5.25 Fracture Toughness (K_{IC}) Results

The Stiffness (S) is represented as the slope of the linear portion of the load-line displacement curve. Lower stiffness values are desirable since this demonstrates a more elastic material that can recover from low-temperature stress accumulations. Figure 5.26 shows the stiffness results from the SCB testing. From these results it can be seen that all ASHphalt mixtures performed better than the Control mixture since the stiffness values were much lower. The TA11 (F) mix demonstrated the lowest stiffness of 5.90 kN/mm whereas the Control mixture obtained the highest stiffness of 14.27 kN/mm. These results reveal that the Control mixture is much more brittle at the low temperature as compared to the ASHphalt mixtures which acted in a more elastic manner.

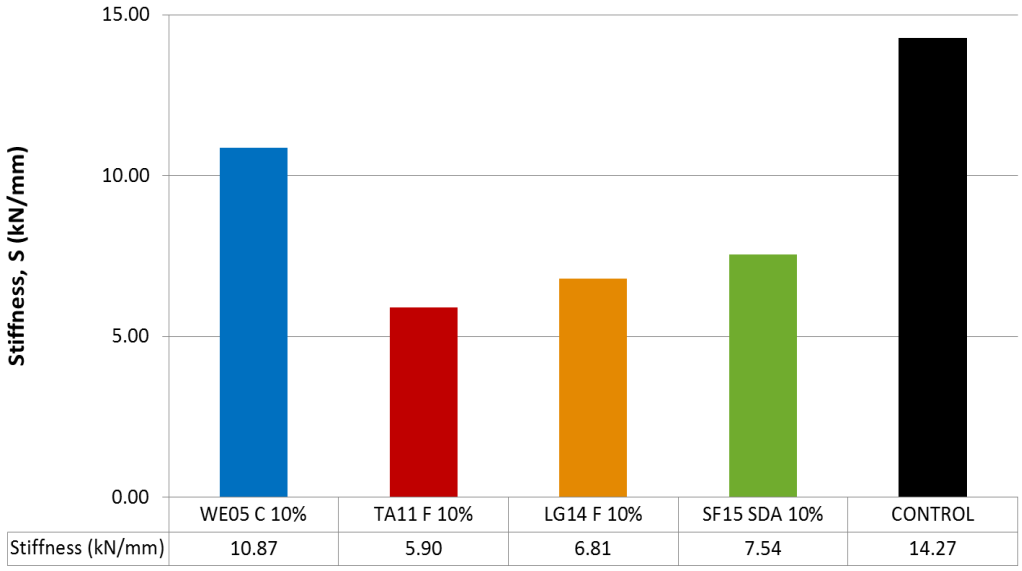

Figure 5.26 Stiffness (S) Results

In terms of thermal cracking resistance, it can be concluded that ASHphalt mixtures resisted the effects of low-temperature cracking better than the Control mixtures for Fracture Energy (Gf) and Stiffness (S) evaluations. For Fracture Toughness (KIC), LG14 (F) was the only material that performed better than the Control mixture. These results prove that adding CCPs to asphalt mixtures enhance low-temperature thermal cracking resistance.

CHAPTER 6.

CONCLUSIONS

The developments of this research produced very promising results which is essential for implementation of ASHphalt pavements. The research findings can be summarized as follows:

1. Asphalt film thickness, which is an important characteristic related to binder coating, was higher for the Control mixtures (9.03 μm) as compared to the ASHphalt mixtures (7.66 μm). However, there were no major differences observed for aggregate coating quality or mixing performance.
2. Preliminary study results demonstrated a need for higher compaction effort for ASHphalt mixtures than Control mixtures when compacted at the same 140^{o}C temperature. The ASHphalt mixtures in the preliminary study had WE05 (C) fly ash at 10% (by mass) binder replacement and this proved to increase stiffness since compaction effort was greater.
3. The workability was used to evaluate the differences in compaction efforts for ASHphalt (compacted at 145^{o}C) and Control mixtures (compacted at 140^{o}C). The increase by 5^{o}C for ASHphalt mixtures reduced the compaction efforts, so WE05 (C), LG14 (F), and SF15 (SDA) mixtures had demonstrated less compaction effort than the Control mixture. The TA11 (F) mix revealed the same densification profile as the Control mixture due to a higher mastic viscosity.
4. The research results proved that the use of fly ash in asphalt can drastically improve the aging resistance. For example, SF15 (SDA) mixtures performed the best in terms of aging resistance since this mixture had the lowest aging index of 1.04 when compared to the Control mixture which had an aging index of 1.07. LG14 (F) also produced excellent results as it yielded an aging index of 1.06.

5. It was demonstrated that all ASHphalt samples produced higher ultimate strengths in dry Indirect Tensile Testing (IDT) than the Control samples. The WE05 (C) and TA11 (F) mixtures developed the highest strengths of 11.97 kN and 12.21 kN. The Control mixtures only produced strengths of 11.50 kN. The SF15 (SDA) demonstrated the highest ultimate deformation at failure of 3.39 mm.
6. The research results demonstrated that all ASHphalt mixtures had improved moisture-damage resistance based on the Tensile Strength Ratio (TSR) parameter as compared to the Control mixtures. The LG14 (F) mixture had the highest TSR of 0.911 and the Control mixture had the lowest TSR of 0.852.
7. Intermediate-temperature fatigue cracking analysis proved that all ASHphalt mixtures performed considerably better than the Control mixtures. The secondary fatigue deformation rate of the TA11 (F) mix was the lowest deformation rate of 6.52E-06 mm/cycle in the vertical direction and 6.95E-06 mm/cycle in the horizontal direction. The Control samples performed the worst as these samples deformed at a rate of 5.72E-05 mm/cycle in the vertical direction and 5.70E-05 mm/cycle and horizontal directions. All ASHphalt mixtures also performed better than the Control mixtures in terms of drop in Complex Modulus (E*). The TA11 (F) mix was able to withstand up to 149,250 loading cycles till there was a drop in E* (i.e., point of failure) which was the most experienced by any mixture. The Control samples were only able to withstand 27,250 cycles till there was a drop in E*. Therefore, the addition of CCPs in asphalt mixtures improves fatigue resistance.
8. Low-temperature thermal cracking resistance demonstrated improved results for ASHphalt mixtures. All ASHphalt mixtures performed better in terms of Fracture Energy (G_f) than the Control mixture. LG14 (F) had the highest G_f value of 1.25 J/m^2 resulting in better performance, and the Control mixture only had a G_f value of 0.57 J/m^2. For Fracture Toughness (K_{IC}), only LG14

(F) performed better than the Control mixture with a K_{IC} value of 1.22 $Pa*m^{0.5}$. All ASHphalt mixtures performed better than the Control mixture in terms of Stiffness (S). TA11 (F) mixtures demonstrated the lowest stiffness of 5.90 kN/mm whereas the Control mixture obtained the highest stiffness of 14.27 kN/mm.

CHAPTER 7.

FUTURE WORK

Even though this research has produced excellent results for ASHphalt evaluations, future work can be developed to investigate other experimental areas where ASHphalt pavement performance could be improved. The following recommendations illustrate areas of future interest:

1. For compaction, the use of softeners, such as plasticizers, could be incorporated into the ASHphalt mixtures to facilitate the compaction effort. Adding softeners to ASHphalt mixtures could reduce the stiffness during mixing, placing, and compacting and this could potentially allow for lower temperature evaluations during these phases.
2. The methodology in this research project can also be used to improve other asphalt technologies such as Cold Mix Asphalt (CMA), Warm-Mix Asphalt (WMA) and even Stone-Mastic Asphalt (SMA). The WMA is useful in that these mixtures can be mixed, placed, and compacted at lower temperatures which reduces the costs associated with production and this can also extend the construction season. The SMA is a dense wearing course material that prevents rutting since the large voids are filled with asphalt mastic. Both asphalt mixture types could also benefit from being mixed with fly ash material as this enhances the performance.
3. Using high-volume CCP based mastics and mixtures could be beneficial as a repair material. The Cold-Mix Asphalt (CMA) produces a weak solution to pothole repair. An alternative would be to incorporate CCPs into CMA mixtures which can be engineered for repair applications and this could ultimately enhance performance during extreme loading and environmental conditions. These mixtures could also develop stronger bonds to the existing materials surrounding the pothole.

CHAPTER 8.

REFERENCES

1. **American Coal Ash Association (ACAA). (2006).** "Fly Ash Facts for Engineers". *Federal Highway Administration*. FHWA-IF-03-019.
2. **Anderson, D. A., Brock, D., & Tarris, J. P. (1982).** "Dust Collector Fines and their Influence on Mixture Design". *AAPT*. Proceeding No. 51, 363-374.
3. **Anagnos, J. N., Kennedy, T. W. (1972).** "Practical Method of Conducting the Indirect Tensile Test". *Center for Highway Research.* University of Texas, Research Report 98-10.
4. **Asphalt Institute. (2001).** "Superpave Mix Design. Superpave Series No. 2 (SP-02)". *Asphalt Institute*. Lexington, KY.
5. **Asphalt Institute. (2003).** "Performance Graded Asphalt Binder Specification and Testing". Superpave Series No. 1 (SP-1). *Asphalt Institute*. Lexington, KY
6. **AASHTO R30-02. (2013).** "Mixture Conditioning of Hot Mix Asphalt (HMA)". *American Association of State Highway and Transportation Officials.*
7. **AASHTO T2830-7. (2013).** "Resistance of Compacted Hot Mix Asphalt (HMA) to Moisture-Induced Damage". *American Association of State Highway and Transportation Officials*.
8. **AASHTO T312-12. (2013).** "Preparing and Determining the Density of Hot Mix Asphalt (HMA) Specimens by Means of the Superpave Gyratory Compactor". *American Association of State Highway and Transportation Officials*.
9. **AASHTO T322-04. (2013).** "Determining the Creep Compliance and Strength of Hot-Mix Asphalt (HMA) Using the Indirect Tensile Test Device". *American Association of State Highway and Transportation Officials.*

10. **AASHTO T342-11. (2013).** “Determining Dynamic Modulus of Hot Mix Asphalt (HMA)”. *American Association of State Highway and Transportation Officials.*
11. **ASTM C136 / C136M-14. (2014).** “Standard Test Method for Sieve Analysis of Fine and Coarse Aggregates”. *ASTM International*. West Conshohocken, PA.
12. **ASTM D4123-82. (2003).** “Standard Test Method for Indirect Tension Test for Resilient Modulus of Bituminous Mixtures”. *ASTM International*, West Conshohocken, PA.
13. **ASTM D4464-15. (2015).** “Standard Test Method for Particle Size Distribution of Catalytic Materials by Laser Light Scattering”. *ASTM International*, West Conshohocken, PA.
14. **ASTM D5550-14. (2014).** “Standard Test Method for Specific Gravity of Soil Solids by Gas Pycnometer”. *ASTM International*, West Conshohocken, PA.
15. **ASTM D6752 / D6752M-11. (2011).** “Standard Test Method for Bulk Specific Gravity and Density of Compacted Bituminous Mixtures Using Automatic Vacuum Sealing Method”. *ASTM International*, West Conshohocken, PA.
16. **ASTM D6857 / D6857M-11. (2011).** “Standard Test Method for Maximum Specific Gravity and Density of Bituminous Paving Mixtures Using Automatic Vacuum Sealing Method”. *ASTM International*, West Conshohocken, PA.
17. **ASTM E986-04. (2010).** “Standard Practice for Scanning Electron Microscope Beam Size Characterization”. *ASTM International*, West Conshohocken, PA.
18. **Bautista, E. G. et al. (2015).** "Experimental Evaluation of the Effect of Coal Combustion Products on Constructability, Damage, and Aging Resistance of Asphalt Mastics". *Theses and Dissertations.* Paper 858.
19. **Bentur, A., Gray, R., Mindess, S., & Young, J. F. (1998).** “The Science and Technology of Civil Engineering Materials”. *Prentice Hall.*

20. **Bianchetto, H., Martinez, A., Miro, R., & Perez, F. (2005).** "Proceedings of the Annual Meeting of the Transportation Research Board: Effect of Filler on the Aging Potential of Asphalt Mixtures". *TRB.* Washington, DC.Asdfadf
21. **Brown, E. R., McRae, J. L., & Crawley, A. (1989).** "Effect of Aggregates on Performance of Concrete". *ASTM*. Special Technical Publication 1016.
22. **Carpenter, C. A. (1952).** "A Comparative Study of Fillers in Asphaltic Concrete". *Public Roads*. 27, 101-110.Asdf
23. **DeFoe, J. H. (1983).** "Evaluation of Sulfur-Asphalt Binder for Bituminous Resurfacing Mixtures". *Michigan Department of Transportation.* Research report R1-1220, Research Project 74-D-29.Asd
24. **Domone, P., & Illston, J. (2010).** "Construction Materials: Their Nature and Behavior (4th Edition*)". Spon Press*, New York, New York. 2010.
25. **Doyle, P. C. (1958).** "Cracking Characteristics of Asphalt Cement". Proceedings *AAPT*, Vol. 27.
26. **Elwardany, M. D., Rad, F. Y., Castorena, C., & Kim, Y. R. (2010).** "Evaluation of Asphalt Mixture Laboratory Long-Term Aging Methods for Performance Testing and Prediction". *Cooperative Highway Research Program.* Project No. 9-39, National Research Council, Washington, D.C.
27. **Faheem, A. F., & Bahia, H. U. (2009).** "Conceptual Phenomenological Model for Interaction of Asphalt Binders with Mineral Fillers". *Doctoral dissertation*. University of Wisconsin-Madison, Madison, WI.
28. **Faheem, A. F., & Bahia H. U. (2010).** "Modelling of Asphalt Mastic in Terms of Filler-Bitumen Interaction".
29. **Faheem, A. F., Hintz, C., & Bahia, H. U. (2011).** "Test Methods and Specification Criteria for Mineral Filler Used in HMA", NCHRP 9-45 Final Report.
30. **Finn, F. N. (1967).** "Factors Involved in the Design of Asphaltic Pavement Surfaces". *HRB*, NCHRP Report 39.

31. **Finn, F. N., Nair, K., & Hilliard, J. M. (1978).** "Minimizing Premature Cracking in Asphaltic Concrete Pavement". *TRB*, NCHRP Report 195.
32. **Fromm, H. J., & Phang, W. A. (1971).** "Temperature Susceptibility Control in Asphalt Cement Specifications". *HRB*, Highway Research Record 350.
33. **Gaw, W. J. (1977).** "Measurement and Prediction of Asphalt Stiffness and Their Use in Developing Specifications to Control Low-Temperature Pavement Transverse Cracking". *ASTM*, Special Technical Publication 628.
34. **Goetz, W. H., & Wood, L. E. (1960).** "Bituminous Materials and Mixtures". *Highway Engineering Handbook.* Ed. K. B. Woods, Section 18, McGraw-Hill, New York, NY.
35. **Goetz, R. O., Tons, E., & Razi, M. (1983).** "Fly Ash as Asphalt Reducer in Bituminous Base Courses". *The Board of Water and Light, Consumer Power Co & Detroit Edison Co.* University of Michigan, Detroit, MI.
36. **Hadley, W. O., Hudson, W. R., & Kennedy, T. W. (1970).** "A Method of Estimating Tensile Properties of Materials Tested in Indirect Tension. *Center for Highway Research*. University of Texas, Research Report 98-7.
37. **Hadley, W. O., Hudson, W.R., & Kennedy, T. W. (1972).** "An Evaluation of Factors Affecting the Tensile Properties of Asphalt-Treated Materials". *Center for Highway Research.* University of Texas, Research Report 98-2.
38. **Hartman, A. M., Gilchrist, M. D., Walsh, G. (2001).** "Effect of Mixture Compaction on Indirect Tensile Stiffness and Fatigue". *Journal of Transportation Engineering.* Journal 127, 370-378.
39. **Henning, N. E. (1974).** "Evaluation of Lignite Fly Ash as a Mineral Filler in Asphaltic Concrete". *Twin Cities Testing and Engineering Laboratory.* Report No. 2, St. Paul, MN.
40. **Hmoud, H. R. (2011).** "Evaluation of VMA and Film Thickness Requirements in Hot-Mix Asphalt". *Modern Applied Science.* Vol. 5, No. 4, Baghdad University, Baghdad, Iraq.

41. **Howell, H. C., Hudson, S. B., & Warden, W. B. (1952).** "Proceedings of the Association of Asphalt Paving Technologists: Evaluation of Mineral Filler in Terms of Practical Pavement Performance". 27, 101-110.
42. **Kandhal, P. S., Sandvig, L.D., Koehler, W. C., & Wenger, M. E. (1973).** "Asphalt Viscosity-Related Properties of In-Service Pavements in Pennsylvania". *ASTM*, Special Technical Publication No. 532, 1973.
43. **Kandhal, P. S., Sandvig, L. D., & Wenger, M. E. (1973).** "Shear Susceptibility of Asphalts in Relation to Pavement Performance". Proceedings *AAPT*, Vol. 42.
44. **Kandhal, P. S. (1978).** "Low Temperature Shrinkage Cracking of Pavements in Pennsylvania". Proceedings of the *AAPT*, Vol. 47.
45. **Kandhal, P. S. (1980).** "Evaluation of Low Temperature Pavement Cracking on Elk County Research Project". *TRB*, Transportation Research Record 77.
46. **Kandhal, P. S. et al. (1988).** "Low-Temperature Properties of Paving Asphalt Cement". *TRB*, State-of-the-Art Report 7.
47. **Mamlouk, M. S., & Zaniewski, J. P. (2006)** "Materials for Civil and Construction Engineering: 2nd Edition. *Pearson Education, Inc*., Upper Saddle River, NJ.
48. **McGennis, R. B. et al. (1994).** "Background of Superpave Asphalt Binder Test Methods". *Federal Highway Administration*. Publication no. FHWA-SA-94-069. Washington, DC.
49. **McGennis, R.B., et al. (1995).** "Background of Superpave Asphalt Mixture Design and Analysis". *Federal Highway Administration*. Publication no. FHWA-SA-95-003. Washington, DC.
50. **McLeod, N. A. (1975).** "The Case for Grading Asphalt Cements by Penetration at 77°F". *CTAA*. Proceedings Canadian Technical Asphalt Association, Vol. 20.

51. **Meininger, R. C., & Nichols, F. P. (1990).** "Highway Materials Engineering, Aggregates, and Unbound Bases". *Federal Highway Administration.* Publication no. FHWA-HI-90-007, NHI Course No. 13123. Washington, D.C.

52. **Perng, J. D. (1989).** "Analysis of Crack Propigation in Asphalt Concrete Using a Cohesive Crack Model". *Thesis.* Ohio State University, Columbus, OH.

53. **Petersen, J. C. (1984).** "Chemical Composition of Asphalt as Related to Asphalt Durability (State-of-the-Art)". *TRB, Transportation Research Record.* No. 999.

54. **Roberts, F. L., Kandhal, P. S., Brown, E. R., Lee, D. Y., & Kennedy, T. W. (1996).** "Hot Mix Asphalt Materials, Mixture Design, and Construction: 2nd Edition". *NAPA Education Foundation*. Lanham, MD.

55. **Shell Bitumen. (2003).** "The Shell Bitumen Handbook", *Shell Bitumen*, UK.

56. **Shu, X., Huang, B., & Vukosavljevic, D. (2007).** "Laboratory Evaluation of Fatigue Characteristics of Recycled Asphalt Mixtures". *Department of Civil and Environmental Engineering.* University of Tennessee, Knoxville, TN.

57. **Siddique, R., & Iqbal Khan, M. (2011).** "Supplementary Cementing Materials". Springer-Verlag Berlin Heidelberg.

58. **Sobolev, K., Flores, I. V., & Wasiuddin, N. M. (2013).** "The Use of Fly Ash as Filler in Asphalt Cement: Phase 1". Final Report, *UWM-We Energies*, 17 p.

59. **Suheibani, A. R. S. (1986).** "The Use of Fly as an Asphalt Extender". *Doctoral dissertation*. University of Michigan, Ann Arbor, MI.

60. **Wang, H. et al (2011).** "Effect of Filler Characteristics on Asphalt Mastic and Mixture Rutting Potential". *TRB.* Transportation Research Board, 2208: 33-39.

61. **Wen, H. (2001).** "Fatigue performance Evaluation of WesTrack Asphalt Mixtures Based on Viscoelastic Analysis of Indirect Tensile Test". *Doctoral dissertation*. North Carolina State University, Raleigh, North Carolina.

62. **Wu, S. P. (2009).** "Effect of Organo-Montmorillonite on Aging Properties of Asphalt". *Elsevier.* Construction and Building Materials Vol. 23, Issue 7, 2636-2640.

63. **Zimmer, F. V. (1970).** "Proceedings of the 2nd Ash Utilization Symposium: Fly Ash as Bituminous Filler". Pittsburgh, PA.